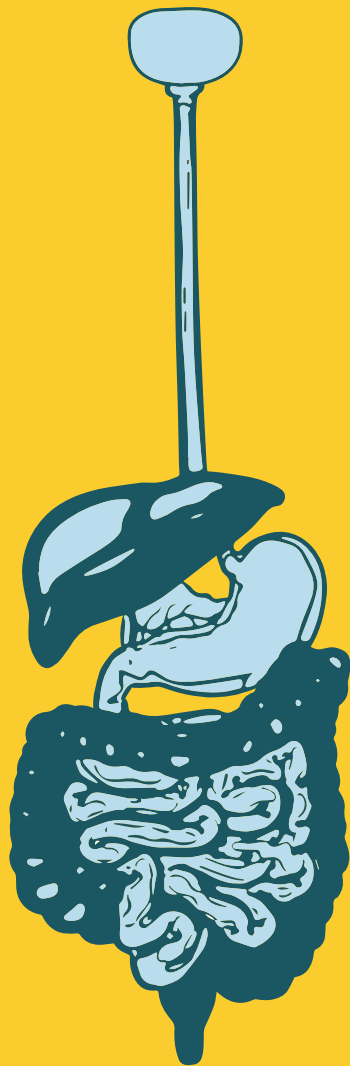


The

ARTIFICIAL GUT

integrating in vitro models of the human
digestive tract with mass spectrometry



Milou J.C. Santbergen

Propositions

1. Integration of a dynamic in vitro intestinal barrier model with mass spectrometry complicates user friendliness and analysis (this thesis)
2. Organ-on-a-chip researchers should start focussing on the application and validation of the model sooner rather than later to reach the end goal of replacing animal testing. (this thesis)
3. Tests studying the effectiveness of an anti-biofouling layer using physiologically irrelevant solutions are bad predictors for real life applications.
4. The interactions between the gut microbiota and the host must be prioritized when designing strategies to treat human intestinal diseases.
5. Overcomplicating the simple is worse than oversimplifying the complex.
6. The corona virus outbreak has restored the appreciation of scientific facts.
7. Positive discrimination in the hiring process is needed to create a balanced workplace.

Propositions belonging to the thesis entitled

“The Artificial Gut: integrating in vitro models of the human digestive tract with mass spectrometry”.

Milou J.C. Santbergen

Wageningen, 17 November 2020

**The Artificial Gut: integrating in vitro models
of the human digestive tract with mass
spectrometry**

Milou J.C. Santbergen

Thesis committee

Promotor

Prof. Dr M.W.F. Nielen
Professor of Analytical Chemistry
Wageningen University & Research

Co-promotors

Dr M. van der Zande
Scientist, Wageningen Food Safety Research
Wageningen University & Research

Dr H. Bouwmeester
Associate professor, Division of Toxicology
Wageningen University & Research

Other members

Prof. Dr R.F. Witkamp, Wageningen University & Research
Prof. Dr L. Connolly, Queen's University Belfast, United Kingdom
Prof. Dr M.H. Lamoree, Vrije Universiteit Amsterdam
Prof. Dr J. Legler, Institute for Risk Assessment Sciences, Utrecht

This research was conducted under the auspices of the Graduate School VLAG (Advanced studies in Food Technology, Agrobiotechnology, Nutrition and Health Sciences).

The Artificial Gut: integrating in vitro models of the human digestive tract with mass spectrometry

Milou J.C. Santbergen

Thesis

submitted in fulfilment of the requirements for the degree of doctor
at Wageningen University
by the authority of the Rector Magnificus,
Prof. Dr A.P.J. Mol,
in the presence of the
Thesis Committee appointed by the Academic Board
to be defended in public
on Tuesday 17 November 2020
at 4 p.m. in the Aula.

Milou J.C. Santbergen

The Artificial Gut: integrating in vitro models of the human digestive tract with mass spectrometry

198 pages

PhD thesis, Wageningen University, Wageningen, NL (2020)

With references, with summaries in English and Dutch

DOI: <https://doi.org/10.18174/532696>

ISBN: 978-94-6395-582-9

May the flowers remind us
why the rain was so necessary
- Xan Oku

Table of contents

1	General introduction	9
2	Online and <i>in situ</i> analysis of organs-on-a-chip	35
3	Development of a dynamic <i>in vitro</i> intestinal barrier model to predict oral bioavailability of chemicals	65
4	Dynamic <i>in vitro</i> intestinal barrier model coupled to chip-based liquid chromatography mass spectrometry for oral bioavailability studies	93
5	An integrated modular <i>in vitro</i> gastrointestinal tract total analysis system for oral bioavailability studies	111
6	The effect of flow on the translocation of gold nanoparticles in a dynamic <i>in vitro</i> intestinal barrier model	137
7	General discussion and future perspectives	155
	Summary	175
	Samenvatting	181
	Curriculum Vitae	187
	Acknowledgements	191
	Overview of Completed Training Activities	197

Chapter 1

General Introduction

1. Introduction

Imagine you are sitting at the dinner table eating your favourite dish, pasta pesto for example, never wondered how the body takes up the nutrients from your favourite dish to fuel the muscles of your body. Or how a medicine you orally ingest is taken up via your intestines and subsequently helps to relieve a headache. Not to mention, what happens when you ingest a toxin through a piece of shellfish. In the fields of nutrition, drug development and toxicology it is of major importance to know how a certain chemical is absorbed, distributed, metabolised and excreted (ADME) by the human body.

It all starts in the mouth, where the food is chewed and physically broken down into smaller parts. The salivary glands start producing saliva, inducing the enzymatic hydrolysis of starch by the enzyme amylase and they add water to the mixture [1]. By the addition of water, the food mixture can easily move down the oesophagus by peristaltic motion into the stomach (Figure 1.1). At the end of the oesophagus is a sphincter (circular muscle) that relaxes when food needs to pass through, for the most part this sphincter is closed to prevent stomach content from flowing back into the oesophagus. In the stomach the ingested compounds encounter a low pH, causing the denaturation of proteins. Furthermore, the enzyme pepsin breaks down proteins into smaller peptides, being most effective in cleaving the bond between amino acids with a hydrophobic side chain, like tryptophan, tyrosine and phenylalanine [2]. The stomach is connected to the small intestine via the pyloric sphincter, which slowly empties the stomach content into the small intestine. Upon reaching the small intestine the pH is neutralized and enzymes produced by the pancreas are added, like proteases and lipases, to further digest the chemicals [3]. A last addition comes from the gall bladder in the form of bile that is helping the emulsification of the fat present in the food mixture [4]. After digestion only the free, or bioaccessible, fraction of dietary, drug or toxic compounds are available for transport across the wall of the small intestine. After passing the intestinal wall the compound reaches the systemic blood (or lymphatic) circulation. Followed by metabolism in the liver and subsequently the compounds are distributed to their target site in the body. Finally, the compounds and metabolites thereof are excreted by the body, usually via the kidneys (urine) or the faeces.

For the risk assessment of toxins or the development of novel drugs good predictions of internal exposure to the bioactive component is crucial. Working in a step wise manner to establish these predictions is essential. Firstly, assessment of compound stability in the digestive tract upon exposure to different salt concentrations, pH levels and digestive enzymes. Secondly, is the compound in such a configuration it can be taken up by the small intestine. The fraction that is taken up is called the (oral) bioaccessible fraction. From a mechanistic point of view it is also interesting to know by which route the compound is absorbed by the intestine. And if the compound undergoes any metabolism inside the intestinal cells before reaching the bloodstream.

To answer all these questions laboratory model systems for the human digestive tract are of great use. In the following part of this introduction the main functions and important anatomical characteristics of the small intestine will be described in more detail followed by discussing model systems that are currently being used to recapitulate and better understand the processes that go on in the gastrointestinal tract upon ingestion of a compound. These studies cannot be performed without robust detection methods. Therefore, the state-of-the-art model systems with integrated analysis are discussed. The introduction ends with the outline and aim of this thesis.

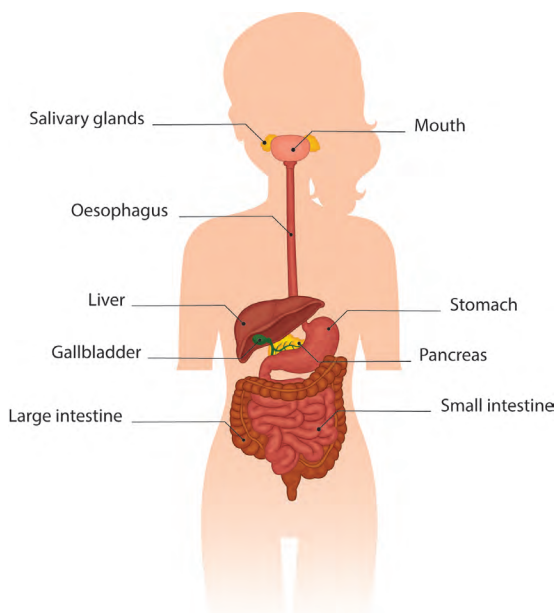


Figure 1.1: Anatomy human gastrointestinal tract

1.1 Small intestine

The small intestine is the most important part of our gastrointestinal tract for the absorption of chemicals and it consists of three distinct regions, namely: the duodenum, jejunum and ileum. The duodenum is the first section after the stomach, here the bile and pancreatic secretions enter the intestine and Brunner's glands are present in the duodenal wall. These glands produce an alkaline secretion to neutralize the acidic content coming from the stomach, optimizing the environment for intestinal enzymatic digestion [5]. The middle section of the small intestine is the jejunum and most nutrients are absorbed here. The last section of the small intestine is the ileum where compounds not absorbed by the jejunum are taken up. Furthermore, the ileum contains lymph nodules, known as Peyer's patches which are not found in the duodenum and the jejunum [6].

Looking more closely at the anatomy of the intestinal wall you will find roughly three layers: the muscular layer, the submucosa and the mucosa. The muscular layer as the name already suggest contains muscles both in circular and longitudinal direction. Allowing for the peristaltic movement of the intestine, directing the food down the intestinal tract. Next in the submucosa, you find blood and lymphatic vessels together with connective tissue and nerves. Finally, the last layer on the inside of the intestinal tract is the mucosa. The mucosa consists of the lamina propria, a layer of connective tissue containing immune cells and the innermost layer the epithelium. The epithelium is the last layer that lines the inside (luminal side) of the small intestine and consists of finger-like structures, called villi, they increase the surface area of the intestine to promote absorption (Figure 1.2).

Six different cell types are found in the (small) intestinal epithelium, namely: stem cells, Paneth cells, microfold (M) cells, goblet cells, enteroendocrine cells and enterocytes. The stem cells and Paneth cells are located at the bottom of the crypts of the small intestine (Figure 1.2). From the stem cells in the crypts all other epithelial cells originate and migrate to the tops of the villi where they are shed. This is a continuous cycle of epithelial renewal and takes 3-5 days [7], while at the same time maintaining the integrity of the intestinal barrier [8]. Paneth cells are part of the innate immune system in the intestine and can be recognized by the large granules in their cytoplasm. These granules

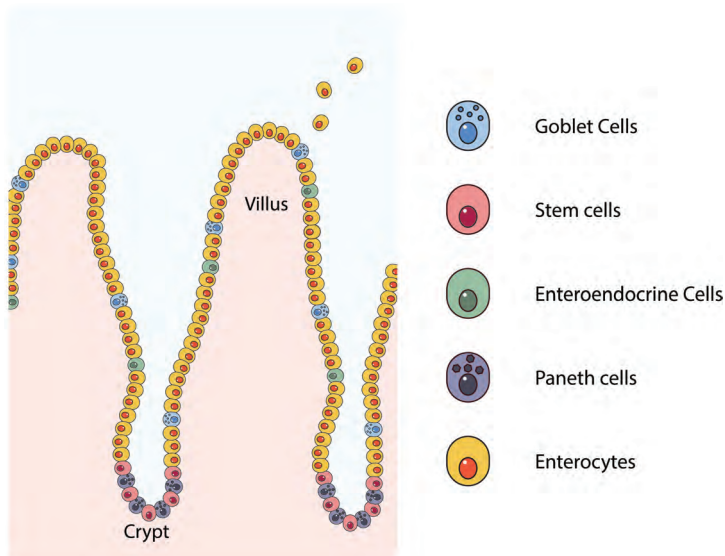


Figure 1.2: Intestinal epithelium with the five main cell types

contain compounds that aid in the host defence mechanism against harmful pathogens [9]. M cells are found within the Peyer's patches in the ileum and their main function is to transport antigens present in the lumen towards the cells of the immune system. Along the crypt villus axis, you find the goblet cells, enteroendocrine cells and enterocytes (Figure 1.2). Goblet cells are mucin producing cells and the mucus creates an extra barrier on top of the epithelium, decreasing the translocation of highly diffusible small molecules and increasing the transport of hydrophilic compounds [10]. Moreover, the mucus layer protects from mechanical induced damage and forms a barrier between the epithelium and the non-commensal bacteria in the lumen. Enteroendocrine cells occupy less than 1% of the epithelium, however they secrete hormones and peptides that influence important pathways in the intestine like, energy metabolism, intestinal motility and mucus secretion [11]. Lastly, the enterocytes are the most abundant cell type in the small intestine and play a crucial role in the absorption and translocation of compounds: during translocation a compound enters the enterocytes, from where it can undergo metabolism, and is excreted towards the systemic circulation, or is routed back into the intestinal lumen [12]. Furthermore, enterocytes express microvilli at the apical side of the cells increasing the surface area, aiding absorption. All cells are tightly connected to each other by tight junction proteins, to form a closed

membrane. More than 40 different proteins are involved in the formation of tight junctions, both intracellular and extracellular membrane proteins [13].

Besides the properties of the epithelium, the specific properties of a chemical, like size, charge and hydrophobicity greatly influences the transport of the chemical. Water and electrolytes can freely diffuse para-cellular (in-between the cells). Lipophilic compounds are assumed to be exclusively transported by the passive trans-cellular (through the cell) route (Figure 1.3). While, nutrients are mostly transported via active carrier mediated transport. Some hydrophobic drugs, depending on their chemical properties and structures, may also be translocated via active transporters (Figure 1.3) [10, 14].

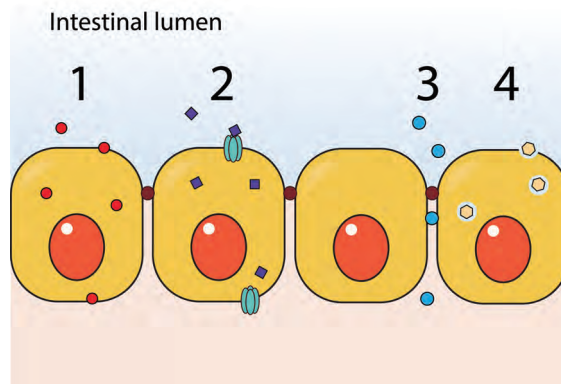


Figure 1.3: Four translocation pathways of the intestinal epithelium. 1) Transcellular (passive diffusion), 2) transcellular (transporter mediated), 3) paracellular (passive diffusion) and 4) transcellular (endocytosis and/or receptor mediated)

To fully understand what happens when chemicals are taken up by the small intestine, laboratory models are of great use. Several different models exist for bioavailability studies like, animal models, barrier models using intestinal cell lines, organoids and the most recent development the gut-on-a-chip. In the next part of this introduction these models for translocation and biotransformation across the intestinal epithelium will be discussed. Stating the biggest advantages and disadvantages of each model system. Followed by the technological advancements of integrating a dynamic *in vitro* model system of the intestine with high-end analytical detection systems.

1.2 Intestinal epithelial models

Biological model systems can range from full organisms, like animals to single cells. A biological model system is used to study a biological phenomenon in a controlled setting with the intention to translate this information to the human situation. The main reason for using model systems is that most research would be deemed unfeasible or unethical to perform in humans. On the other hand, the biggest difficulty when using model systems is how translatable the observations are to the human situation. Therefore, better biological model systems are desired and there is a need for robust detection methods to study these models. The gastrointestinal tract is one of the most complex and fascinating sites in the human body as it can protect us from exogenous compounds and pathogen invasions, but tolerates the harmless bacteria that aid in digestion. Furthermore, it effectively takes up nutrients from our food. One of the biggest challenges within the field of intestinal biology is the development of physiologically relevant model systems that better represent the human intestine. Before designing an experiment, scientists must assess the tools and methods available for establishing an appropriate model system capable of answering the research question at hand. Many different model systems exist for the gastrointestinal tract all allowing the investigation of different aspects, like transport of nutrients and chemicals, responses of the mucosal immune system or interactions with the microbiome either in a healthy or diseased state. In this thesis, the focus is on the bioavailability and uptake of chemicals by the intestine, below model systems suited for that purpose are discussed.

1.2.1 *in vivo/ ex vivo*

In the scientific literature several different animal species are used to study oral bioavailability of a compound, like mice, rats, dogs, pigs and non-human primates. However, the translation of this information to human oral bioavailability depends on the knowledge available on the physiological, anatomical and biochemical differences between the animal model and a human. In the early stages of drug development generally two types of animals are used a rodent (e.g. mice or rats) and a non-rodent (dogs, pigs or non-human primates). In the field of toxicology mostly rodents are used as animal model [15]. Advantages of using mice and rats are the relatively low costs compared to

other animals and a lot of permeability data is available for these animal models [16]. However, still many drug candidates fail at the clinical stage due to the bad predictive power of an animal model. Considerations to take into account when correlating rat data with human data are that rats have a different pH profile in the GI tract and a different transit time [17, 18]. Using non-human primates is considered to be the closest animal model there is to humans, even though differences still exist. Furthermore, the use of non-human primates is time consuming, expensive and difficult to get accepted by an ethical committee. Another larger animal frequently used is a dog, biggest consideration when using dogs is that their stomach pH is on average much higher than that of a human [19]. Besides differences between species that are hard to correct for in calculations, performing an animal study has low throughput and it is difficult to sample. Furthermore, because of the complexity of a full organism changing a specific parameter can be difficult, for example comparing healthy versus diseased. Along with the ethical issues involving animal testing the biggest disadvantages using full animals for intestinal uptake studies is where to sample (lumen/plasma levels).

A solution for this, is to take the intestine out of the animal and study intestinal permeability in a more controlled setting. The two most important, so-called *ex vivo* techniques are the everted sac and Ussing chamber technique. The everted sac was firstly introduced by Wilson and Wiseman in 1954 [20]. The main principle of the everted sac technique starts with the removal of 5 to 6 cm of small intestine and a washing step. The intestinal tissue is then everted (turned inside out) and tied off on one end, subsequently it is filled with a salt solution and tied off at the other end. Then the everted sac is placed inside an incubation flask that contains the compound of interest [21]. Main advantages of this technique are the presences of all cell types with their transporters, metabolic activity and a relative large surface area. However, the everted sac is only viable for up to two hours and the presence of the muscular layer of the intestine results in an underestimation of the absorption of the chemical studied [21]. The Ussing chamber was invented by Hans Ussing in 1951 [22], an intestinal section is taken from an animal and opened, subsequently it is placed as a flat sheet in a chamber to create an apical and a basolateral compartment. Microelectrodes are integrated into the system to detect current changes of the cellular membrane due to transport and both sides of the barrier can be

sampled. Same benefits and issues apply for the Ussing chamber as for the everted sac technique [23].

1.2.2 Static *in vitro* models

As discussed in the previous part, animal models have been the method of choice for the interpretation of absorption of chemicals. However, the translation to the human situation is hard to make. In 1959 Russel and Burch described the three R's principle for the use of laboratory animals, the three R's stand for refinement, reduction and replacement [24]. Stating the importance of minimizing the pain and distress of the animals used for scientific purposes (refinement), critically looking at the amount of animals needed to answer the research question or increasing the amount of information obtained per animal (reduction) and lastly replacing the animal all together for an *in vitro* or computer model (replacement) [25]. The use of animals has already been banned for the cosmetic industry [26] and more pressure is been put on the scientific community to reduce the use of animals as well. Therefore, good *in vitro* cell culture models are needed that give a more accurate prediction of the human situation, compared to animal models. *In vitro* models are used to study specific mechanistic *in vivo* processes in a simplified and well controlled manner. Thus, cell lines can be a great way to investigate the transport of a compound of interest through the intestinal epithelium, considering the specific properties of the compound and the research question at hand. Ideally, primary intestinal cell cultures are used for permeability studies expressing all cell types. However, stable long-term cultures of primary intestinal cells have failed, therefore researchers have established immortalized cell lines derived from intestinal tumours for *in vitro* intestinal model systems. The most wide spread used cell line is the human colorectal carcinoma cell line (Caco-2). Differentiated Caco-2 cells resemble mature enterocytes found in the small intestine, even though the cell line is derived from the colon. Caco-2 cells include several influx and efflux transporters from the ATP-binding cassette (ABC) and solute carrier (SLC) transporter families [27]. As well as tight junctions between the cells, however the tight junctions in a Caco-2 monolayer are less permeable compared to the *in vivo* situation in the small intestine [28-30]. For transport studies Caco-2 cells are grown on a porous membrane insert, called the transwell, with cell culture media on both sides creating a cellular intestinal barrier. Because Caco-2 cells are universally used for mimicking the intestinal barrier a lot of data is

generated for proper comparison to the *in vivo* situation. High correlations between *in vitro* Caco-2 monolayers and *in vivo* data have been shown for lipophilic compounds that cross the intestinal barrier via passive transcellular diffusion [10]. Largest issue with Caco-2 cell cultures is that different culture condition across labs can influence the cells and can lead to selection of cells with certain differentiation characteristics during sub culturing [31]. Resulting in different reported permeability of the same drug. Another drawback of Caco-2 cells is the low expression of some members of the cytochrome P450 protein family [32], like CYP3A4 which is the most prevalent oxidative enzyme involved in gut metabolism *in vivo* [33]. A subclone of the Caco-2 cell line are TC-7 cells, they have shown higher enzymatic activity compared to Caco-2 cells [34], but otherwise show the same morphology. Caco-2 cells mimic the enterocytes within the intestinal epithelium, the most important cell type for permeability of compounds across the epithelial barrier. However, *in vivo* a mucus layer is present on top of the epithelial cell layer introducing an extra barrier element. A monoculture of Caco-2 cells lacks this characteristic. Therefore, a co-culture of Caco-2 cells and a goblet cell line would be a closer mimic to the *in vivo* microenvironment of the gut. HT29-MTX cells resemble intestinal goblet cells and are derived from the parent cell line HT29 originating from a human adenocarcinoma. The HT29-MTX cells have been modified so they produce mucin, just like goblet cells, yet with a slightly different composition [35-37]. Generally HT29-MTX cells are grown in co-culture with Caco-2 cells resulting in a layer of cells that produces mucus and the barrier is more loose compared to a monoculture of Caco-2 cells, thus more representative of the *in vivo* microenvironment [38, 39].

In 2009 Sato and colleagues developed a small intestinal model called the organoid [40]. Organoids are three-dimensional (3D) cell cultures derived from adult stem cells in intestinal crypts or from induced pluripotent stem cells (iPSCs), reproducing complex cell-cell interaction and spatial morphology. They are generally cultured within an artificial extracellular matrix (ECM) and supplemented with a mixture of growth factors. Once the organoids are seeded they start growing in a spherical shape with crypt like structures. The luminal side of the organoid is on the inside of the sphere. All five different cell types that are found in the epithelial layer in the human body are also present in the organoid culture [41, 42]. Furthermore, just like in the *in vivo* situation cells

shed into the luminal space. Using biopsies of patients to create an intestinal organoid culture would be very beneficial for the development towards personalized medicine [43]. Yet, the absence of supporting tissues like blood vessels and the immune system limit the applicability of the organoid cultures for pharmacokinetic studies and disease modelling. Another disadvantage mainly for permeability experiments is the fact that the luminal side is on the inside of the sphere and hard to reach. Adding to that, cells are shed into the luminal space which causes the organoids to burst open at a certain point releasing the debris of cells into the ECM. It is hard to predict when this happens. A solution to this is the two dimensional (2D) growth of intestinal organoids making the luminal side easily accessible just like in a traditional transwell culture with immortal cell lines [44]. Another solution is introducing flow either by puncturing an individual 3D organoid and using capillaries to supply liquids [45] or by subjecting a 2D organoid culture to flow [46]. Characterization and applicability of organoid cultures for transport studies is still in its developmental stages but looks like a promising replacement for immortal cell lines.

1.2.3 Dynamic *in vitro* models

In the previous sections animal models and static *in vitro* cell culture models of the intestine for permeability studies were discussed. However, over the past decade techniques from the field of microfluidics have been incorporated with *in vitro* cell culture models with the aim to better mimic the biochemical and mechanical triggers present *in vivo* and eventually, together with improved biology, eradicate (or at least reduce) the use of animals for research purposes. The field quickly expanded with the development of the lung-on-a-chip by Huh et al. (2010), where they have incorporated the mechanical triggers of breathing and blood flow into the cell culture system [47]. After this a plethora of different chip systems have been developed for almost every organ in the body [48, 49], also for the intestinal tract. In its most basic form these intestinal models consist of a cell culture chamber subjected to flow. The cell culture chamber contains living cells derived from the intestine, either an immortal cell line or an organoid culture. The incorporation of flow allows for the continuous supply of cell culture medium for maintaining the cells and the induction of *in vivo* like shear stresses on the cells. Several different names are used across literature to describe these types of models like, gut-on-a-chip [50], dual

flow bioreactor [51], intestine-on-a-chip [52], small intestine-on-a-chip [53], gastrointestinal tract microscale cell culture analog [54] and more. In this thesis the term dynamic *in vitro* intestinal barrier model will be used to describe all types of intestinal cell barrier models that are subjected to flow.

Even though the core principals of dynamic intestinal models are similar across literature, there are also many differences. Firstly, models described in the literature can be roughly divided in two types of design. One design resembles the traditional transwell, having a large round cell culture area [51, 55]. And the other has a straight channel or tube-like design with relatively smaller cell culture area [50, 56]. Secondly, different materials are used to fabricate the cell culture systems. Polydimethylsiloxane (PDMS) is a popular material for microfluidic chip fabrication [57], mainly because it is easy to use and cheap. However, PDMS is known to absorb hydrophobic compounds and by this limiting the exposure of a particular compound to the cells. Coating the PDMS helps to reduce the absorption of chemicals to the surface [58]. Furthermore, uncrosslinked polymer fragments can end up in the cell culture medium and have toxic effects on the cells. Therefore, other materials have also been used for dynamic intestinal models like, glass [59], polycarbonate [60] and poly methyl methacrylate [61]. Because the main focus of organ-on-a-chip models is to better mimic the *in vivo* microenvironment the models get more and more complex. Like for the dynamic *in vitro* intestinal barrier model besides including flow on the cells mimicking the bloodstream and the passing of the food matrix, systems have incorporated peristaltic motion. This results in mechanical strain on the cells by stretching and releasing of the cell culture membrane [50]. Just like the traditional transwell system, dynamic intestinal cell systems are suited for intestinal barrier function studies [62, 63] and uptake studies of nutrients, drugs or toxins [64-66]. The dynamic model can even be expanded to study the interaction with different cell types like cells from the immune system [67], vascular system [52], and the microbiome [50, 68]. Especially, the addition of the microbiome is a big advantage compared to static culture systems as there the biggest problem was the overgrowth of the bacteria in the system with the incorporation of flow the excess of bacteria is washed off [68]. Also, the ability to grow under anaerobic circumstances has become possible in a dynamic cell culture device [52]. Another benefit of having a flowing system is that different organs can be connected via the bloodstream compartments of the individual

organ-on-a-chip modules allowing for pharmacokinetics studies [55, 69, 70]. The biggest advantages of the previously discussed organoid cultures are the presence of multiple cell types and the three-dimensional structure representing the crypts and villi present in the human intestinal tract, dynamic intestinal barrier systems are mainly flat cultures. However, some research has shown the induction of villi like structures under flow [50]. Others have tried to incorporate villi like scaffolds in the systems to incorporate the three-dimensional structure on chip [71, 72].

Besides the many advantages of dynamic intestinal cultures on chip, there are also some disadvantages (Table 1.1). Most work on dynamic *in vitro* cell culture systems of the intestine are performed in academic laboratories and there is a high diversity in the designs of the models. This is making comparison between the different models available difficult, furthermore most chips require a skilled technician to perform a robust experiment. Luckily, in recent years multiple companies have commercialized organ-on-a-chip technology bringing down the costs and increase robustness and ease of use (Figure 1.4). Analysing the dynamic culture systems has been limited to mainly antibody staining's, subsequently visualizing the presence of different cell types or for example mucin proteins by confocal microscopy. Recently, more papers have been focussed on characterizing the transport mechanisms in a dynamic culture systems [59, 65, 66, 73-75], however still not enough to determine a standardised system that can be used for drug development or for risk assessment purposes.

Table 1.1 Advantages and disadvantages of the different intestinal model systems for intestinal uptake

	Model	Pros	Cons
In vivo	Animals	<ul style="list-style-type: none"> ADME 	<ul style="list-style-type: none"> unethical expensive translation to human sample location
Ex vivo	Everted sac	<ul style="list-style-type: none"> presence of all transporters metabolically active 	<ul style="list-style-type: none"> static environment short life span animal origin
	Ussing Chamber	<ul style="list-style-type: none"> presence of all transporters metabolically active 	<ul style="list-style-type: none"> static environment short life span animal origin
In vitro	Cell lines	<ul style="list-style-type: none"> easy to use human origin cheap high through put 	<ul style="list-style-type: none"> static environment no supporting tissue only limited number of cell types present different metabolic/transporter activity
	Organoids	<ul style="list-style-type: none"> all intestinal epithelial cell types present biopsy/iPSC/adult stem cells 2D or 3D structure metabolically active 	<ul style="list-style-type: none"> static environment no supporting tissue labour intensive
	Dynamic intestinal models	<ul style="list-style-type: none"> flow some models included peristaltic motion possibility to include automated online analysis 	<ul style="list-style-type: none"> no generally agreed upon flow system minimal literature discussing intestinal permeability no supporting tissue

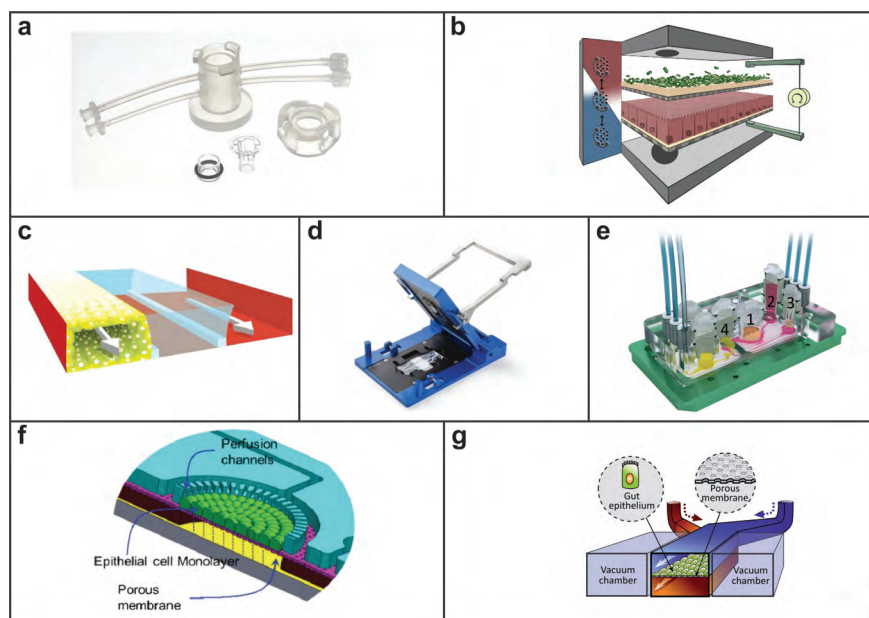


Figure 1.4: a) QV600 system from Kirkstall, b) human-microbial crosstalk (HuMix) model [76] c) OrganoPlate from Mimetas [77], d) organ-on-a-chip system from Micronit Microtechnologies, e) four organ chip from TissUse [69], f) Nutrichip [78] g) gut-on-a-chip [50]. Images e, f and g were reproduced with permission from The Royal Society of Chemistry

1.3 Integration of mass spectrometry with dynamic cellular models of the intestine

Miniaturization of the cell culture models of the intestine and the inclusion of flow in these models has the benefit of lower consumption of cell culture medium (including antibiotics) and the compound of interest. However, this also decreases the sample size for analytical measurements. Incorporation of sensors and online coupling to analytical equipment is beneficial to validate and improve the quality of data that can be gained from dynamic cell culture models. Currently, only a few integrations have been made of dynamic *in vitro* cell culture models of the intestine with analytical systems [52, 60, 64, 79]. Mass spectrometry is one of the few analytical techniques that is suited for highly sensitive multi analyte detection to analyse translocation and (un)known product formation by the cells.

1.3.1 Mass Spectrometry

Mass spectrometry (MS) is an analytical technique that measures the molecular mass of ionized molecules and fragments thereof based on their mass-to-charge ratio (m/z). MS is a highly sensitive technique compared to spectroscopic techniques such as ultra violet visible light (UV-Vis) absorbance spectroscopy, vibrational spectroscopy (infrared and Raman) and nuclear magnetic resonance (NMR). Mass spectrometry is used in many different fields of study for the elucidation/identification of organic molecules and in inorganic analysis of metals and salts. All mass spectrometers consist of three components: an ionization source, a mass analyzer and a detector. The mass analyzer is at the center of a mass spectrometer, it differentiates the ions based on their mass-to-charge ratio. Several different types of mass analyzers have been developed over the years. Quadrupole and magnetic sector mass analyzers are so called scanning instruments, depending on the settings, only ions with a given m/z pass through the analyzer at a time. A quadrupole instrument consists of four parallel rods on which DC and AC voltages are applied creating an oscillating field. The applied voltages affect the stability of the flight path of the ions in between the four rods. For a certain set of voltages, only ions with a particular m/z will pass and reach the detector. In other types of mass analyzers all ions pass the mass analyzer and are eventually detected, for example in a time-of-flight (TOF) or orbitrap instrument. In TOF mass spectrometry all ions in

the sample are accelerated with the same kinetic energy and, following the kinetic energy equation $E=0.5mv^2$ the difference in velocity and, at a fixed drift tube length, in flight time, separates the ions on the basis of their mass-to-charge ratio [80]. Tandem MS instruments have multiple similar or different mass analyzers in series allowing for the selection of a particular m/z value in a first quadrupole analyzer, fragmentation in a collision cell (often a second quadrupole) and MS analysis of a single or multiple fragment ion(s) by a third mass analyzer (quadrupole, TOF, ion trap or orbitrap). After the (final) mass analyzer the detector is positioned, for example a multichannel plate or an electron multiplier, that converts the impact of the (fragment) ions into an electrical current. But before, a molecule can be separated based on their m/z in a mass analyzer it first needs to be ionized. The ionization techniques used in this thesis are fully compatible with analysis-in-solution, i.e. the sample matrix effluents from the dynamic *in vitro* model of the intestine. In the next section the ionization techniques used in this thesis are discussed namely, electrospray ionization and inductively coupled plasma ionization.

1.3.2 Electrospray ionization

The first electrospray ionization (ESI) source for MS analysis was developed by the Fenn group in the 1980s [81], and resulted in the Nobel prize for Chemistry in 2002. Their work mainly focused on the detection of proteins [82, 83], however the field extended to also measure other biopolymers, synthetic polymers and small molecules. In particular small molecules with a polar character such as drugs, food and environmental contaminants. With ESI the analyte is in solution and pumped through a metal capillary to which a positive or negative high voltage is applied (2-5 kV), as a result charged solvent is generated (Figure 1.5). Due to the destabilization of the accumulated charges at the liquid surface and the high electric field a so-called Taylor cone is formed, which was theoretically described by Geoffrey Taylor for the first time in 1964 [84]. From the Taylor cone charged droplets are produced that move along the direction of the electric field towards the mass analyzer. The charged droplets become smaller due to solvent evaporation and droplet fission. For small molecules it is assumed that a charged analyte is created via the ion evaporation model, where the ion is ejected from a charged nanodroplet. Whereas, for large proteins it is widely accepted that charged analytes are created via the charged residue model. Here, the nanodroplet completely evaporates transferring the charge to the

analyte [85]. Finally, the charged analytes pass through a sample cone or heated capillary interface into the high vacuum mass analyser. ESI is a highly sensitive technique and has been coupled to high performance liquid chromatography (HPLC) and capillary electrophoresis [86]. Furthermore, the electrospray emitter has been integrated into a “plug and play” chip format containing an analytical column [87]. In this thesis I have used the latter approach for the detection of small molecules transported across a dynamic *in vitro* intestinal culture system. This so-called iKey system consisted of a micro ultra-performance liquid chromatography column (50 mm x 150 μm I.D.) in a credit card size format, packed with 1.7 μm C18 stationary phase particles and having an integrated nano electrospray emitter. However, ionization suppression may occur in ESI due to the coelution of salts, proteins, etc. present in the sample matrix, thereby dramatically reducing the sensitivity of analyte detection by up to several orders of magnitude. As a mitigation measure sample preparation using, for example, a solid phase extraction (SPE) ‘trap’ column is crucial prior to ESI-MS analysis.

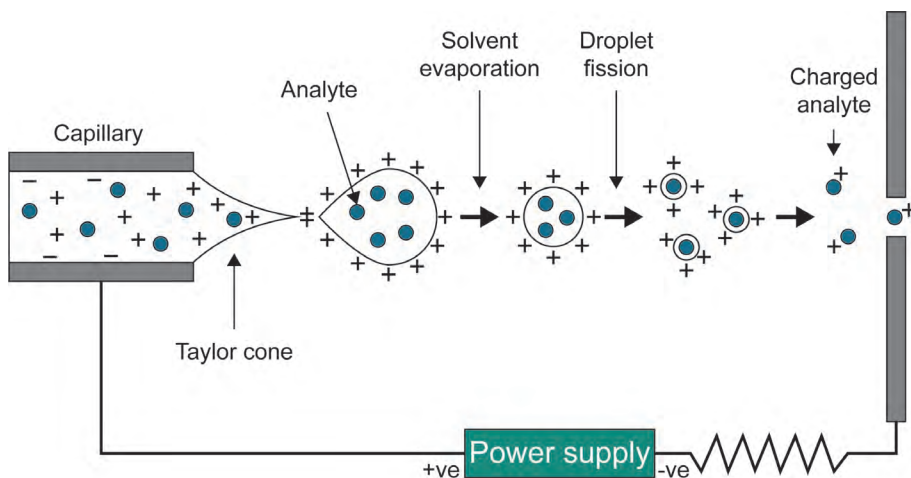


Figure 1.5: Schematic representation of electrospray ionization

1.3.3 Inductively coupled plasma ionization

Inductively coupled plasma mass spectrometry (ICP-MS) is an analytical method that ionizes, separates and detects a wide range of metal and non-metal compounds (minerals), it is even suited for the detection of metal nanoparticles in solution. Sample is introduced into the ICP-MS via a nebulizer,

thus creating an aerosol. The droplets formed are directed towards an argon plasma at a temperature between 6,000 to 8,000 Kelvin. The plasma is maintained by a radio frequency generator providing a stable source of energy through an induction coil (Figure 1.6). The argon plasma consists of electrons and positively charged argon ions. Due to the plasma the molecular structure of a compound is entirely lost, and molecules split into its individual atoms that lose an electron, thus becoming positively charged. ICP-MS has excellent elemental specificity based on m/z values and is therefore an ideal technique for the (multi-analyte) detection of metal-based nanoparticles. Typical mass analysers in ICP-MS are still quadrupole-based. An inherent limitation of the argon plasma used in ICP-MS is the occurrence of interferences at specific m/z values in the mass spectrum due to clusters of ionic species formed from the argon gas. In many cases these interferences can be mitigated using tandem or high-resolution mass analysers. For nanoparticle analysis the use of the so-called single particle analysis mode is highly relevant, since it allows for the detection of individual particles in a solution [88].

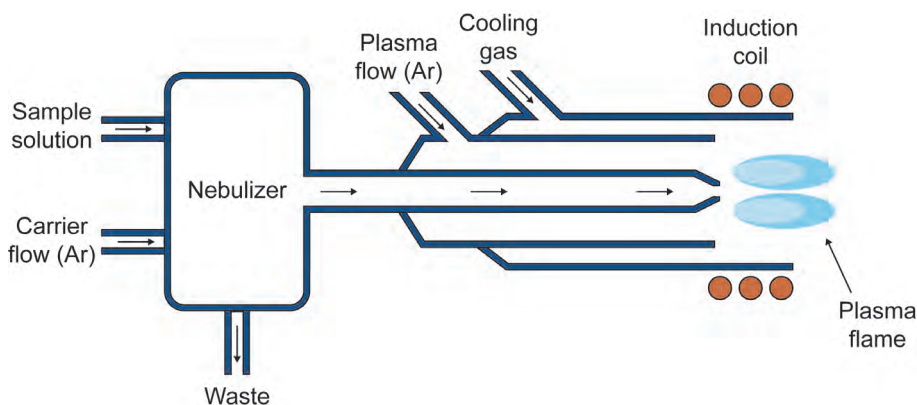


Figure 1.6: Schematic representation of inductively coupled plasma ionization. Ar =Argon

1.4 Aim and outline of this thesis

Currently, static *in vitro* cell culture assays are used in early phases of drug development, food research and hazard identification of chemicals. However, these *in vitro* models lack organ specific functionality, hampering mechanism-

based research needed for novel drug development and next generation risk assessment. Recent advances in microchip- and bio-engineering enabled the development of organ-on-a-chip models. The main technical advantages of organ-on-a-chip technology are the ability to spatiotemporally control the microenvironment and the low reagent consumption. On the other hand, micro-engineered organ-on-a-chip models may still lack robustness for reproducible and bio-relevant studies. In addition, also the low flow rates present a major challenge of organ-on-a-chip technology: how to detect drug uptake and compound metabolism in real-time and at a high temporal resolution at the microscale.

In this thesis a dynamic intestinal cell culture device is coupled to highly advanced mass spectrometry equipment, aiming for automated and online analysis of translocation of drugs, natural toxins and nanoparticles, while maintaining the bio-integrity of the cell system. Apart from technical robustness challenges, the fundamental chemical incompatibility between complex biological systems used in cell culturing and the clean sample requirements of sensitive advanced analytical instrumentation need to be resolved. Furthermore, the dynamic cell culture model is placed outside of an incubator for the integration with the mass spectrometer. However, physiological relevant temperatures and pH levels still need to be regulated for a reliable biological experiment. As well as the evaluation of the barrier integrity of the intestinal cell layer an aspect largely overlooked by current literature.

In **Chapter 2** an overview is provided of the current knowledge regarding analytical techniques integrated with organ-on-a-chip systems. In **Chapter 3a** a dynamic flow-through *in vitro* model was developed to predict permeability across the intestine using a well-known model drug, verapamil, to benchmark our results against literature. In **Chapter 3b** the stereoselective permeability of the natural mycotoxin ergotamine was examined using the model established in chapter 3a. The dynamic flow-through *in vitro* model system was expanded in **Chapter 4**. A novel bio-integrated online total analysis system for intestinal absorption and metabolism was developed by successfully interfacing a flow-through transwell with electrospray ionization mass spectrometry. The main advantages of this system being the integration of a relevant biological model with fully automated online analysis, which was missing before. **Chapter 5**

combines a digestion-on-a-chip with the bio-integrated analysis system developed in chapter 4, including the complexity of digestion creating a more complete bio-availability model. In **Chapter 6** the integration of the flow-through transwell with inductively coupled plasma mass spectrometry was realized for the evaluation of the translocation of model gold nanoparticles. Lastly, in **Chapter 7** a general discussion on the topics described in this thesis is provided and look to the future of organ-on-a-chip technology, with special emphasis on the integration with mass spectrometry analysis.

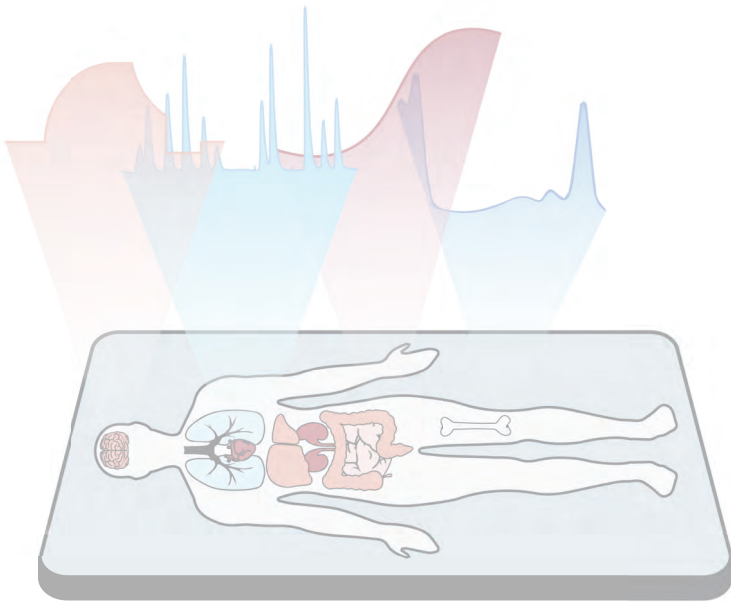
References

- [1] DeSesso JM, Jacobson CF. Anatomical and physiological parameters affecting gastrointestinal absorption in humans and rats. *Food Chem Toxicol.* 2001;39(3):209-228.
- [2] Trout GE, Fruton JS. Side-chain specificity of pepsin. *Biochemistry-U.S.* 1969;8(10):4183-4190.
- [3] Whitcomb DC, Lowe ME. Human pancreatic digestive enzymes. *Digest Dis Sci.* 2007;52(1):1-17.
- [4] Carey MC, Small DM, Bliss CM. Lipid digestion and absorption. *Annu Rev Physiol.* 1983;45(1):651-677.
- [5] Krause WJ. Brunner's glands: A structural, histochemical and pathological profile. *Prog Histochem Cyto.* 2000;35(4):255-367.
- [6] Jung C, Hugot JP, Barreau F. Peyer's Patches: The immune sensors of the intestine. *Int J Inflam.* 2010;2010:823710.
- [7] van der Flier LG, Clevers H. Stem cells, self-renewal, and differentiation in the intestinal epithelium. *Annu Rev Physiol.* 2009;71:241-260.
- [8] Watson AJM, Hughes KR. TNF-alpha-induced intestinal epithelial cell shedding: implications for intestinal barrier function. *Ann Ny Acad Sci.* 2012;1258:1-8.
- [9] Bevins CL, Salzman NH. Paneth cells, antimicrobial peptides and maintenance of intestinal homeostasis. *Nat Rev Microbiol.* 2011;9(5):356-368.
- [10] Artursson P, Palm K, Luthman K. Caco-2 monolayers in experimental and theoretical predictions of drug transport. *Adv Drug Deliv Rev.* 2001;46(1-3):27-43.
- [11] Sternini C, Anselmi L, Rozengurt E. Enteroendocrine cells: a site of 'taste' in gastrointestinal chemosensing. *Curr Opin Endocrinol.* 2008;15(1):73-78.
- [12] Roberts DJ, Hall RI. Drug absorption, distribution, metabolism and excretion considerations in critically ill adults. *Expert Opin Drug Met.* 2013;9(9):1067-1084.
- [13] Alberts B, Johnson A, Lewis J, Raff M, Roberts K, Walter P. Cell junctions. *Molecular Biology of the Cell* 4th edition: Garland Science; 2002.
- [14] Ehrhardt C, Kim KJ. Drug absorption studies: in situ, in vitro and in silico models: Springer Science & Business Media; 2007.
- [15] OECD. Test No. 417: Toxicokinetics 2010.
- [16] Fagerholm U, Johansson M, Lennernas H. Comparison between permeability coefficients in rat and human jejunum. *Pharmaceut Res.* 1996;13(9):1336-1342.
- [17] Cao XH, Gibbs ST, Fang LY, Miller HA, Landowski CP, Shin HC, et al. Why is it challenging to predict intestinal drug absorption and oral bioavailability in human using rat model. *Pharmaceut Res.* 2006;23(8):1675-1686.
- [18] Hurst S, Loi CM, Brodfuehrer J, El-Kattan A. Impact of physiological, physicochemical and biopharmaceutical factors in absorption and metabolism mechanisms on the drug oral bioavailability of rats and humans. *Expert Opin Drug Metab Toxicol.* 2007;3(4):469-489.
- [19] Akimoto M, Nagahata N, Furuya A, Fukushima K, Higuchi S, Suwa T. Gastric pH profiles of beagle dogs and their use as an alternative to human testing. *Eur J Pharm Biopharm.* 2000;49(2):99-102.
- [20] Wilson TH, Wiseman G. The use of sacs of everted small intestine for the study of the transference of substances from the mucosal to the serosal surface. *J Physiol-London.* 1954;123(1):116-125.
- [21] Alam MA, Al-Jenoobi FI, Al-mohizea AM. Everted gut sac model as a tool in pharmaceutical research: limitations and applications. *J Pharm Pharmacol.* 2012;64(3):326-336.
- [22] Ussing HH, Zerahn K. Active transport of sodium as the source of electric current in the short-circuited isolated frog skin. *Acta Physiol Scand.* 1951;23(2-3):110-127.
- [23] Neirinckx E, Vervaet C, Michiels J, de Smet S, van den Broeck W, Remon JP, et al. Feasibility of the Ussing chamber technique for the determination of in vitro jejunal permeability of passively absorbed compounds in different animal species. *J Vet Pharmacol Ther.* 2011;34(3):290-297.
- [24] Russell WMS, Burch RL. The principles of humane experimental technique: Methuen; 1959.
- [25] Balls M. The principles of humane experimental technique: timeless insights and unheeded warnings. *Altex-Altern Anim Ex.* 2010;27(2):144-148.

- [26] EU. Directive 2003/15/EC of the European Parliament and of the Council of 27 February 2003 amending Council Directive 76/768/EEC on the approximation of the laws of the Member States relating to cosmetic products. *Official Journal of the European Union*. 2003;66:26-35.
- [27] Maubon N, Le Vee M, Fossati L, Audry M, Le Ferrec E, Bolze S, et al. Analysis of drug transporter expression in human intestinal Caco-2 cells by real-time PCR. *Fund Clin Pharmacol*. 2007;21(6):659-663.
- [28] Hayeshi R, Hilgendorf C, Artursson P, Augustijns P, Brodin B, Dehertogh P, et al. Comparison of drug transporter gene expression and functionality in Caco-2 cells from 10 different laboratories. *Eur J Pharm Sci*. 2008;35(5):383-396.
- [29] Anderson JM, Van Itallie CM, Peterson MD, Stevenson BR, Carew EA, Mooseker MS. ZO-1 mRNA and protein expression during tight junction assembly in Caco-2 cells. *J Cell Biol*. 1989;109(3):1047-1056.
- [30] Sun H, Chow ECY, Liu S, Du Y, Pang KS. The Caco-2 cell monolayer: usefulness and limitations. *Expert Opin Drug Met*. 2008;4(4):395-411.
- [31] Sambuy Y, Angelis I, Ranaldi G, Scarino ML, Stammati A, Zucco F. The Caco-2 cell line as a model of the intestinal barrier: influence of cell and culture-related factors on Caco-2 cell functional characteristics. *Cell Biol Toxicol*. 2005;21(1):1-26.
- [32] Sun D, Lennernas H, Welage LS, Barnett JL, Landowski CP, Foster D, et al. Comparison of human duodenum and Caco-2 gene expression profiles for 12,000 gene sequences tags and correlation with permeability of 26 drugs. *Pharm Res*. 2002;19(10):1400-1416.
- [33] Cummins CL, Mangravite LM, Benet LZ. Characterizing the expression of CYP3A4 and efflux transporters (P-gp, MRP1, and MRP2) in CYP3A4-transfected Caco-2 cells after induction with sodium butyrate and the phorbol ester 12-O-tetradecanoylphorbol-13-acetate. *Pharmaceut Res*. 2001;18(8):1102-1109.
- [34] Gres MC, Julian B, Bourrie M, Meunier V, Roques C, Berger M, et al. Correlation between oral drug absorption in humans, and apparent drug permeability in TC-7 cells, a human epithelial intestinal cell line: Comparison with the parental Caco-2 cell line. *Pharmaceut Res*. 1998;15(5):726-733.
- [35] Behrens I, Stenberg P, Artursson P, Kissel T. Transport of lipophilic drug molecules in a new mucus-secreting cell culture model based on HT29-MTX cells. *Pharmaceut Res*. 2001;18(8):1138-1145.
- [36] Mahler GJ, Shuler ML, Glahn RP. Characterization of Caco-2 and HT29-MTX cocultures in an in vitro digestion/cell culture model used to predict iron bioavailability. *J Nutr Biochem*. 2009;20(7):494-502.
- [37] Navabi N, McGuckin MA, Linden SK. Gastrointestinal cell lines form polarized epithelia with an adherent mucus layer when cultured in semi-wet interfaces with mechanical stimulation. *Plos One*. 2013;8(7):e68761.
- [38] Li N, Wang DD, Sui ZG, Qi XY, Ji LY, Wang XL, et al. Development of an improved three-dimensional in vitro intestinal mucosa model for drug absorption evaluation. *Tissue Eng Part C-Me*. 2013;19(9):708-719.
- [39] Pontier C, Pachot J, Botham R, Lenfant B, Arnaud P. HT29-MTX and Caco-2/TC7 monolayers as predictive models for human intestinal absorption: Role of the mucus layer. *J Pharm Sci*. 2001;90(10):1608-1619.
- [40] Sato T, Vries RG, Snippert HJ, van de Wetering M, Barker N, Stange DE, et al. Single Lgr5 stem cells build crypt-villus structures in vitro without a mesenchymal niche. *Nature*. 2009;459(7244):262-U147.
- [41] Jung P, Sato T, Merlos-Suarez A, Barriga FM, Iglesias M, Rossell D, et al. Isolation and in vitro expansion of human colonic stem cells. *Nat Med*. 2011;17(10):1225-1227.
- [42] Sato T, van Es JH, Snippert HJ, Stange DE, Vries RG, van den Born M, et al. Paneth cells constitute the niche for Lgr5 stem cells in intestinal crypts. *Nature*. 2011;469(7330):415-418.
- [43] Fatehullah A, Tan SH, Barker N. Organoids as an in vitro model of human development and disease. *Nat Cell Biol*. 2016;18(3):246-254.
- [44] van der Hee B, Loonen LMP, Taverne N, Taverne-Thiele JJ, Smidt H, Wells JM. Optimized procedures for generating an enhanced, near physiological 2D culture system from porcine intestinal organoids. *Stem Cell Res*. 2018;28:165-171.
- [45] Sidar B, Jenkins BR, Huang S, Spence JR, Walk ST, Wilking JN. Long-term flow through human intestinal organoids with the gut organoid flow chip (GOFlowChip). *Lab chip*. 2019;19(20):3552-3562.
- [46] Schweinlin M, Wilhelm S, Schwedhelm I, Hansmann J, Rietscher R, Jurowich C, et al. Development of an advanced primary human in vitro model of the small intestine. *Tissue Eng Part C-Me*. 2016;22(9):873-883.

- [47] Huh D, Matthews BD, Mammoto A, Montoya-Zavala M, Hsin HY, Ingber DE. Reconstituting organ-level lung functions on a chip. *Science*. 2010;328(5986):1662-1668.
- [48] Kimura H, Sakai Y, Fujii T. Organ/body-on-a-chip based on microfluidic technology for drug discovery. *Drug Metab Pharmacok*. 2018;33(1):43-48.
- [49] Ahadian S, Civitarese R, Bannerman D, Mohammadi MH, Lu R, Wang E, et al. Organ-on-a-chip platforms: A convergence of advanced materials, cells, and microscale technologies. *Adv Healthc Mater*. 2018;7(2).
- [50] Kim HJ, Huh D, Hamilton G, Ingber DE. Human gut-on-a-chip inhabited by microbial flora that experiences intestinal peristalsis-like motions and flow. *Lab chip*. 2012;12(12):2165-2174.
- [51] Giusti S, Sbrana T, La Marca M, Di Patria V, Martinucci V, Tirella A, et al. A novel dual-flow bioreactor simulates increased fluorescein permeability in epithelial tissue barriers. *Biotechnol J*. 2014;9(9):1175-1184.
- [52] Jalili-Firoozinezhad S, Gazzaniga FS, Calamari EL, Camacho DM, Fadel CW, Bein A, et al. A complex human gut microbiome cultured in an anaerobic intestine-on-a-chip. *Nat Biomed Eng*. 2019;3(7):520-531.
- [53] Kasendra M, Tovaglieri A, Sontheimer-Phelps A, Jalili-Firoozinezhad S, Bein A, Chalkiadaki A, et al. Development of a primary human small intestine-on-a-chip using biopsy-derived organoids. *Sci Rep-Uk*. 2018;8.
- [54] Mahler GJ, Esch MB, Glahn RP, Shuler ML. Characterization of a gastrointestinal tract microscale cell culture analog used to predict drug toxicity. *Biotechnol Bioeng*. 2009;104(1):193-205.
- [55] Esch MB, Mahler GJ, Stokor T, Shuler ML. Body-on-a-chip simulation with gastrointestinal tract and liver tissues suggests that ingested nanoparticles have the potential to cause liver injury. *Lab on a chip*. 2014;14(16):3081-3092.
- [56] Imura Y, Sato K, Yoshimura E. Micro Total Bioassay System for Ingested Substances: Assessment of intestinal absorption, hepatic metabolism, and bioactivity. *Anal chem*. 2010;82(24):9983-9988.
- [57] Berthier E, Young EW, Beebe D. Engineers are from PDMS-land, biologists are from polystyrenia. *Lab chip*. 2012;12(7):1224-1237.
- [58] van Meer BJ, de Vries H, Firth KSA, van Weerd J, Tertoolen LGJ, Karperien HBJ, et al. Small molecule absorption by PDMS in the context of drug response bioassays. *Biochem Bioph Res Co*. 2017;482(2):323-328.
- [59] Kulthong K, Duivenvoorde L, Mizera BZ, Rijkers D, ten Dam G, Oegema G, et al. Implementation of a dynamic intestinal gut-on-a-chip barrier model for transport studies of lipophilic dioxin congeners. *Rsc Adv*. 2018;8(57):32440-32453.
- [60] Henry OYF, Villenave R, Cronce MJ, Leineweber WD, Benz MA, Ingber DE. Organs-on-chips with integrated electrodes for trans-epithelial electrical resistance (TEER) measurements of human epithelial barrier function. *Lab chip*. 2017;17(13):2264-2271.
- [61] Lee DW, Ha SK, Choi I, Sung JH. 3D gut-liver chip with a PK model for prediction of first-pass metabolism. *Biomed Microdevices*. 2017;19(4).
- [62] Odijk M, van der Meer AD, Levner D, Kim HJ, van der Helm MW, Segerink LI, et al. Measuring direct current trans-epithelial electrical resistance in organ-on-a-chip microsystems. *Lab chip*. 2015;15(3):745-752.
- [63] Maoz BM, Herland A, Henry OYF, Leineweber WD, Yadid M, Doyle J, et al. Organs-on-Chips with combined multi-electrode array and transepithelial electrical resistance measurement capabilities. *Lab on a chip*. 2017;17(13):2294-2302.
- [64] Gao D, Liu HX, Lin JM, Wang YN, Jiang YY. Characterization of drug permeability in Caco-2 monolayers by mass spectrometry on a membrane-based microfluidic device. *Lab on a chip*. 2013;13(5):978-985.
- [65] Imura Y, Asano Y, Sato K, Yoshimura E. A Microfluidic system to evaluate intestinal absorption. *Anal Sci*. 2009;25(12):1403-1407.
- [66] Pocock K, Delon L, Bala V, Rao S, Priest C, Prestidge C, et al. Intestine-on-a-chip microfluidic model for efficient in vitro screening of oral chemotherapeutic uptake. *Acs Biomater Sci Eng*. 2017;3(6):951-959.
- [67] Shin W, Kim HJ. Intestinal barrier dysfunction orchestrates the onset of inflammatory host-microbiome cross-talk in a human gut inflammation-on-a-chip. *Proc Natl Acad Sci USA*. 2018;115(45):E10539-E10547.

- [68] Kim HJ, Li H, Collins JJ, Ingber DE. Contributions of microbiome and mechanical deformation to intestinal bacterial overgrowth and inflammation in a human gut-on-a-chip. *Proc Natl Acad Sci USA*. 2016;113(1):E7-E15.
- [69] Maschmeyer I, Lorenz AK, Schimek K, Hasenberg T, Ramme AP, Hubner J, et al. A four-organ-chip for interconnected long-term co-culture of human intestine, liver, skin and kidney equivalents. *Lab chip*. 2015;15(12):2688-2699.
- [70] Kimura H, Ikeda T, Nakayama H, Sakai Y, Fujii T. An on-chip small intestine-liver model for pharmacokinetic studies. *Jala-J Lab Autom*. 2015;20(3):265-273.
- [71] Shim KY, Lee D, Han J, Nguyen NT, Park S, Sung JH. Microfluidic gut-on-a-chip with three-dimensional villi structure. *Biomed Microdevices*. 2017;19(2).
- [72] Wang YL, Gunasekara DB, Reed MI, DiSalvo M, Bultman SJ, Sims CE, et al. A microengineered collagen scaffold for generating a polarized crypt-villus architecture of human small intestinal epithelium. *Biomaterials*. 2017;128:44-55.
- [73] Kulthong K, Duivenvoorde L, Sun H, Confederat S, Wu J, Spenkelink B, et al. Microfluidic chip for culturing intestinal epithelial cell layers: Characterization and comparison of drug transport between dynamic and static models. *Toxicol in Vitro*. 2020:104815.
- [74] Tan HY, Trier S, Rahbek UL, Dufva M, Kutter JP, Andresen TL. A multi-chamber microfluidic intestinal barrier model using Caco-2 cells for drug transport studies. *Plos One*. 2018;13(5).
- [75] Marin TM, Indolfo ND, Rocco SA, Basei FL, de Carvalho M, Goncalves KD, et al. Acetaminophen absorption and metabolism in an intestine/liver microphysiological system. *Chem-Biol Interact*. 2019;299:59-76.
- [76] Shah P, Fritz JV, Glaab E, Desai MS, Greenhalgh K, Frchet A, et al. A microfluidics-based in vitro model of the gastrointestinal human-microbe interface. *Nat Commun*. 2016;7:11535.
- [77] Trietsch SJ, Naumovska E, Kurek D, Setyawati MC, Vormann MK, Wilschut KJ, et al. Membrane-free culture and real-time barrier integrity assessment of perfused intestinal epithelium tubes. *Nat Commun*. 2017;8.
- [78] Ramadan Q, Jafarpoorchehab H, Huang C, Silacci P, Carrara S, Koklu G, et al. NutriChip: nutrition analysis meets microfluidics. *Lab chip*. 2013;13(2):196-203.
- [79] van der Helm MW, Henry OYF, Bein A, Hamkins-Indik T, Crounce MJ, Leineweber WD, et al. Non-invasive sensing of transepithelial barrier function and tissue differentiation in organs-on-chips using impedance spectroscopy. *Lab chip*. 2019;19(3):452-463.
- [80] de Hoffmann E, Stroobant V. *Mass Spectrometry: Principles and Applications*, 3rd Edition: Wiley-Interscience; 2007.
- [81] Yamashita M, Fenn JB. Electrospray ion-source - Another variation on the free-jet theme. *J Phys Chem-Us*. 1984;88(20):4451-4459.
- [82] Mann M, Meng CK, Fenn JB. Interpreting mass-spectra of multiply charged ions. *Anal chem*. 1989;61(15):1702-1708.
- [83] Fenn JB, Mann M, Meng CK, Wong SF, Whitehouse CM. Electrospray ionization for mass-spectrometry of large biomolecules. *Science*. 1989;246(4926):64-71.
- [84] Taylor G. Disintegration of water drops in electric field. *Proc R Soc Lon Ser-A*. 1964;280(1382):383-397.
- [85] Konermann L, Ahadi E, Rodriguez AD, Vahidi S. Unraveling the mechanism of electrospray ionization. *Anal chem*. 2013;85(1):2-9.
- [86] Smyth WF, Brooks P. A critical evaluation of high performance liquid chromatography-electrospray ionisation-mass spectrometry and capillary electrophoresis-electrospray-mass spectrometry for the detection and determination of small molecules of significance in clinical and forensic science. *Electrophoresis*. 2004;25(10-11):1413-1446.
- [87] Gallagher R, Dillon L, Grimsley A, Murphy J, Samuelsson K, Douce D. The application of a new microfluidic device for the simultaneous identification and quantitation of midazolam metabolites obtained from a single micro-litre of chimeric mice blood. *Rapid Commun Mass Sp*. 2014;28(11):1293-1302.
- [88] Peters R, Herrera-Rivera Z, Undas A, van der Lee M, Marvin H, Bouwmeester H, et al. Single particle ICP-MS combined with a data evaluation tool as a routine technique for the analysis of nanoparticles in complex matrices. *J Anal At Spectrom*. 2015;30(6):1274-1285.



Chapter 2

Online and *in situ* analysis of organs-on-a-chip

This chapter was published as:

M.J.C. Santbergen, M. van der Zande, H. Bouwmeester and M.W.F. Nielen. Online and *in situ* analysis of organs-on-a-chip. *TrAC Trends in Analytical Chemistry* (2019);115:138-146

Abstract

Organ-on-a-chip technology is used to study biological processes that involve multiple cell types and temporal changes like, homeostasis, metabolism of compounds and responses to chemical triggers. Main benefits of organ-on-a-chip systems include: improved mimicking of the *in vivo* situation, easy manipulation of the microenvironment and low reagent consumption. Exploiting the unique dynamic aspects of organ-on-a-chip technology, such as liquid flow, automated online measurement of parameters by sensors or online coupling to analytical equipment becomes feasible. Apart from the challenge to detect drug uptake and chemical changes in real-time with high resolution at the microscale, the biggest challenge, is the detection of the analyte of interest in cell culture medium, as this contains high amounts of salts, sugars and proteins required by the living cells. In this review online and *in situ* analytical techniques integrated with organ-on-a-chip devices are discussed with special emphasis on maintaining the biological relevance, achieving analytical compatibility, system integration and final applicability.

Keywords: organ-on-a-chip, mass spectrometry, online analysis, electrochemical sensor, optical detector

2.1 Introduction

Reliable experimental models that mimic the function of human organs play an important role in the development of novel drugs, assessment of the toxicological effect of chemicals and monitoring the health benefits of dietary compounds. Animal models capture complex processes like absorption, distribution, metabolism and excretion of chemicals, but do not always represent human physiology adequately due to important differences between species [1]. Furthermore, worldwide scientific and socio-political organizations strive to reduce, refine and replace the use of animals for research purposes [2, 3]. Standardized, *in vitro* cell culture assays are currently used in early phases of drug development, food research and hazard identification of chemicals [4, 5]. However, these *in vitro* models lack organ specific functionality, hampering mechanism-based research needed for novel drug development and next generation risk assessment.

Recent advances in microchip- and bio-engineering enabled the development of organ-on-a-chip models, an *in vitro* cell culture model that includes dynamic physical and functional features of a human organ [6]. In recent years, several organ-on-a-chip models have been developed, for brain- [7, 8], lung- [9], heart- [10], kidney- [11], liver [12], skin [13], gut [14, 15] and even models that comprise multiple organ systems [16]. To establish an organ-on-a-chip model, cells are cultured within a microfluidic device simulating a tissue specific physical microenvironment. For example, Kim and colleagues have developed a human gut-on-a-chip, in which intestinal cells were grown on a permeable membrane. Interestingly, upon exposure of these cells to mechanical forces, simulating peristaltic motion, and a liquid flow, resulting in physiological relevant fluid shear stresses, tissue functionality closer resembled *in vivo* responses [14]. The permeable membrane separates the microfluidic channel in a top and bottom compartment which makes this model well suited for uptake studies of dietary, pharmaceutical and chemical compounds. Often multiple cell types are combined in organ-on-a-chip models, like endothelial cells [17], immune cells [18] and components of the intestinal microbiome [19], allowing mechanistic studies of more complex tissue interactions. This can be taken a step further by growing primary human cells, adults stem cells or

induced pluripotent stem cells in the chip, allowing for personalized medicine testing using organ-on-a-chip technology [20].

The main scientific and technological advantages of organ-on-a-chip technology are the ability to spatiotemporally control the microenvironment and the low reagent consumption. Exploiting the unique dynamic aspects of organ-on-a-chip technology, automated online measurement of chemicals by sensors or online coupling to analytical equipment is becoming realistic. However, apart from the technical challenge to detect compounds and metabolites at very low concentrations in such miniaturized formats, the analytes will be present in cell culture medium which contains very high levels of sugar, salts, amino acids and proteins (table 2.1) that may interfere with the measurement.

Table 2.1: General composition of cell culture medium

Compound	Concentration (mg/L)	Compound	Concentration (mg/L)
Calcium Chloride	200	L-Threonine	95.2
Dextrose	4500	L-Tryptophan	16
Ferric Nitrate	0.1	L-Valine	93.6
Magnesium Sulphate	97.7	Vitamin B5	4
Potassium Chloride	400	Choline Chloride	4
Sodium Bicarbonate	3700	Folic Acid	4
Sodium Chloride	6400	I-Inositol	7
L-Arginine	84	Nicotinamide	4
L-Glutamine	584	Pyridoxine	4
Glycine	30	Vitamin B2	0.4
L-Histidine	42	Vitamin B1	4
L-Isoleucine	104.8	Phenol Red	15
L-Leucine	104.8	Pyruvic Acid Sodium Salt	110
L-Lysine	146.2	L-Tyrosine Disodium Salt	103.7
L-Methionine	30	L-Cystine 2HCl	62.5
L-Phenylalanine	66	Sodium Phosphate	108.6
L-Serine	42	Added Protein/Serum	variable

In this review, we discuss various online and *in situ* techniques to analyse organ-on-a-chip devices, excluding end-point measurements that require fixation or destruction of the cells. Here, online is defined as a direct connection between the organ-on-a-chip device and the detection method requiring no user involvement. Furthermore, *in situ* is defined as in close proximity to the cells. The focus is on the analysis of mammalian cell cultures rather than organ slices

or single cell analysis, which have been reviewed recently [21]. Literature from 2000 till 2019 has been searched using the databases from PubMed, Scholar, Scopus and Web of Science with the following keywords: organ-on-a-chip (and organ specific variations), mass spectrometry, sensor, optical detection, *in situ* sensing, coupling, real-time and online analysis. The first part of the review will mainly focus on the electrochemical monitoring of the microenvironment in the organ-on-a-chip device to confirm proper biological functionality of the model, discussing cell layer integrity, mitochondrial function, extracellular oxygen and acidification. In the second part, the integration of analytical techniques with organ-on-a-chip devices will be addressed, focussing on optical detection, electrochemical sensing and mass spectrometric analysis of target molecules.

2.2 Electrochemical monitoring of the microenvironment of organ-on-a-chip systems to assure biological integrity

Dynamic *in vitro* models like organ-on-a-chip models allow for the control of the cellular environment in great detail. However, this is only relevant if the local microenvironment can be strictly monitored [22]. Some important parameters to monitor are cell layer integrity, mitochondrial function, extracellular oxygen and acidification as they influence major chemical and biological processes in the cellular model (Fig. 2.1). A fast and accurate detection of these parameters is a prerequisite for fast control (feedback) of the microenvironment to correct for unwanted derivations from the normal situation. Active control of the microenvironment has been extensively reviewed for organ-on-a-chip purposes [23-25]. In the following part we will discuss the integration of electrochemical sensors for organ-on-a-chip applications to measure: cell layer integrity, mitochondrial function, extracellular oxygen and acidification. Kieninger and colleagues [26] recently reviewed microsensors in static 2D and 3D cell cultures. Therefore, here we focus on the integration of sensors in dynamic cell based microfluidic chip systems.

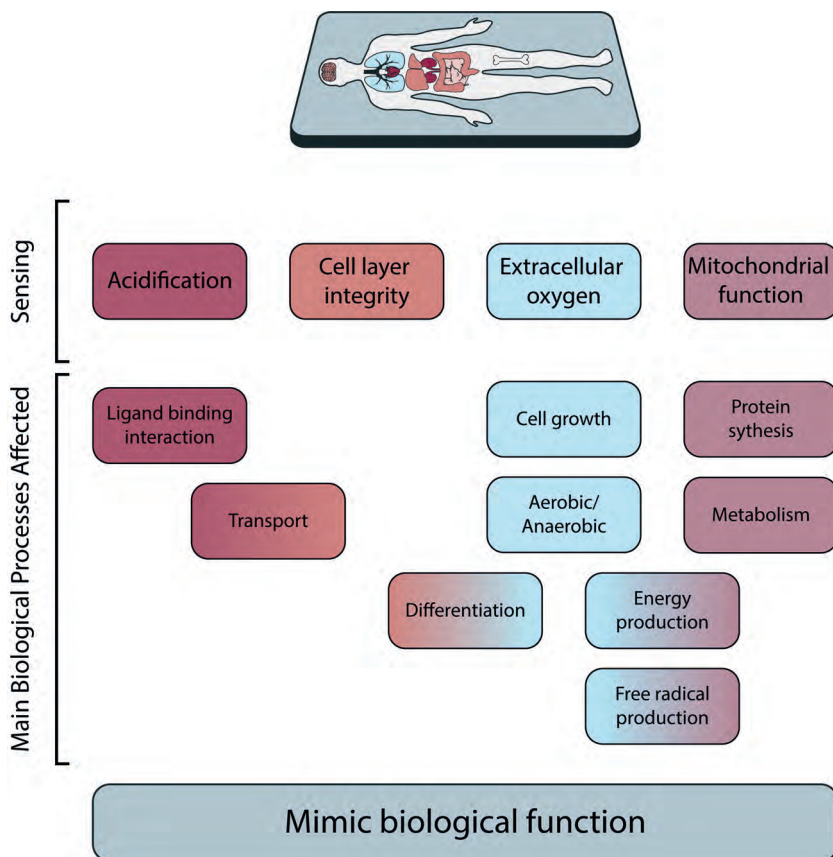


Figure 2.1: Simplified representation of sensing parameters in relation to cell function.

2.2.1 Cell layer integrity

Transepithelial electrical resistance (TEER) is a measure for the barrier integrity of epithelial and endothelial cell layers [27]. In a classical experimental setup, TEER measurements are performed before and after exposure to compounds as barrier integrity quality control. Alternatively, TEER data is used as read out of diseased “leaky” models, or as a marker of toxicity upon exposure to a compound. TEER measurements are non-invasive, label-free and performed in real-time. In the conventional *in vitro* transwell system (Fig. 2.2), TEER is measured by manually submerging (silver) electrodes in the top and bottom compartment of the transwell insert. The electric resistance is measured over the cell layer, which increases with an increasing tightness of the cell layer [27]. However, manually submerging these electrodes in the confined closed areas in organ-on-a-chip devices is rather tricky. The cell culture area in microfluidic

devices is generally much smaller compared to transwell systems which makes positioning of the electrodes in close proximity of the cells, crucial for a stable measurement. Attachment of the electrodes to the device itself would eliminate the noise generated by the movement of the electrode by the user.

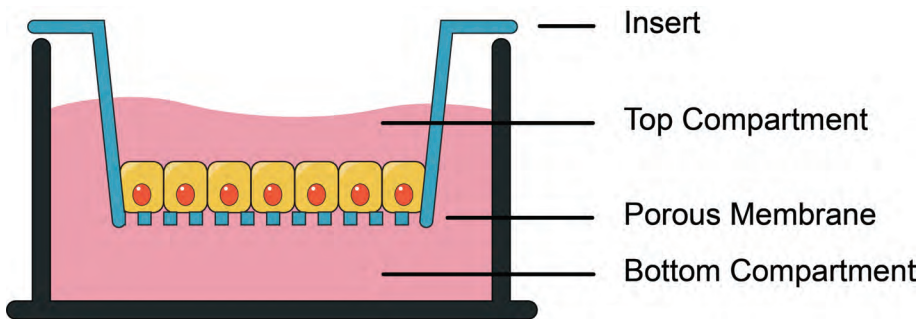


Figure 2.2: Conventional transwell insert

TEER measurement electrodes have been incorporated in organ-on-a-chip models like the blood-brain-barrier- [7, 8], gut-, lung- [28, 29], heart- [30] and skin-on-a-chip [13]. For example, a chip consisting of two polydimethylsiloxane (PDMS) channels, separated by a membrane, was closed on either side by glass slides. On these glass slides, 25 nm thick transparent gold electrodes were sputter-coated along the full length of the channel and attached to thin copper wires, which were connected to a multimeter for TEER analysis [28]. Currently, TEER electrodes are not attached to flexible surfaces that are used for stretching the cell layer, for instance in lung-, or gut-on-a-chip systems. Such sensor integration for flexible surfaces has been shown for other purposes [31, 32]. Possible solutions for TEER analysis lie in further miniaturization of the electrodes and synthesizing the electrode from a flexible material. Moving away from static transwell barrier models, raises the question which TEER values in organ-on-a-chip devices are considered as indicative of a mature monolayer barrier. Data from literature has shown that TEER values in microfluidic chips are rather different compared to values measured in transwells using the same cell type [27]. It has been reported that this is most likely due to different geometries and materials of microfluidic chips, compared to a traditional transwell system rather than being a result of biological differences in chip systems. To account for these differences a mathematical model was developed [33]. In this model, several parameters like channel height and width, membrane length,

conductivity of the cell culture medium and resistance of the membrane material are taken into account [33]. Clearly, integration of electrodes for TEER measurements adds to the complexity of fabrication and use of organ-on-a-chip devices resulting in higher costs. But barrier models on chip greatly benefit from the incorporation of TEER electrodes to be able to reliably measure the integrity of epithelial and endothelial cell layers.

Electric cell substrate impedance sensing (ECIS) is another sensing technique for cellular monolayer integrity that is integrated in organs-on-a-chip devices. This method is not only used to assess barrier integrity, but also is a well-known non-invasive method to measure cytotoxicity, cell proliferation or wound healing properties [34]. With ECIS, cells are grown on a gold electrode, the impedance of the electrode is measured at one or more frequencies versus time. As cell membranes have insulating properties the more cells that are present, the higher the impedance measurement. ECIS has successfully been integrated in different types of organ-on-a-chip models like a hydrogel based model [35] and PDMS based models [36, 37].

A general problem for all types of *in situ* electrochemical sensors is the continuous exposure to cell culture medium, which can result in fouling of the electrode. Frequent cleaning, shorter experiments or the incorporation of antifouling layers would minimize the effect of fouling on the electrode [38].

2.2.2 Mitochondrial function

Mitochondria are the powerhouses of the cell, producing adenosine triphosphate through the respiration chain. Monitoring mitochondrial activity is essential for evaluating the energy demand of the cell and is commonly used to monitor the viability of cells. Measurement of glucose and lactate levels in the surrounding cell culture medium is a frequently used procedure to analyse mitochondrial activity in organ-on-a-chip models [39-42]. The production of lactate, parallel to the decline of glucose through glycolysis, is a sign of mitochondrial dysfunction. Bavli and colleagues measured glucose and lactate levels in a liver-on-a-chip device, in which a sensor unit was attached downstream of the microfluidic device [43]. The sensor included membrane embedded glucose and lactate oxidase and platinum electrodes, which were stable for 24 hours of measurements. Every hour, cell culture medium from the

liver chip was introduced to the sensor unit where both glucose and lactate were oxidized under the formation of hydrogen peroxide (H_2O_2), the latter being measured using the platinum electrode. The disadvantage of this sensor is that as a result of the production of H_2O_2 and the use of oxygen (O_2) for this process, the sensor unit must be separated from the cells [43]. In addition, the measurements are not continuous and fouling issues apply again. Fouling issues are circumvented by shorter experiments, which is not ideal for chronic biological experiments. Nevertheless, monitoring glucose and lactate levels in organ-on-a-chip device is important for the evaluation of proper mitochondrial activity.

2.2.3 Extracellular oxygen

Oxygen is crucial for the conversion of nutrients into energy within the cell. Reduced levels of oxygen result in anaerobic cell respiration, causing less efficient energy transfer, which can only be sustained for a limited time. During cellular respiration carbon dioxide (CO_2) is produced, resulting in the acidification of the cell culture medium if not properly buffered. Traditional in vitro cell culture models are grown in a culture plate or flask and are placed inside an incubator where CO_2 levels are controlled. Culture plates and flasks are open systems and O_2 and CO_2 exchange takes place inside the incubator [44]. Gas exchange is rather different in organ-on-a-chips, as these are commonly closed systems. Aspects to consider are chip material, smaller media-to-cell volume and ambient environment. Nowadays, most microfluidic chips are made of PDMS, which has a high gas diffusion coefficient. This allows for sufficient exchange of O_2 and CO_2 , when the PDMS layer is thin enough ($\sim 100 \mu m$) [45].

Alternative microfluidic chip materials are being studied because of some important disadvantages of PDMS from a biological perspective. A well-known disadvantage of PDMS is the high likelihood of absorption of hydrophobic compounds to PDMS, even though several coating procedures have been proposed to avoid this [46]. Much less-known, but very relevant in terms of potentially limiting the online coupling to sensitive analytical detection systems is the leaching of uncross-linked oligomers and polymer additives into the media [46]. Several other materials like, glass [47] and polycarbonate [48] are used for chip fabrication, but are less permeable to gasses. All these

factors influence O_2 and CO_2 exchange in organ-on-a-chip devices, which is why integration of oxygen sensors in chip systems is of great importance. Incorporation of oxygen sensors also allows for studying the respiration chain by precise monitoring of energy production. Lastly, the incorporation of oxygen sensors is pivotal for the development of advanced gut-on-a-chip models. In these models tight monitoring (and adjustments) of low oxygen levels are required to maintain anaerobic growth conditions needed for the inclusion of a human relevant intestinal microbiome [19, 49].

The most often applied approach for sensing oxygen is by the use of metal electrodes, like silver, gold or platinum. Oxygen levels are measured based on the amperometric reduction of dissolved oxygen [12, 39, 40, 47, 50, 51]. A major disadvantage of using metal electrodes in microfluidic systems however is the reduction of O_2 to H_2O_2 during the measurement. This makes the sensor unsuitable for placement in close contact with the cells. To sum up, oxygen levels in organ-on-a-chip devices can be variable depending on chip material and ambient environment, therefore incorporation of oxygen sensors on chip is crucial for maintaining a biological relevant microenvironment.

2.2.4 Acidification

Mammalian cells function best at a neutral pH. As mentioned in paragraph 2.2.3, the improper exchange of CO_2 , can result in an undesirable acidification of the extracellular environment. To keep track of the cellular environment, most cell culture media contain phenol red, as a pH indicator. However, due to the small volumes in organ-on-a-chip devices colorimetric changes are difficult to observe visually. Integration of pH sensors in organ-on-a-chip systems would allow for direct feedback and control measurements to prevent undesirable pH fluctuations. Zhang and colleagues described a liver-heart chip model with an incorporated pH sensor that detected changes in absorbance of phenol red [52]. More widespread are silicon based chemical sensors, like the light-addressable potentiometric sensors (LAPS) [53, 54]. LAPS in conventional cell culture applications are constructed of silicon chips that are placed at the bottom of a cell culture chamber (Fig. 2.3).

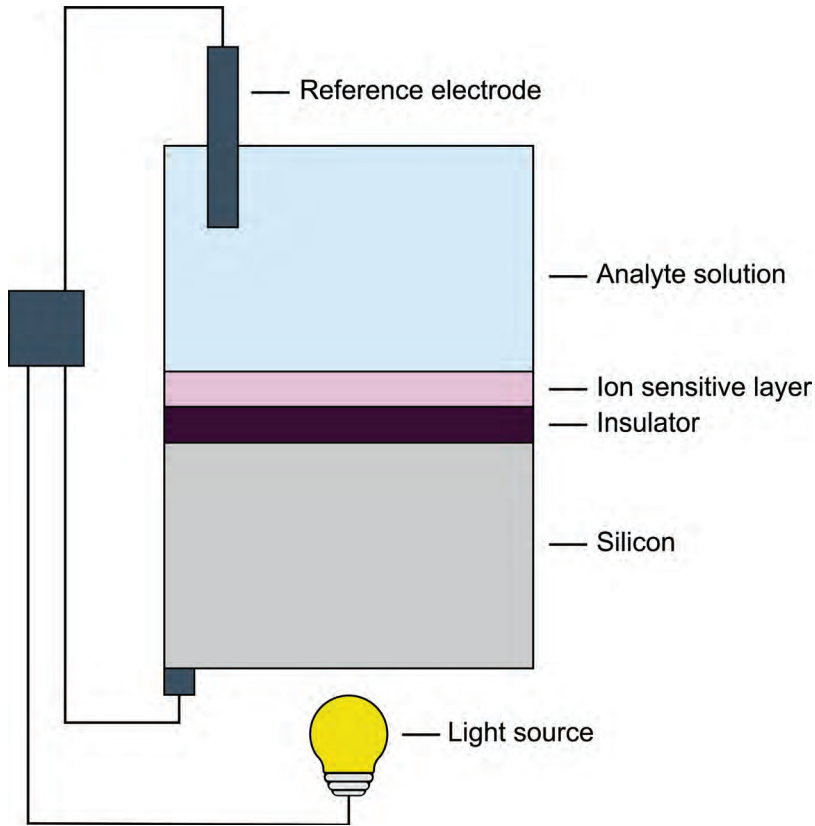


Figure 2.3: Schematic representation of LAPS

The silicon chip has an insulating layer and an ion sensitive layer consisting of silicon oxide and silicon nitride. The ion sensitive layer interacts with the protons within the cell culture medium, affecting the surface potential of the layer. The surface charge of the ion sensitive layer, together with an applied voltage to the chip and pulsed infrared light produces a photocurrent. Changes in pH can either be measured by changes in photocurrent or applied voltage.

Ion-sensitive field-effect transistor (ISFET) is another silicon based electrochemical sensor used in organ-on-a-chip devices to detect pH changes [55-58]. An ISFET sensor consists of a source, drain, gate and reference electrode. Between the source and drain electrode is the gate, which is covered by a pH sensitive insulator material, mostly silicon nitride, aluminium oxide, or tantalum oxide. A current runs through the source and drain electrode and the resulting

potential on the gate is influenced by the pH of the solution. Even though both LAPS and ISFET are sensitive pH sensors, LAPS sensors are preferred because of the simple design and low production costs [59]. As mentioned before, fouling of the electrode has a major effect on the sensitivity of the electrode. In current literature LAPS and ISFET sensors are regularly cleaned, sterilized and used for short experiments to mitigate the impact of fouling.

In conclusion, many different integrated electrochemical sensors have been developed to monitor the cellular microenvironment in organ-on-a-chip devices over the past couple of years. Optical sensing techniques, like photoacoustic imaging and luminescence detection have been or have the potential to be incorporated on chip as well, however they require a dye or labelled substrate for visualisation [60-62]. Electrochemical sensors do not have this drawback, which explains the more widespread use of these type of sensors. Ideally, all parameter measurements, pH, TEER, glucose, lactate and oxygen, are combined to establish a broader picture of cell functioning in homeostasis and under stress. Future work should concentrate on the combination of different robust sensors in one user friendly format to study various biological processes within organ-on-a-chip devices.

2.3 Integration of analytical techniques for target substance detection

Organ-on-a-chip devices have been integrated with multiple analytical techniques, like optical spectroscopy, electrochemical sensors and mass spectrometry. These integrations widen the applicability of organ-on-a-chip models for drug uptake and dietary studies and unravelling biological processes. In the following part we will discuss the different integrations and the major challenges that relate to sensitivity and selectivity of detection in organ-on-a-chip systems in the highly complex and abundant cell culture medium (table 2.1).

2.3.1 Optical spectroscopy detection of target analytes

Optical detection instruments are abundant in most laboratories and ultraviolet visible (UV-Vis) spectroscopy, infrared (IR) spectroscopy, luminescence, and

microscopy versions thereof, have been applied for the detection of a wide range of analytes in organ-on-a-chip devices. Integration of a spectrophotometric detection system in an organ-on-a-chip model has been shown in a membrane based kidney-on-a-chip. The chip was connected with two flow channels, one for either side of the membrane. Each channel was directed through quartz cuvettes allowing real-time analysis of caffeine and vitamin B12 permeability [11, 63]. Another label-free option reported is IR spectroscopy. The main problem with IR and organ-on-a-chip technology is the liquid barrier on top of the cells since IR absorption by water will interfere with the signal. However, Loutharback and colleagues came up with a solution for this problem [48]. They created a chip containing two channels, separated by a gold coated porous membrane on which neuronal cells were grown. During measurements little to no liquid was present on top of the cells, but a flow of 100 nL/min was maintained to the lower channel of the device to still provide the cells with the right nutrients and prevent them from drying. Different regions as a function of cell stress could be visualised within the cell culture on the basis of the peak intensity of vibrational modes of C-O-C, C-O-P and C-O stretching of glycogen/glycoprotein and they demonstrated continuous measurements for up till a week [48]. Despite this achievement, the application seems more suited for skin- or lung-on-a-chip that grow at the air liquid interface.

Optical biosensors are popular techniques to detect target peptides and proteins in organ-on-a-chip models. Two types of biorecognition elements are found in organ-on-a-chip integrations namely, aptamers like deoxyribonucleic acid or ribonucleic acid [64, 65], or antibodies [52, 66]. In organ-on-a-chip models, the biggest concern for the applicability of integrated biosensors is the overabundance of nonspecific proteins compared with the trace levels of the analyte of interest. A nanoplasmonic platform that employs an antibody based biosensor was integrated with an organ-on-a-chip to quantitatively determine cellular cytokine release in real-time and label-free [67]. The platform consisted of two parts: a cellular compartment and an optical detection compartment where secreted cytokines were detected (Fig. 2.4). The optical detection module contained three inline nanohole arrays, one as negative control and the other two functionalized with a specific antibody against the cytokine of interest. A beam of broadband light was directed onto the nanohole array and the transmitted light was measured by a spectrometer. Binding of the cytokine

to the antibody caused a detectable wavelength shift of the transmitted light [67]. Besides antibodies, aptamer based biosensors are also used in organ-on-a-chip devices. Claimed advantages of aptamers compared to antibodies are: better binding capacities to any given target and highly reproducible animal free production methods with high purity [68]. However, the presence of deoxyribonuclease and ribonuclease enzymes in biological samples makes aptamers susceptible to degradation. An example of an aptamer biosensor is the integrated vascular endothelial growth factor (VEGF) aptamer biosensor for cervical cancer cells on chip. The biosensor consisted of a functional nucleic acid, designed to bind to VEGF and was immobilized onto the surface of the chip. The aptamer was coupled to a G-quadruplex DNzyme, acid, hemin and peroxide system which upon binding of VEGF catalysed the reaction resulting in a blue-green colour that was analysed by Vis spectroscopy [65].

Fluorescent dyes have been used to visualize target molecules in an organ-on-a-chip by fluorescence microscopy [8, 19, 47]. Alternatively, fibre optics [69] and even smartphones [70] have been exploited as miniaturized fluorescent detectors for organ-on-a-chip devices. The fluorescence microscope developed by Cho et al. [70] consisted of three white light emitting diodes, two optical filters and an objective lens. Images were taken with the smartphone and analysed separately on a computer. They demonstrated its use in combination with a kidney-on-a-chip device. The cells on the chip were exposed to a specific kidney toxin, which induced the release of a brush border enzyme. Subsequently, an antibody, conjugated to a fluorescent nanoparticle label, bound to the enzyme and the fluorescence signal was detected using the smartphone microscope. Using a smartphone as a read-out simplifies and decreases the cost of analysis, however it may also compromise the sensitivity in comparison to a conventional fluorescence microscope.

Integration of optical detection methods with organ-on-a-chip devices is one of the few *in situ* techniques that allows for long term analysis, because cells are generally not disrupted during the measurements. However, some integrative techniques require a labelled substrate to visualize the compound in the cell culture matrix.

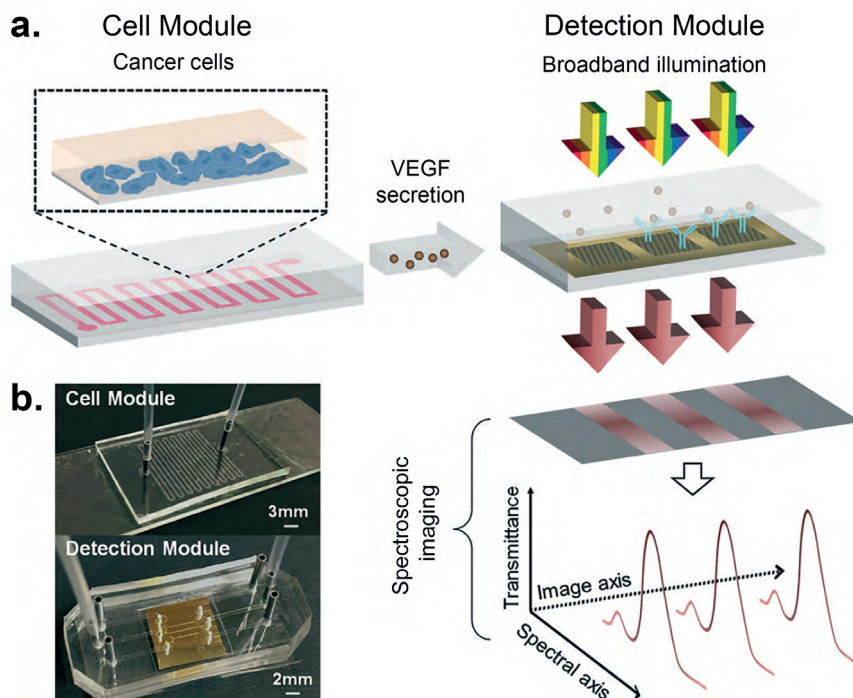


Figure 2.4: a) Schematic representation of a microfluidic integrated biosensor for real-time cytokine analysis. b) Photo of cell culture module and detection module. Reproduced from Ref. [67] with permission of The Royal Society of Chemistry.

2.3.2 Electrochemical detection of target analytes

Amperometric models for the detection of target analytes have been proposed in several organ-on-a-chip systems [71, 72], showing an alternative application of electrochemical sensors next to the previously discussed application as tools to monitor the extracellular microenvironment. An example of an electrochemical sensor based on amperometric reduction was described by Li et al. [72]. They designed a PDMS microchip with an integrated electrochemical sensor measuring a redox reaction at the surface of a platinum electrode at the bottom of the channel. In the chip, immobilized neuronal cells were grown and subsequently stimulated with calcium ions to induce the release of dopamine. Using the platinum electrode, the oxidation and release of catecholamine (dopamine/epinephrine) could be measured in the micromolar range. The disadvantage of this method is that no distinction between dopamine and epinephrine could be made, since they have the same redox potential [72].

Another method described is an impedance spectroscopy antibody biosensor platform with a built-in regeneration function to prevent sensor saturation [66]. A series of on chip pressure driven microfluidic valves allowed for the regeneration of the sensor and detection without manual interference, thus decreasing the possibility of human error. Regeneration of the sensor was established by flowing a cleaning solution over the chip at a high speed and an electrical sweep. To demonstrate robustness of the method they compared the results from the impedance spectroscopy sensor with a conventional enzyme linked immunosorbent assay which showed similar sensitivity [66]. The biggest challenge for electrochemical detection is fouling of the electrode surface, decreasing the overall sensitivity and robustness of the sensor. The integration of cleaning steps or a selective antifouling layer would greatly improve the usability of electrochemical detection of target analytes in microfluidic chips [38].

2.3.3 Mass Spectrometric detection of target analytes

Organ-on-a-chip devices accommodate minimal amounts of analytes in a highly complex cellular environment, which puts high demands on the analytical instrumentation in terms of sensitivity and sample preparation. Mass spectrometry (MS) is a label-free and multi analyte detection technique that meets these challenges provided that ion suppression due to the cellular environment can be overcome. The integration of a microfluidic chip to MS has been reviewed recently [73-76]; here we focus on the online analysis of organ-on-a-chip models with MS.

2.3.3.1 Electrospray ionization MS

Electrospray ionization (ESI) is ideal for interfacing with dynamic organ-on-a-chip devices, as ionization of target compounds occurs in the liquid phase. Clearly, a major challenge is the complex mixture with high concentrations of sugars, salts and proteins in the cell culture medium (table 2.1) causing severe ion suppression thereby compromising the detection of the analyte of interest. A solution is the integration of a solid phase extraction (SPE) column, either incorporated on the same chip [77] or coupled to the chip [78]. On chip SPE coupled to ESI-MS has been studied by the group of Jin-Ming Lin [77, 79-85]. For example, a microfluidic system was developed to characterize curcumin permeability across an intestinal epithelial layer (Fig. 2.5). The system consists

of two parts, part one a membrane based cell culture chip, where intestinal cells were cultured on a permeable membrane separating a top and bottom chamber. The bottom chamber of the membrane was connected to the second part of the system, a chip containing a micro-SPE column. The SPE column captured curcumin that permeated through the cell layer and was washed offline with a water-methanol mixture to remove any unwanted sugars and salts. Then, the micro-SPE chip was connected to the ESI-MS via fused silica capillaries for the detection of curcumin [77]. A major drawback of this system is the offline washing step of the SPE column which compromises the overall online nature and time resolution of the system. Similarly, the group of Jin-Ming Lin was able to couple several other organs-on-a-chip systems to ESI-MS, such as neurons-[81, 82, 84], liver-[79, 83, 85] and lung-on-a-chip [80].

Others used separate SPE columns coupled to their chip to capture their analyte of interest. For instance, Dugan et al. [86] developed a chip to analyse the release of non-esterified fatty acids from fat tissue cells. An on-chip sample loop collected the released fatty acids and was subsequently eluted by an on-chip automated valve system to a separate SPE column [86]. Another exciting example is a system using a series of three switching valves to measure the effect of cocaine on cells of the immune system in near real-time. This system included two loops for continuous sample collection and SPE columns for desalting [78]. The advantage of sample preparation in a column isolated from the chip is that commercially SPE columns can be applied and elution and wash steps can be easily automated.

Maintaining a stable cell temperature of 37°C and controlling O₂/CO₂ gas flows together with online analysis is a serious challenge of organ-on-a-chip systems integrated with large footprint analytical equipment, such as MS. In table 2.2 an overview is given of organ-on-a-chip systems hyphenated with mass spectrometry detection evaluating the biological relevance and online nature of the systems. From this table it is clearly shown that either the biological relevance of the organ-on-a-chip mimic or the online analysis of the system is significantly compromised.

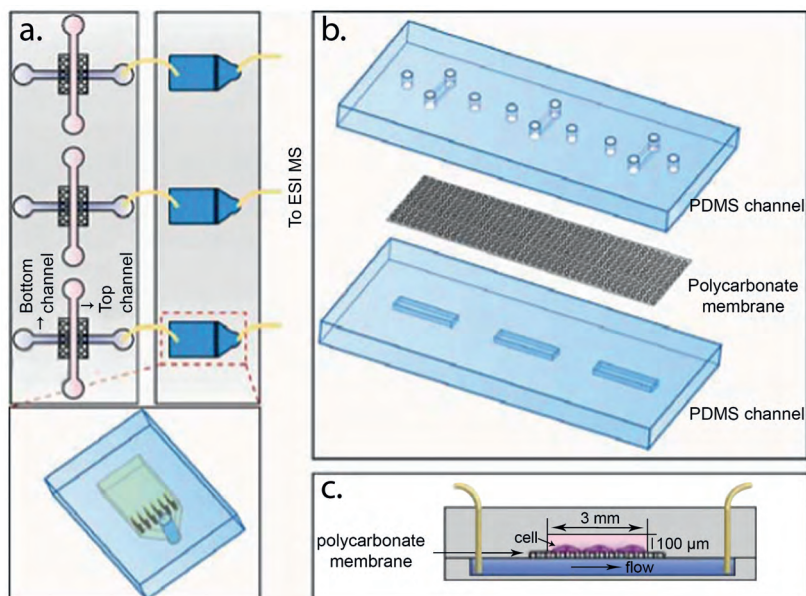


Figure 2.5: a) Schematic representation of microfluidic device for cell culture and ESI-MS detection. b) The three layers of the membrane based cell culture chip. c) Side view cell culture chip, not to scale. Reproduced from Ref. [77] with permission of The Royal Society of Chemistry.

2.3.3.2 Ambient ionization MS

Ambient ionization MS was pioneered by Cooks and Cody by the invention of desorption electrospray ionization [87] and direct analysis in real-time [88]. Nowadays, a plethora of related designs have become available [89]. Paper spray ionization (PSI) is an ambient ionization technique where the sample is deposited on a triangular piece of paper in front of the MS entrance [90]. The main advantages of using paper includes low costs, wide availability and the possibility of chemical modification of the paper [91]. Two types of integrations are reported in literature coupling PSI to organ-on-a-chip systems. The first type is a microdialysis PSI-MS system which monitored the glucose concentration in the media [92]. Human liver cells were stimulated with insulin and the decrease in glucose levels within the system was followed [92]. However, the cells were grown in a static petri dish, opposed to a dynamic microfluidic system. Later the same group developed a four channel microfluidic chip in which they monitored lactate production of normal cells versus tumour cells [93]. The second type of integration is a system in which cells were directly grown on the paper substrate. However, conventional chromatography paper for cell culture

has its drawbacks, mainly in mechanically supporting the cells [94]. Both glass and polycarbonate substrates have been used to provide a scaffold for cell culture and direct PSI-MS analysis [95, 96]. However, in both cases, cells are lysed by isopropanol for PSI-MS analysis making it an end-point measurement. PSI is in theory a well suited method for fast screening of a cell-based microfluidic chip. Nevertheless, temperature and CO₂ control remain a big challenge for any method operated in an open ambient environment.

2.3.3.3 Other MS options

The majority of MS coupling methods to organs-on-a-chip considered the coupling to ESI-MS and PSI-MS rather than other ionization techniques. Two alternative types of ionization techniques that would be beneficial in the field of organ-on-a-chip are inductively coupled plasma (ICP) MS and matrix assisted laser desorption/ionization (MALDI) MS. ICP-MS would be beneficial for the analysis of metal ions or particles frequently present in food products, as an additive, or for pharmaceutical purposes [97]. MALDI-MS imaging has been used for the analysis of neuropeptide release from *Aplysia* neuronal cells on chip [98], but further studies are limited.

Organ-on-a-chip models have been integrated with several different analytical techniques for the detection of target analytes, all dealing with issues of sensitivity and selectivity. The most promising integration in terms of sensitivity, selectivity and multi analyte detection seems to be ESI-MS with the integration of a SPE column to get rid of the interference of the cell culture medium. However, when truly *in situ* analysis is required for a specific biological application, optical or electrochemical sensing techniques provide a simpler coupling solution.

Table 2.2: Overview of organ-on-a-chip systems hyphenated with mass spectrometry. Biological relevance and full online analysis were evaluated.

Detection Method	Cell Model	Biological relevance			Fully Online Analysis (yes/no)	Analyte	Ref
		Temp	CO ₂	Cell Viability			
ESI-MS	Caco-2 cells	+	+	+	no	Curcumin	[77]
ESI-MS	Jurkat cells	+	+	+	yes	Cocaine	[78]
ESI-MS	A549 cells	+	+	+	no	Vitamin E	[80]
ESI-MS	PC12 cells	+	+	+	no	Glutamate	[81]
ESI-MS	PC12 and GH3 cells	+	+	-	no	Growth hormone	[82]
ESI-MS	HepG2 cells	+	+	+	no	Acetaminophen	[83]
ESI-MS	293 and L-02 cells	-	-	+	no	Epinephrine and glucose	[84]
ESI-MS	HepG2 and MCF-7 cells	+	+	+	no	Capecitabine metabolites	[85]
ESI-MS	3T3-L1	-	-	-	yes	Non-esterified fatty acids	[86]
PSI-MS	HepG2 and L-02 cells	+	+	n.a.	yes	Glucose	[92]
PSI-MS	A549, L-02 and MCF-7 cells	+	+	n.r.	yes	Lactate	[93]

n.r. = not reported, n.a. = not applicable

2.4 Conclusions

Recent advances in integrated analytical techniques with organ-on-a-chip devices were discussed. Main advantages of these integrations are reduction of (bio)reagents, automation allowing unattended prolonged experiments and real-time analytical data for feedback on nutrient composition and detection of target analytes and metabolites thereof. Organ-on-a-chip devices are living cellular systems, therefore careful real-time monitoring of the functioning of the cells is crucial to ensure the biological relevance of the micro tissue. Main challenges for integrated analytical techniques comprise sensitivity, selectivity, robustness, user friendliness and multi analyte detection. *In situ* optical and/or electrochemical sensors are easy to use analytical devices and small enough to be placed inside a gas and temperature controlled incubator. Issues that remain to be solved however are, lower sensitivity compared to conventional benchtop analytical equipment, susceptibility to fouling and measurement of only one (or a limited number) of parameters at a time. Future analytical solutions for online organ-on-a-chip systems can be found in the design of multisensor platforms. Surfaces of such multisensors should have tailor made antifouling layers to mitigate nonspecific binding and the sensors should provide active feedback control loops, thus ensuring a stable microenvironment for biological relevant *in vitro* experiments.

Online coupling to high-end instrumentation such as a mass spectrometer is another crucial future development. That would enable the semi-continuous identification and quantification of multiple target analytes, and (un)expected metabolites thereof, in a small sample volume with high sensitivity. Continuous online mass spectrometric detection of organ-on-a-chip systems is currently not feasible, due to the presence of high levels of interfering substances in the cell culture medium that require the incorporation of SPE columns and a wash step to prevent ionization suppression. In recent interfacing designs, the organ-on-a-chip device is generally placed outside the gas and temperature controlled incubator to allow interfacing with a mass spectrometer. Obviously, this is still a serious drawback as it compromises a biological accurate environment.

Organ-on-a-chip technology is moving towards replacing animal models for drug development trials and may, in the far future, even function as a diagnostic tool for personalized medicine. Analytical techniques connected or included in the organ-on-a-chip must enable these developments. Therefore, future advancements should aim to create total analysis systems for organ-on-a-chip devices (Fig. 2.6), ultimately making the systems cheaper, more robust and more user friendly. To achieve such a system future work should consider the following aspects and solve current problems. Firstly, advanced self-regulating organ-on-a-chip systems having sensor-based active feedback control regulating nutrient demand. Secondly, creating robust electrochemical sensors by solving fouling issues with antifouling layers based on covalent surface chemistry. Where necessary, these electrode materials may be adapted to mechanical stretching organ-on-a-chip systems, for example through the development of polymeric electrode materials. A last remaining issue is the formation of hydrogen peroxide while sensing oxygen or glucose/lactate, which might cause biological damage to the cells grown in the organ-on-a-chip device. We envisage the further integration of organ-on-a-chip systems with miniaturized analytical equipment in order to provide continuous read outs of target analytes and metabolites thereof. Eventually this will yield online systems that provide continuous online data and mimic real life *in vivo* biological processes. This would greatly advance the widespread use of organ-on-a-chip approaches in research and development of novel drugs, assessment of toxicological effect of chemicals and monitoring of health benefits of dietary compounds.

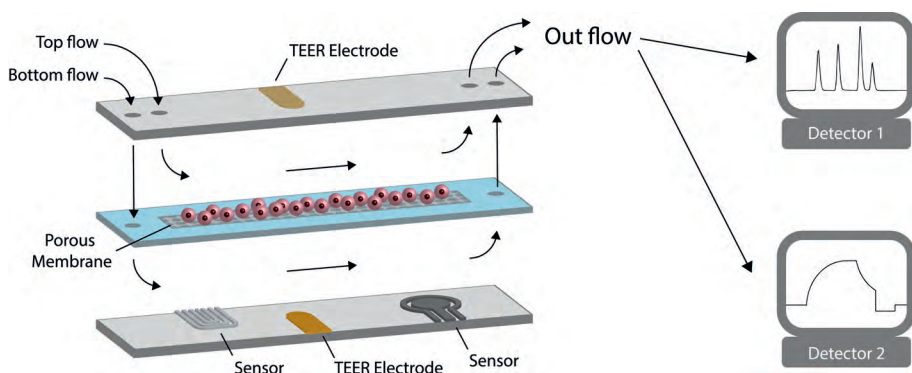


Figure 2.6: Advanced organ-on-a-chip model with several integrated sensors for monitoring and feedback of biological integrity and hyphenated to one or more online detectors for detection of target analytes and metabolites thereof.

Acknowledgements

This research receives funding from the Dutch Research Council (NWO) in the framework of the Technology Area PTA-COAST3 (project nr. 053.21.116) of the Fund New Chemical Innovations with Wageningen University, University of Groningen, Wageningen Food Safety Research, FrieslandCampina, Micronit Microtechnologies, Galapagos and Europroxima as partners.

References

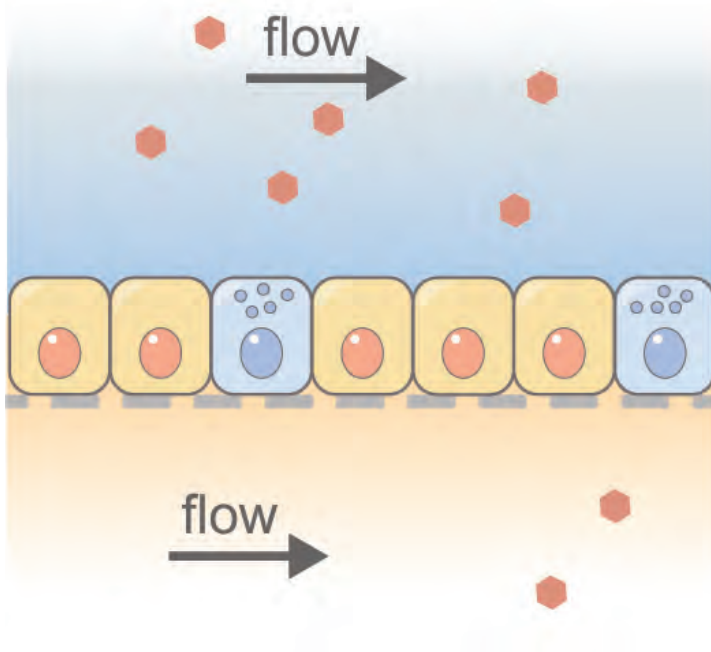
- [1] Shanks N, Greek R, Greek J. Are animal models predictive for humans? *Philos Ethics Humanit Med.* 2009;4:2.
- [2] Directive 2010/63/EU of the European Parliament and of the Council of 22 September 2010 on the protection of animals used for scientific purposes, Pub. L. No. L276 Stat. L276 (2010).
- [3] Ward PA, Blanchard, R. J., & Bolivar, V. Recognition and alleviation of distress in laboratory animals. Washington (DC): National Academies Press; 2008.
- [4] Carere A, Stamatii A, Zucco F. In vitro toxicology methods: impact on regulation from technical and scientific advancements. *Toxicol Lett.* 2002;127(1-3):153-160.
- [5] Fotaki N. Pros and cons of methods used for the prediction of oral drug absorption. *Expert Rev Clin Pharmacol.* 2009;2(2):195-208.
- [6] Marx U, Walles H, Hoffmann S, Lindner G, Horland R, Sonntag F, et al. 'Human-on-a-chip' developments: A translational cutting-edge alternative to systemic safety assessment and efficiency evaluation of substances in laboratory animals and man? *Atla-Altern Lab Anim.* 2012;40(5):235-257.
- [7] Griep LM, Wolbers F, de Wagenaar B, ter Braak PM, Weksler BB, Romero IA, et al. BBB on chip: microfluidic platform to mechanically and biochemically modulate blood-brain barrier function. *Biomed Microdevices.* 2013;15(1):145-150.
- [8] Booth R, Kim H. Characterization of a microfluidic in vitro model of the blood-brain barrier (muBBB). *Lab Chip.* 2012;12(10):1784-1792.
- [9] Huh D, Matthews BD, Mammoto A, Montoya-Zavala M, Hsin HY, Ingber DE. Reconstituting organ-level lung functions on a chip. *Science.* 2010;328(5986):1662-1668.
- [10] Grosberg A, Alford PW, McCain ML, Parker KK. Ensembles of engineered cardiac tissues for physiological and pharmacological study: heart on a chip. *Lab Chip.* 2011;11(24):4165-4173.
- [11] Desrousseaux C, Prot JM, Dufresne M, Pautier P, Leclerc E. Evaluation of the mass transfers of caffeine and vitamin B12 in chloroacetaldehyde treated renal barrier model using a microfluidic biochip. *Sensor Actuat B-Chem.* 2012;174:465-472.
- [12] Moya A, Ortega-Ribera M, Guimera X, Sowade E, Zea M, Illa X, et al. Online oxygen monitoring using integrated inkjet-printed sensors in a liver-on-a-chip system. *Lab Chip.* 2018;18(14):2023-2035.
- [13] Alexander FA, Eggert S, Wiest J. Skin-on-a-Chip: Transepithelial electrical resistance and extracellular acidification measurements through an automated air liquid interface. *Genes-Basel.* 2018;9(2):114.
- [14] Kim HJ, Huh D, Hamilton G, Ingber DE. Human gut-on-a-chip inhabited by microbial flora that experiences intestinal peristalsis-like motions and flow. *Lab Chip.* 2012;12(12):2165-2174.
- [15] Kulthong K, Duivenvoorde L, Mizera BZ, Rijkers D, ten Dam G, Oegema G, et al. Implementation of a dynamic intestinal gut-on-a-chip barrier model for transport studies of lipophilic dioxin congeners. *Rsc Adv.* 2018;8(57):32440-32453.
- [16] Sung JH, Wang Y, Narasimhan Sriram N, Jackson M, Long C, Hickman JJ, et al. Recent advances in body-on-a-chip systems. *Anal Chem.* 2019;91(1):330-351.
- [17] Chen LJ, Ito S, Kai H, Nagamine K, Nagai N, Nishizawa M, et al. Microfluidic co-cultures of retinal pigment epithelial cells and vascular endothelial cells to investigate choroidal angiogenesis. *Sci Rep.* 2017;7(1):3538.
- [18] Irimia D, Wang X. Inflammation-on-a-chip: Probing the Immune system ex vivo. *Trends Biotechnol.* 2018;36(9):923-937.
- [19] Kim HJ, Li H, Collins JJ, Ingber DE. Contributions of microbiome and mechanical deformation to intestinal bacterial overgrowth and inflammation in a human gut-on-a-chip. *P Natl Acad Sci USA.* 2016;113(1):E7-E15.
- [20] Ahadian S, Civitarese R, Bannerman D, Mohammadi MH, Lu R, Wang E, et al. Organ-on-a-chip platforms: A convergence of advanced materials, cells, and microscale technologies. *Adv Healthc Mater.* 2018;7(2):1700506.
- [21] Reece A, Xia BZ, Jiang ZL, Noren B, McBride R, Oakey J. Microfluidic techniques for high throughput single cell analysis. *Curr Opin Biotech.* 2016;40:90-96.

- [22] Varma S, Voldman J. Caring for cells in microsystems: principles and practices of cell-safe device design and operation. *Lab Chip*. 2018;18(22):3333-3352.
- [23] Kamble H, Barton MJ, Jun M, Park S, Nguyen NT. Cell stretching devices as research tools: engineering and biological considerations. *Lab Chip*. 2016;16(17):3193-3203.
- [24] Toh AGG, Wang ZP, Yang C, Nguyen NT. Engineering microfluidic concentration gradient generators for biological applications. *Microfluid Nanofluid*. 2014;16(1-2):1-18.
- [25] Ergir E, Bachmann B, Redl H, Forte G, Ertl P. Small force, big impact: Next generation organ-on-a-chip systems incorporating biomechanical cues. *Front Physiol*. 2018;9:1417.
- [26] Kieninger J, Weltin A, Flamm H, Urban GA. Microsensor systems for cell metabolism - from 2D culture to organ-on-chip. *Lab Chip*. 2018;18(9):1274-1291.
- [27] Srinivasan B, Kolli AR, Esch MB, Abaci HE, Shuler ML, Hickman JJ. TEER measurement techniques for in vitro barrier model systems. *Jala-J Lab Autom*. 2015;20(2):107-126.
- [28] Walter FR, Valkai S, Kincses A, Petnehazi A, Czeller T, Veszelka S, et al. A versatile lab-on-a-chip tool for modeling biological barriers. *Sensor Actuat B-Chem*. 2016;222:1209-1219.
- [29] Henry OYF, Villenave R, Crounce MJ, Leineweber WD, Benz MA, Ingber DE. Organs-on-chips with integrated electrodes for trans-epithelial electrical resistance (TEER) measurements of human epithelial barrier function. *Lab Chip*. 2017;17(13):2264-2271.
- [30] Maoz BM, Herland A, Henry OYF, Leineweber WD, Yadid M, Doyle J, et al. Organs-on-Chips with combined multi-electrode array and transepithelial electrical resistance measurement capabilities. *Lab Chip*. 2017;17(13):2294-2302.
- [31] Zhao S, Li J, Cao D, Zhang G, Li J, Li K, et al. Recent advancements in flexible and stretchable electrodes for electromechanical sensors: strategies, materials, and features. *ACS Appl Mater Interfaces*. 2017;9(14):12147-12164.
- [32] Bandodkar AJ, Nunez-Flores R, Jia WZ, Wang J. All-printed stretchable electrochemical devices. *Adv Mater*. 2015;27(19):3060-3065.
- [33] Odijk M, van der Meer AD, Levner D, Kim HJ, van der Helm MW, Segerink LI, et al. Measuring direct current trans-epithelial electrical resistance in organ-on-a-chip microsystems. *Lab Chip*. 2015;15(3):745-752.
- [34] Xu Y, Xie X, Duan Y, Wang L, Cheng Z, Cheng J. A review of impedance measurements of whole cells. *Biosens Bioelectron*. 2016;77:824-836.
- [35] Tran TB, Cho S, Min J. Hydrogel-based diffusion chip with electric cell-substrate impedance sensing (ECIS) integration for cell viability assay and drug toxicity screening. *Biosens Bioelectron*. 2013;50:453-459.
- [36] Xu YC, Lv Y, Wang L, Xing WL, Cheng J. A microfluidic device with passive air-bubble valves for real-time measurement of dose-dependent drug cytotoxicity through impedance sensing. *Biosens Bioelectron*. 2012;32(1):300-304.
- [37] van der Helm MW, Henry OYF, Bein A, Hamkins-Indik T, Crounce MJ, Leineweber WD, et al. Non-invasive sensing of transepithelial barrier function and tissue differentiation in organs-on-chips using impedance spectroscopy. *Lab Chip*. 2019;19(3):452-463.
- [38] Lange SC, van Andel E, Smulders MMJ, Zuilhof H. Efficient and tunable three-dimensional functionalization of fully zwitterionic antifouling surface coatings. *Langmuir*. 2016;32(40):10199-10205.
- [39] Weltin A, Slotwinski K, Kieninger J, Moser I, Jobst G, Wego M, et al. Cell culture monitoring for drug screening and cancer research: a transparent, microfluidic, multi-sensor microsystem. *Lab Chip*. 2014;14(1):138-146.
- [40] Eklund SE, Thompson RG, Snider RM, Carney CK, Wright DW, Wikswo J, et al. Metabolic discrimination of select list agents by monitoring cellular responses in a multianalyte microphysiometer. *Sensors-Basel*. 2009;9(3):2117-2133.
- [41] Misun PM, Rothe J, Schmid YRF, Hierlemann A, Frey O. Multi-analyte biosensor interface for real-time monitoring of 3D microtissue spheroids in hanging-drop networks. *Microsyst Nanoeng*. 2016;2:16022.
- [42] Curto VF, Marchiori B, Hama A, Pappa AM, Ferro MP, Braendlein M, et al. Organic transistor platform with integrated microfluidics for in-line multi-parametric in vitro cell monitoring. *Microsyst Nanoeng*. 2017;3:17028.

- [43] Bavli D, Prill S, Ezra E, Levy G, Cohen M, Vinken M, et al. Real-time monitoring of metabolic function in liver-on-chip microdevices tracks the dynamics of mitochondrial dysfunction. *P Natl Acad Sci USA*. 2016;113(16):E2231-E2240.
- [44] Halldorsson S, Lucumi E, Gomez-Sjoberg R, Fleming RMT. Advantages and challenges of microfluidic cell culture in polydimethylsiloxane devices. *Biosens Bioelectron*. 2015;63:218-231.
- [45] Kim L, Toh YC, Voldman J, Yu H. A practical guide to microfluidic perfusion culture of adherent mammalian cells. *Lab Chip*. 2007;7(6):681-694.
- [46] Berthier E, Young EW, Beebe D. Engineers are from PDMS-land, biologists are from polystyrenia. *Lab Chip*. 2012;12(7):1224-1237.
- [47] Schulze T, Mattern K, Fruh E, Hecht L, Rustenbeck I, Dietzel A. A 3D microfluidic perfusion system made from glass for multiparametric analysis of stimulus-secretion coupling in pancreatic islets. *Biomed Microdevices*. 2017;19(3):47.
- [48] Louterback K, Chen L, Holman HYN. Open-channel microfluidic membrane device for long-term FT-IR spectromicroscopy of live adherent cells. *Anal Chem*. 2015;87(9):4601-4606.
- [49] Shah P, Fritz JV, Glaab E, Desai MS, Greenhalgh K, Frachet A, et al. A microfluidics-based in vitro model of the gastrointestinal human-microbe interface. *Nat Commun*. 2016;7:11535.
- [50] Bonk SM, Stubbe M, Buehler SM, Tautorat C, Baumann W, Klinkenberg ED, et al. Design and characterization of a sensorized microfluidic cell-culture system with electro-thermal micro-pumps and sensors for cell adhesion, oxygen, and pH on a glass chip. *Biosensors-Basel*. 2015;5(3):513-536.
- [51] Oomen PE, Skolimowski MD, Verpoorte E. Implementing oxygen control in chip-based cell and tissue culture systems. *Lab Chip*. 2016;16(18):3394-3414.
- [52] Zhang YS, Aleman J, Shin SR, Kilic T, Kim D, Shaegh SAM, et al. Multisensor-integrated organs-on-chips platform for automated and continual in situ monitoring of organoid behaviors. *P Natl Acad Sci USA*. 2017;114(12):E2293-E2302.
- [53] Hafner F. Cytosensor microphysiometer: technology and recent applications. *Biosens Bioelectron*. 2000;15(3-4):149-158.
- [54] Hu N, Wu CX, Ha D, Wang TX, Liu QJ, Wang P. A novel microphysiometer based on high sensitivity LAPS and microfluidic system for cellular metabolism study and rapid drug screening. *Biosens Bioelectron*. 2013;40(1):167-173.
- [55] Alborzinia H, Can S, Holenya P, Scholl C, Lederer E, Kitanovic I, et al. Real-time monitoring of cisplatin-induced cell death. *Plos One*. 2011;6(5):e19714.
- [56] Brischwein M, Motrescu ER, Cabala E, Otto AM, Grothe H, Wolf B. Functional cellular assays with multiparametric silicon sensor chips. *Lab Chip*. 2003;3(4):234-240.
- [57] Buehler SM, Stubbe M, Bonk SM, Nissen M, Titipornpun K, Klinkenberg ED, et al. Cell monitoring and manipulation systems (CMMSs) based on glass cell-culture chips (GC(3)s). *Micromachines-Basel*. 2016;7(7):106.
- [58] Lehmann M, Baumann W, Brischwein M, Ehret R, Kraus M, Schwinde A, et al. Non-invasive measurement of cell membrane associated proton gradients by ion-sensitive field effect transistor arrays for microphysiological and bioelectronic applications. *Biosens Bioelectron*. 2000;15(3-4):117-124.
- [59] Hu N, Ha D, Wu CX, Zhou J, Kirsanov D, Legin A, et al. A LAPS array with low cross-talk for non-invasive measurement of cellular metabolism. *Sensor Actuat a-Phys*. 2012;187:50-56.
- [60] Grist SM, Chrostowski L, Cheung KC. Optical oxygen sensors for applications in microfluidic cell culture. *Sensors-Basel*. 2010;10(10):9286-9316.
- [61] Sin A, Chin KC, Jamil MF, Kostov Y, Rao G, Shuler ML. The design and fabrication of three-chamber microscale cell culture analog devices with integrated dissolved oxygen sensors. *Biotechnol Progr*. 2004;20(1):338-345.
- [62] Lee CH, Folz J, Tan JWY, Jo J, Wang X, Kopelman R. Chemical imaging in vivo: Photoacoustic-based 4-dimensional chemical analysis. *Anal Chem*. 2019;91(4):2561-2569.
- [63] Ramello C, Paullier P, Ould-Dris A, Monge M, Legallais C, Leclerc E. Investigation into modification of mass transfer kinetics by acrolein in a renal biochip. *Toxicol in Vitro*. 2011;25(5):1123-1131.
- [64] Shin SR, Zhang YS, Kim DJ, Manbohi A, Avci H, Silvestri A, et al. Aptamer-based microfluidic electrochemical biosensor for monitoring cell-secreted trace cardiac biomarkers. *Anal Chem*. 2016;88(20):10019-10027.

- [65] Lin X, Chen Q, Liu W, Zhang J, Wang S, Lin Z, et al. Oxygen-induced cell migration and on-line monitoring biomarkers modulation of cervical cancers on a microfluidic system. *Sci Rep*. 2015;5:9643.
- [66] Shin SR, Kilic T, Zhang YS, Avci H, Hu N, Kim D, et al. Label-free and regenerative electrochemical microfluidic biosensors for continual monitoring of cell secretomes. *Adv Sci*. 2017;4(5):1600522.
- [67] Li XK, Soler M, Ozdemir CI, Belushkin A, Yesilkoy F, Altug H. Plasmonic nanohole array biosensor for label-free and real-time analysis of live cell secretion. *Lab Chip*. 2017;17(13):2208-2217.
- [68] Lee JF, Stovall GM, Ellington AD. Aptamer therapeutics advance. *Curr Opin Chem Biol*. 2006;10(3):282-289.
- [69] Kimura H, Yamamoto T, Sakai H, Sakai Y, Fujii T. An integrated microfluidic system for long-term perfusion culture and on-line monitoring of intestinal tissue models. *Lab Chip*. 2008;8(5):741-746.
- [70] Cho S, Islas-Robles A, Nicolini AM, Monks TJ, Yoon JY. In situ, dual-mode monitoring of organ-on-a-chip with smartphone-based fluorescence microscope. *Biosens Bioelectron*. 2016;86:697-705.
- [71] Li YT, Zhang SH, Wang XY, Zhang XW, Oleinick AI, Svir I, et al. Real-time monitoring of discrete synaptic release events and excitatory potentials within self-reconstructed neuromuscular junctions. *Angew Chem Int Ed Engl*. 2015;54(32):9313-9318.
- [72] Li MW, Spence DM, Martin RS. A microchip-based system for immobilizing PC 12 cells and amperometrically detecting catecholamines released after stimulation with calcium. *Electroanal*. 2005;17(13):1171-1180.
- [73] Feng XJ, Liu BF, Li JJ, Liu X. Advances in coupling microfluidic chips to mass spectrometry. *Mass Spectrom Rev*. 2015;34(5):535-557.
- [74] Oedit A, Vulto P, Ramautar R, Lindenburg PW, Hankemeier T. Lab-on-a-chip hyphenation with mass spectrometry: strategies for bioanalytical applications. *Curr Opin Biotech*. 2015;31:79-85.
- [75] Gao D, Liu HX, Jiang YY, Lin JM. Recent advances in microfluidics combined with mass spectrometry: technologies and applications. *Lab Chip*. 2013;13(17):3309-3322.
- [76] Mao S, Li W, Zhang Q, Zhang W, Huang Q, Lin J-M. Cell analysis on chip-mass spectrometry. *Trac-Trend Anal Chem*. 2018;107:43-59.
- [77] Gao D, Liu HX, Lin JM, Wang YN, Jiang YY. Characterization of drug permeability in Caco-2 monolayers by mass spectrometry on a membrane-based microfluidic device. *Lab Chip*. 2013;13(5):978-985.
- [78] Marasco CC, Enders JR, Seale KT, McLean JA, Wikswo JP. Real-time cellular exometabolome analysis with a microfluidic-mass spectrometry platform. *Plos One*. 2015;10(2):e0117685.
- [79] Gao D, Li HF, Wang NJ, Lin JM. Evaluation of the absorption of methotrexate on cells and its cytotoxicity assay by using an integrated microfluidic device coupled to a mass spectrometer. *Anal Chem*. 2012;84(21):9230-9237.
- [80] Gao D, Wei HB, Guo GS, Lin JM. Microfluidic cell culture and metabolism detection with electrospray ionization quadrupole time-of-flight mass spectrometer. *Anal Chem*. 2010;82(13):5679-5685.
- [81] Wei HB, Li HF, Gao D, Lin JM. Multi-channel microfluidic devices combined with electrospray ionization quadrupole time-of-flight mass spectrometry applied to the monitoring of glutamate release from neuronal cells. *Analyst*. 2010;135(8):2043-2050.
- [82] Wei HB, Li HF, Mao SF, Lin JM. Cell signaling analysis by mass spectrometry under coculture conditions on an integrated microfluidic device. *Anal Chem*. 2011;83(24):9306-9313.
- [83] Mao SF, Gao D, Liu W, Wei HB, Lin JM. Imitation of drug metabolism in human liver and cytotoxicity assay using a microfluidic device coupled to mass spectrometric detection. *Lab Chip*. 2012;12(1):219-226.
- [84] Mao SF, Zhang J, Li HF, Lin JM. Strategy for signaling molecule detection by using an integrated microfluidic device coupled with mass spectrometry to study cell-to-cell communication. *Anal Chem*. 2013;85(2):868-876.
- [85] Zhang J, Wu J, Li HF, Chen QS, Lin JM. An in vitro liver model on microfluidic device for analysis of capecitabine metabolite using mass spectrometer as detector. *Biosens Bioelectron*. 2015;68:322-328.
- [86] Dugan CE, Grinias JP, Parlee SD, El-Azzouny M, Evans CR, Kennedy RT. Monitoring cell secretions on microfluidic chips using solid-phase extraction with mass spectrometry. *Anal Bioanal Chem*. 2017;409(1):169-178.

- [87] Takats Z, Wiseman JM, Gologan B, Cooks RG. Mass spectrometry sampling under ambient conditions with desorption electrospray ionization. *Science*. 2004;306(5695):471-473.
- [88] Cody RB, Laramée JA, Durst HD. Versatile new ion source for the analysis of materials in open air under ambient conditions. *Anal Chem*. 2005;77(8):2297-2302.
- [89] Lu HY, Zhang H, Chingin K, Xiong JL, Fang XW, Chen HW. Ambient mass spectrometry for food science and industry. *Trac-Trend Anal Chem*. 2018;107:99-115.
- [90] Liu JJ, Wang H, Manicke NE, Lin JM, Cooks RG, Ouyang Z. Development, characterization, and application of paper spray ionization. *Anal Chem*. 2010;82(6):2463-2471.
- [91] Klampfl CW, Himmelsbach M. Direct ionization methods in mass spectrometry: An overview. *Anal Chim Acta*. 2015;890:44-59.
- [92] Liu W, Wang NJ, Lin XX, Ma Y, Lin JM. Interfacing microsampling droplets and mass spectrometry by paper spray ionization for online chemical monitoring of cell culture. *Anal Chem*. 2014;86(14):7128-7134.
- [93] Liu W, Lin JM. Online monitoring of lactate efflux by multi-channel microfluidic chip-mass spectrometry for rapid drug evaluation. *Acs Sensors*. 2016;1(4):344-347.
- [94] Wang H, Manicke NE, Yang QA, Zheng LX, Shi RY, Cooks RG, et al. Direct analysis of biological tissue by paper spray mass spectrometry. *Anal Chem*. 2011;83(4):1197-1201.
- [95] Chen QS, He ZY, Liu W, Lin XX, Wu J, Li HF, et al. Engineering cell-compatible paper chips for cell culturing, drug screening, and mass spectrometric sensing. *Adv Healthc Mater*. 2015;4(15):2291-2296.
- [96] Wu J, Jie M, Dong X, Qi H, Lin JM. Multi-channel cell co-culture for drug development based on glass microfluidic chip-mass spectrometry coupled platform. *Rapid Commun Mass Spectrom*. 2016;30(S1):80-86.
- [97] Bouwmeester H, Brandhoff P, Marvin HJP, Weigel S, Peters RJB. State of the safety assessment and current use of nanomaterials in food and food production. *Trends Food Sci Tech*. 2014;40(2):200-210.
- [98] Zhong M, Lee CY, Croushore CA, Sweedler JV. Label-free quantitation of peptide release from neurons in a microfluidic device with mass spectrometry imaging. *Lab Chip*. 2012;12(11):2037-2045.



Chapter 3

Development of a dynamic *in vitro* intestinal barrier model to predict oral bioavailability of chemicals

This chapter was adapted from

M.J.C. Santbergen, M. van der Zande, A. Gerssen, H. Bouwmeester and M.W.F. Nielen. Dynamic *in vitro* intestinal barrier model coupled to chip-based liquid chromatography mass spectrometry for oral bioavailability studies. *Analytical and Bioanalytical Chemistry* (2020);412:1111-1122

Chapter 3a – Verapamil

Abstract

The oral bioavailability of a chemical is essential information for novel drug development and in the field of toxicology. Intestinal uptake of the chemical is a crucial factor in oral bioavailability, highlighting the importance of *in vitro* intestinal models that correctly predict this phenomenon. For this, various *in vitro* intestinal barrier models have been developed in the past decades. Advancements in the field of organ-on-a-chip technology have resulted in dynamic *in vitro* models of the gut that better mimic the *in vivo* microenvironment of the intestine than their static counterparts. In this study, we developed and evaluated a dynamic *in vitro* model of the intestine for permeability studies of chemicals. A co-culture of Caco-2 and HT29-MTX-E12 cells was grown in a flow-through transwell system. We assessed proper gut barrier function by showing absence of Lucifer yellow permeability, and further examined the morphology of the cell barrier using confocal microscopy. We determined the permeability of the model compound verapamil and compared it to the permeability in a traditional static transwells and benchmarked against *in vitro* and *in vivo* permeability data found in literature.

Keywords: gut-on-a-chip, oral bioavailability, verapamil, transwell

3.1 Introduction

To study oral bioavailability of chemicals, *in vitro* models can be used to assess the transport across the intestinal epithelial barrier. Currently, well-established static *in vitro* cell culture models of the intestine are used for this purpose. Monolayers of differentiated Caco-2 cells are frequently used to mimic the intestinal epithelium [1, 2]. Caco-2 cells are derived from a colorectal adenocarcinoma, however they express the morphological and functional characteristics of small intestinal enterocytes [3]. Upon culturing for 21 days the Caco-2 cells polarize and express an apical brush border with microvilli. Furthermore, tight junctions are formed between the cells creating a tight cell barrier [4]. Good correlations have been found for Caco-2 monolayers and human absorption data, especially for compounds that diffuse paracellularly [5-7]. *In vivo* a mucus layer is covering the epithelial cells, and acts like an extra barrier for chemicals, and protect the enterocytes from the harsh content of the intestinal lumen. However, monolayers of Caco-2 cells alone, do not secrete mucus. To better mimic the *in vivo* intestinal barrier, cocultures of enterocytes and mucus producing goblet cells have been developed [8]. HT29-MTX cells are human mucin producing goblet cells, which, when grown in co-culture with Caco-2 cells, deposit mucin on top of the cell barrier, thereby better mimicking the *in vivo* situation [9].

The *in vitro* models (both mono- and co-cultures) are typically grown in a so called transwell system (Figure 3.1a), which is a well described system for permeability studies [2, 10, 11]. Transwells are cell culture plate inserts containing a porous membrane on which cells can be grown, creating an apical (lumen) and basolateral (blood) compartment. A compound of interest can be applied apically and its transport across the intestinal cell layer can be determined. For this, samples are taken periodically from the apical and basolateral compartment for measurement, and the permeability of the compound is calculated. However, such a transwell system has its limitations as the cells are grown in a static environment, thus ignoring the dynamic flow of the lumen content as well as the blood flow. Additional disadvantages of using the static transwell are: the accumulation of toxic metabolites, a concentration equilibrium influencing permeability and the limited possibilities for online automated analysis [12].

Recent advances in biochip technology have led to state-of-the-art *in vitro* cell culture systems that include mechanical and functional features present in the human body, resulting in a much better representation of the *in vivo* microenvironment [13-15]. For dynamic *in vitro* intestinal models this means: mimicking the passing of food by the inclusion of fluid flow, incorporation of peristaltic motion by mechanical stretching of the cells and a more *in vivo* like volume to surface ratio [16]. Several different geometries and designs have been developed for dynamic *in vitro* intestinal cell culture devices, but two main types of designs are commonly found in literature. The first type is based on the traditional transwell system, where intestinal cells are grown on a circular porous membrane [17-20]. The second type is based on culturing cells on a porous membrane that separates two sides of a straight channel or tube [21-25]. Both types of systems at least contain flow of cell culture medium on the apical side inducing *in vivo* relevant shear forces on the cells. Another advantages of dynamic *in vitro* intestinal barrier systems is that they provide the possibility to fully automate the system by integration with an analytical detection system [26]. Dynamic intestinal barrier systems have the potential to replace animals in safety testing. However, a major drawback of current dynamic systems is the limited studies examining the absorptive capacity of the intestinal barrier in these devices, which is essential when developing novel oral drugs.

In this study, we developed and evaluated a dynamic *in vitro* model of the intestine that can be used for permeability studies of chemicals. A co-culture of Caco-2 and HT29-MTX-E12 cells was grown in a flow-through transwell system (Figure 3.1b). To confirm gut barrier integrity, we assessed Lucifer yellow permeability and cell morphology. The permeability of verapamil, a well-known model compound, was examined in both the static transwell and the dynamic *in vitro* model system. This allowed benchmarking against *in vitro* and *in vivo* permeability data found in literature.

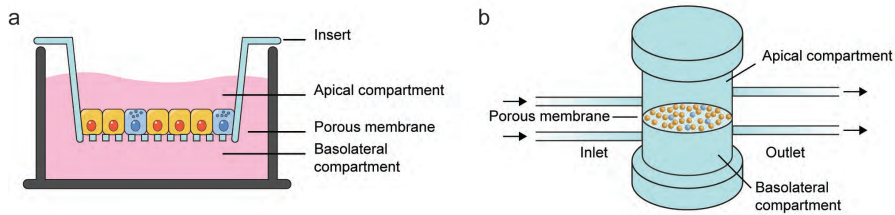


Figure 3.1: Schematic representation of a) traditional transwell insert and b) dynamic flow-through transwell system.

3.2 Materials and Methods

3.2.1 Chemicals and reagents

Verapamil hydrochloride, ergotamin(in)e d-tartrate, penicillin-streptomycin, formic acid, Lucifer yellow, 4-(2-hydroxyethyl)-1-piperazineethanesulfonic acid (HEPES), sodium bicarbonate (NaHCO_3), ammonium carbonate, sodium pyruvate, Dulbecco's Modified Eagle Medium (DMEM) with 4.5 g/L glucose, l-glutamine and 25 mM HEPES powder, Triton-X100 and Hank's balanced salt solution (HBSS), with and without phenol red, were purchased from Sigma-Aldrich/Merck (Zwijndrecht, the Netherlands). DMEM with 4.5 g/L glucose and l-glutamine with and without phenol red, bovine serum albumin (BSA) and heat-inactivated fetal bovine serum (FBS) were purchased from Gibco (Bleiswijk, the Netherlands). Rabbit polyclonal antibody ZO-1/TJP1 – Alexa fluor 594, 4',6-diamidino-2-phenylindole (DAPI), Prolong Diamond Antifade Mountant, dimethyl sulfoxide (DMSO), phosphate buffered saline (PBS) and non-essential amino acids (NEAA) were obtained from Thermo Fisher Scientific (Landsmeer, the Netherlands). Acetonitrile and methanol were purchased from Actua-all chemicals (Oss, the Netherlands). UPLC-MS grade water was purchased from Biosolve (Valkenswaard, the Netherlands). Paraformaldehyde was purchased from VWR (Amsterdam, the Netherlands), WST-1 reagent from Roche Diagnostics GmbH (Mannheim, Germany) and water was prepared daily using a Milli-Q Reference Water Purification System from Millipore (Burlington, MA, USA).

3.2.2 Cell culture

The human colonic adenocarcinoma Caco-2 cell line was obtained from the American Type Culture Collection (ATCC, Manassas, VA, USA) and the human colon adenocarcinoma mucus secreting HT29-MTX-E12 cell line was obtained from the European Collection of Authenticated Cell Cultures (ECACC, Salisbury, UK). Caco-2 cells were used at passage numbers 29-40 and HT29-MTX-E12 cells were used at passage numbers 52-70 for all experiments. Cells were cultured in DMEM containing 10% FBS, 1% NEAA and 1% penicillin-streptomycin and maintained at 37°C in a 5% CO₂-humidified air atmosphere and subcultured every 2 to 3 days. For permeability experiments cells were seeded at a density of 40,000 cells/cm² on a polycarbonate transwell insert (area 0.6 cm², 0.4 µm pore size, Millipore) as follows: Caco-2 and HT29-MTX-E12 cells were seeded in a 3:1 ratio on the apical side of the transwell and allowed to attach for 24 hours. After 24 hours, cell culture medium was refreshed every 2-3 days and, transwells were used for permeability experiments after 21 days of culturing.

3.2.3 Cell culture medium comparison

Caco-2 and HT29-MTX-E12 cells were cultured in T-75 flasks for 3 days and exposed to either CO₂ dependent DMEM (discussed above), at 37°C in a 5% CO₂-humidified air atmosphere or exposed to CO₂ independent cell culture medium consisting of DMEM high glucose powder with 25mM HEPES, 0.84 g/L sodium bicarbonate, 1mM sodium pyruvate, 10% FBS, 1% penicillin-streptomycin and 1% NEAA, at 37°C in an ambient air atmosphere. Phase-contrast (4x magnification) microscopic images of the flasks were acquired using an Olympus IX51 microscope (Leiderdrop, the Netherlands) for comparison.

3.2.4 Cell layer integrity

Cell layer integrity was evaluated using the transport marker Lucifer yellow. Following permeability experiments, the cells were incubated with Lucifer yellow at a concentration of 500 µg/mL for 30 minutes on the apical side of the transwell insert. Cell culture medium was collected from the apical and basolateral side at t=0 and t=30 minutes and analysed for fluorescence at 458/530 nm using a Bio-Tek (Winooski, VT, USA) Synergy HT Multi-Mode microplate reader. Cell layers that transported more than 5% of Lucifer yellow to the basolateral compartment were judged as leaking. Cell layer integrity was also examined by confocal microscopy. Cells were cultured on a transwell

membrane for 21 days and subsequently stained for tight junction protein ZO-1 and the cell nuclei. For this, the cells were washed with PBS and fixed with 4% paraformaldehyde (w/v) for 15 min. Cells were permeabilized with 0.25% Triton-X100 (v/v) and blocked with 1% BSA (w/v). The cells were then incubated with the conjugated antibody ZO-1/TJP1-Alexa Fluor 594 for 45 min (10 µg/mL). Subsequently, DAPI was used to stain the nuclei for 10 min (5 µg/mL). Between incubations cells were washed with PBS three times. Cells were mounted in a 120 µm spacer (Sigma-Aldrich) on a microscope slide (Thermo Scientific) with ProLong Diamond Antifade Mountant. Slides were then examined using a Zeiss (Jena, Germany) LSM 510-META confocal microscope. Samples were excited with 405 and 543 nm lasers and the pinholes were in the range of 90-94 µm at a magnification of 40 X.

3.2.5 Cell viability

Possible cytotoxic effects of verapamil were evaluated using the cell proliferation WST-1 assay. With the WST-1 assay mitochondrial activity of the cell is measured by the conversion of water soluble tetrazolium salt (WST-1) into formazan dye by mitochondrial dehydrogenase enzymes. The assay is performed as follows: Caco-2 and HT29-MTX-E12 cells (ratio 3:1) were seeded in Greiner bio-one (Alphen aan den Rijn, the Netherlands) flat bottom 96-well plates at a concentration of 1×10^5 cells/mL in cell culture medium (100 µL/well). Plates were incubated for 24 hours at 37°C under 5% CO₂. Cell culture medium was removed and subsequently the cells were exposed to 100 µL/well serial dilutions of verapamil (0 - 500 µg/mL) in cell culture medium for 24 hours, at 37°C. Then, the exposure media containing verapamil was discarded and the cells were washed with pre-warmed HBSS. WST-1 reagent (in cell culture medium without phenol red) was added to the cells (1:10, 100 µL/well) and incubated for 1.5 hour at 37°C. The absorbance of each well was measured at 440nm using a Bio-Tek Synergy HT Multi-Mode microplate reader. The viability of the cells for each concentration of verapamil was expressed as a percentage of the negative control consisting of cell culture medium. Triton-X100 (0.25%, v/v) was used as a positive control and decreased the cell viability to $0.2 \pm 0.2\%$.

3.2.6 Cell permeability experiments

For the static and dynamic cell permeability experiments 5 µg/mL verapamil was suspended in HBSS (without phenol red) containing 25 mM of HEPES and

0.35 g/L NaHCO_3 as the donor solution. For the static transwell experiments the donor solutions was directly applied on the apical side of the cells (400 μL /insert), at day 21 of culturing. The basolateral side of the insert was filled with the same solution (600 μL /insert), but without the compound of interest (receiving solution). Samples (100 μL) were collected and replenished on the basolateral side at the following time points: 15, 30, 45, 60, 120 and 180 minutes. Apical samples were taken at $t=0$ and $t=180$ minutes. For the dynamic experiments the transwell inserts were placed into the QV600 system from Kirkstall (Rotherham, UK), further referred to as a flow-through transwell (see also Figure 3.1b), at day 20 of culture. CO_2 independent cell culture medium containing 25 mM HEPES was perfused into the apical compartment (200 $\mu\text{L}/\text{min}$) and basolateral compartment (100 $\mu\text{L}/\text{min}$) of the flow-through transwell system using a New Era pump systems (Farmingdale, NY, USA) syringe pump for 24 h at 37°C , as described by Giusti et al. (2014) [27]. After 24 hours, the apical syringe was replaced by a syringe containing the donor solution and the basolateral syringe was replaced by a syringe containing the receiving solution. Syringe heaters (New Era Pump Systems) were used to heat the medium and keep the cells at 37°C without the need for an additional incubator. Both effluent flows were attached to a Gilson 234 autosampler (Villiers-le-Bel, France) which was used as a fraction collector, collecting samples every two minutes in 96-well plates (Figure 3.2). All experiments were conducted in biological triplicates.

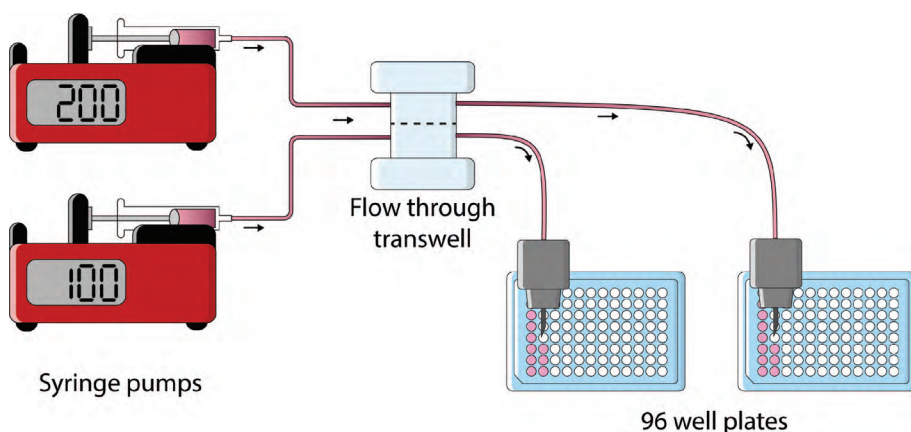


Figure 3.2: Schematic representation sample collection flow-through transwell.

3.2.7 LC-MS/MS analysis

Verapamil samples were diluted 500 times in water, prior to LC-MS/MS analysis. Chromatographic separation was achieved using a Waters (Milford, MA, USA) Acquity I-Class UPLC system equipped with an Acquity UPLC BEH C18 (100 mm x 2.1 mm, 1.7 μm) column (Waters). The column temperature was kept at 50°C and the autosampler was set at 10°C. A 2.5 μL injection volume was used. Mobile phase A was water and mobile phase B was acetonitrile, both containing 5 mM formic acid. The mobile phase gradient started at 10% B and after 0.8 min was linearly increased to 40% B in 2 min followed by an increase to 99% B in 0.1 min. This composition was kept for 3 min and returned to 10% B in 0.1 min, all at a constant flow rate of 0.6 mL/min. A mobile phase equilibration time of 1.1 min was allowed prior to the next injection. The first minute of the gradient elution was directed to waste to prevent any salts from the HBSS matrix to enter the ionization source. Mass spectrometric detection was performed using a Waters Xevo TQS tandem mass spectrometer equipped with an electrospray ionisation interface (ESI) and operated in positive ion mode, with a capillary voltage of 3.1 kV, a desolvation temperature of 450 °C, a gas flow rate of 800 L/h, a source temperature of 150 °C and a cone gas flow rate of 150 L/h. For verapamil three multiple reaction monitoring (MRM) transitions were acquired for compound conformation: m/z 445.4 > 150.1, 445.4 > 165.1 and 455.4 > 303.4 with a cone voltage of 40V and a collision energy of 25 eV. For quantification of verapamil a calibration curve was constructed in HBSS and subsequently diluted in water similar as the samples. Resulting in a calibration curve with the following points: 0, 0.01, 0.05, 0.1, 0.25, 0.5, 1 and 5 $\mu\text{g/mL}$. Limit of detection (LOD) and quantification (LOQ) were calculated as the average signal of five blank samples plus three (LOD) or ten (LOQ) times the standard deviation (SD) of the blank samples divided by the sensitivity (slope of the calibration curve) using the transition m/z 455.4 > 165.1 resulting in a LOD of 3.3 ng/mL and LOQ of 9.6 ng/mL. The concentration of verapamil in the unknown samples was then calculated using peak area measurements in the reconstructed ion current (RIC) of the transition m/z 455.4 > 165.1 via interpolation of the external matrix-matched calibration curve ($r^2=0.99$).

3.2.8 Data analysis

The apparent permeability coefficient (P_{app} , cm/s) was calculated as described by Yeon and Park (2009) [28], according to the following equation:

$$P_{app} = \frac{dQ}{dt} \frac{1}{A C_0}$$

Where dQ/dt is the cumulative transport rate in the basolateral compartment ($\mu\text{mol/s}$), A is the surface area of the cell layer (0.6 cm^2) and C_0 is the initial concentration of the compounds in the apical compartment ($\mu\text{mol/cm}^3$).

3.3 Results and Discussion

3.3.1 Evaluation intestinal barrier function

Conventionally, cells are cultured in an incubator at 37°C and $5\% \text{ CO}_2$. However, the flow-through transwell system is connected to syringe pumps and fraction collectors, which are placed outside of the incubator. Furthermore, the system is to be integrated with analytical equipment in future experiments (Chapter 4) therefore, we optimised the system to perform experiments outside the incubator, while maintaining good cell culturing conditions. Regular cell culture medium uses sodium bicarbonate as a pH buffer mechanism and therefore requires a stable level of CO_2 . In the present study, a well-known buffering agent (*i.e.* HEPES, a zwitterionic sulfonic acid) was used in the cell culture medium, which has a buffering capacity independent of the CO_2 concentration [21]. We examined the morphology and growth speed of the Caco-2 and HT29-MTX-E12 cells after 3 days of culture in a T-75 flask in cell culture medium containing HEPES grown independent of CO_2 and compared it with cells grown in conventional cell culture medium at $5\% \text{ CO}_2$ (Figure 3.3). No differences were observed either in morphology or growth speed between the cells exposed to CO_2 dependent or independent medium.

The human gastrointestinal tract is in close contact with the external environment. It protects our body from pathogens and toxic compounds [29, 30]. On the other hand, it effectively absorbs nutrients from our food as well as orally administrated drugs [31]. A reliable *in vitro* intestinal barrier model should reflect this gatekeeper function. A prerequisite for *in vitro* permeability experiments is the formation of a leak free monolayer of intestinal cells grown on a permeable membrane (*i.e.* transwell). In our *in vitro* model, confocal imaging showed a network of the tight junctions, visualized by staining the tight junction protein ZO-1 (Figure 3.4a) demonstrating a tight monolayer of

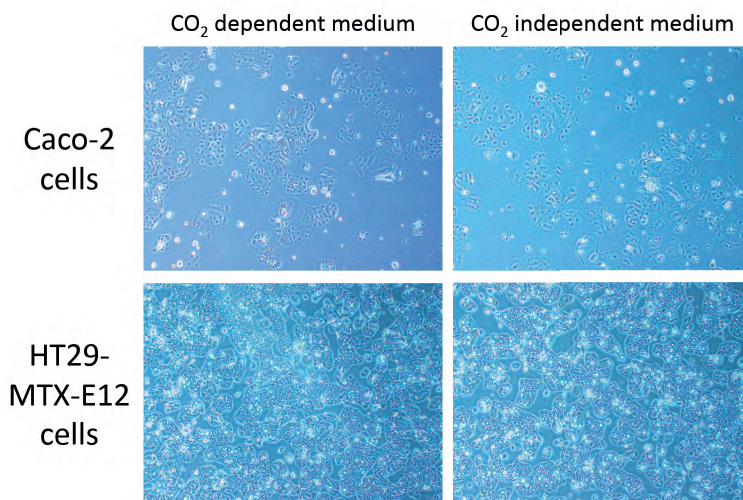


Figure 3.3: Light microscope images of Caco-2 cells and HT29-MTX-E12 cells after three days of culture in a T-75 flask. In the images on the left the cells were exposed to CO₂ dependent medium and in the images on the right the cells were exposed to CO₂ independent medium (magnification was 4X).

cells after 21 days of culture in the transwell. Tight junction proteins are present on the apical side of the cells, connecting individual cells together creating a closed barrier [32]. Furthermore, absence of paracellular transport was shown, by performing a Lucifer yellow permeability test. After exposure to verapamil the low Lucifer yellow permeability indicated good barrier integrity of the monolayer. Less than 5% Lucifer yellow permeability is generally used as a cut-off value for a leaky monolayer [33]. We obtained an average permeability of $0.18\% \pm 0.06\%$ (Figure 3.4b).

To assess the flow-through transwell model as a model for oral absorption, we examined its permeability characteristics using the model compound verapamil (Figure 3.4c), of which extensive *in vitro* and *in vivo* permeability data can be found in literature. Prior to permeability experiments, a non-toxic dose of verapamil was determined to ensure proper cell viability during experiments. For this we incubated non-differentiated cells for 24 hours with increasing concentrations of verapamil to establish the desired non-toxic concentration for subsequent studies. These are worst-case conditions as in the permeability experiments, the exposure lasted three hours and was executed on fully differentiated cells. The combination of a longer exposure time and the use of proliferating cells results in a higher sensitivity towards

cytotoxicity, compared to the shorter incubation and fully differentiated cells used in permeability experiments [34]. Results showed that the cell viability of the co-culture of Caco-2 and HT29-MTX-E12 cells was >80% [35] after exposure to concentrations of verapamil at or below 10 $\mu\text{g}/\text{mL}$ (Figure 3.4d). Therefore, a concentration of 5 $\mu\text{g}/\text{mL}$ was selected for permeability experiments in both the static and dynamic model system.

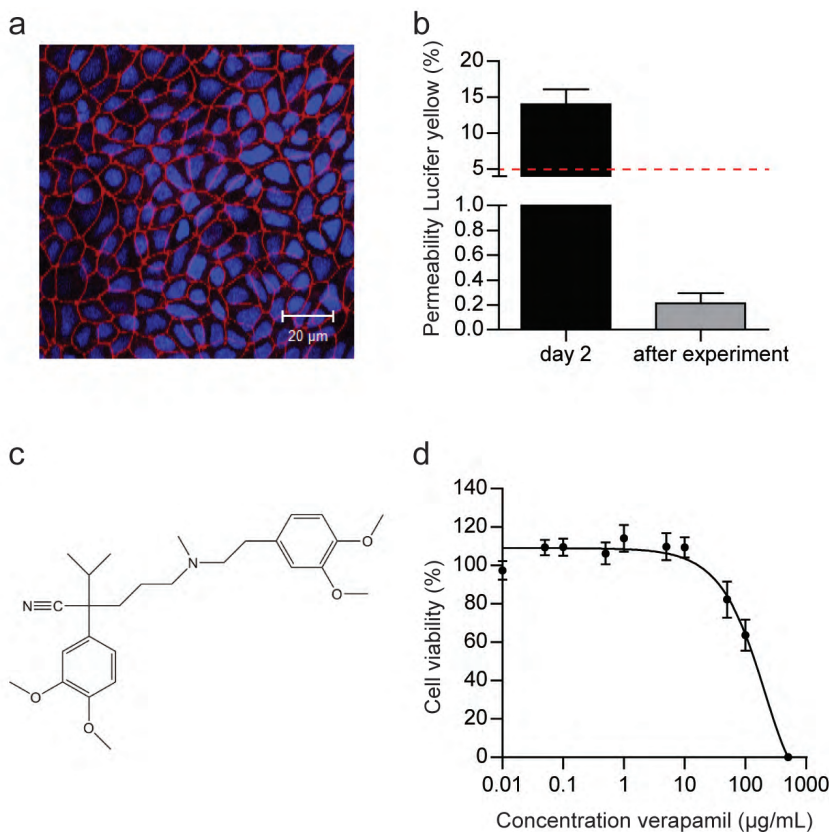


Figure 3.4: **a)** Confocal image of Caco-2/HT29-MTX-E12 cells before the exposure experiments in the dynamic flow-through transwell system (*i.e.* 21 days). Cells were stained for tight junction protein ZO-1/TJP1 (red) and cell nuclei (blue). **b)** Permeability of Lucifer yellow across a monolayer of Caco-2/HT29-MTX-E12 cells after two days of culture and after permeability experiments in the dynamic flow-through transwell system, given as a percentage of the apical concentration ($\% \pm$ standard error of the mean (SEM)). **c)** Molecular structure verapamil. **d)** Cell viability after 24 h exposure to increasing concentrations of verapamil. Viability is given as a percentage of the control ($\% \pm$ SEM; $n=3$).

3.3.2 Comparison of verapamil permeability in the static versus dynamic intestinal barrier model

In order to assess the flow-through transwell model as a model for intestinal absorption, we examined the permeability of model compound verapamil. Verapamil is a drug classified in category II of the biopharmaceutics classification system (BCS), meaning it is a high permeability compound, and it is known to cross the intestinal epithelium predominantly via passive transcellular diffusion [36, 37]. As discussed in the introduction Caco-2 cells are a well-suited model for testing permeability of passively transported compounds, like verapamil. For the static experiment, samples were collected on the basolateral side of the membrane at $t=0, 15, 30, 45, 60, 120$ and 180 minutes. In the flow-through transwell system samples were collected every two minutes by a fraction collector in a 96 well plate (Figure 3.2). The concentration of verapamil in these samples was determined by LC-MS/MS. Cumulative transport of verapamil across the intestinal layer in the static and flow-through transwell system after three hours was 13.5% and 12.7% of the exposure concentration, respectively, and followed a similar trend over time in both models (Figure 3.5). Variation among the biological samples in the flow-through transwell system was larger, compared to the static system. This is probably due to some flow induced shear stresses on the cells [38]. The apparent permeability coefficients (P_{app}) were calculated for all verapamil experiments, allowing comparison of our results against *in vitro* permeability data found in literature (Table 3.1). As shown in Table 3.1 the apparent permeability coefficients observed in our study fall within the range of *in vitro* data found in literature. *In vivo* P_{app} values for verapamil are ten to a hundred times higher ($6.7 \pm 2.9 \times 10^{-4}$ cm/s) [39] compared to *in vitro* data, however good correlations has been shown between *in vivo* and *in vitro* permeability data for verapamil [40].

A major drawback of current dynamic *in vitro* systems of the intestine is the high variety in designs and limited studies examining the absorptive capacity of the devices and benchmarking them against the golden standard, the transwell [18, 22, 34, 41]. For future research predicting oral bioavailability using dynamic intestinal barrier models more data needs to be generated testing the permeability of model compounds with different transport mechanisms, this will allow comparison to the static transwell and *in vivo* permeability data. Furthermore, characterization of the cell layer is essential looking at barrier

integrity and expression of transporters and metabolic enzymes. In the end we strive for better predictive *in vitro* models of oral bioavailability that can replace the animals currently used in regulatory analysis and novel drug development trails.

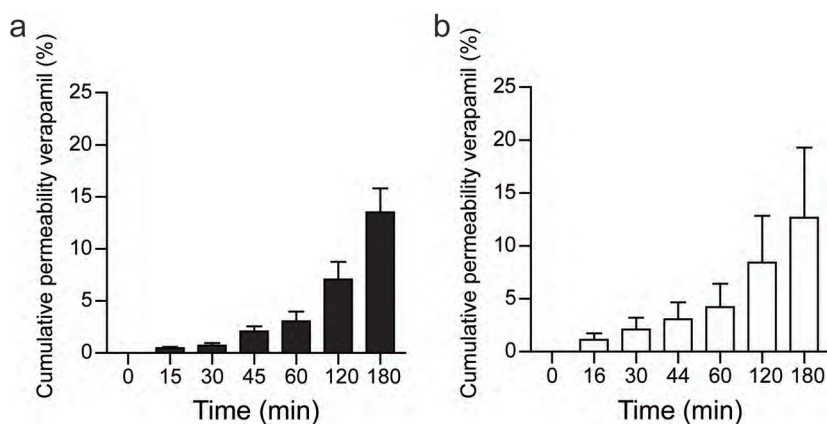


Figure 3.5: a) Permeability of verapamil across a monolayer of Caco-2/HT29-MTX-E12 cells in a static transwell. Permeability is given as a percentage of the apical concentration (% \pm SEM; n=3). b) Permeability of verapamil across a monolayer of Caco-2/HT29-MTX-E12 cells in the dynamic flow-through transwell. Permeability is given as a calculated cumulative percentage of the apical concentration (% \pm SEM; n=3).

Table 3.1 Apparent permeability coefficient of verapamil described in literature for different static *in vitro* model systems.

Cell Model	$P_{app} \times 10^{-6}$ cm/s	ref.
Caco-2	9.17-62.4	[42-45]
Caco-2 (TC-7) ^a	2.98 \pm 0.55	[46]
Caco-2/HT29-MTX	41.7 \pm 4.7	[47]
Caco-2/HT29-MTX/Raji B ^b	42.7 \pm 5.6	[47]
LLC-PK1 ^c	24 \pm 15.3	[42]
L-MDR1 ^c	18.8 \pm 0.7	[42]
Caco-2/HT29-MTX-E12 (static)	20.9 \pm 3.9	This study
Caco-2/HT29-MTX-E12 (dynamic)	19.5 \pm 10.3	This study

^aTC-7 is a clone of the Caco-2 cell line, ^b Raji B is a human B lymphocyte cell line and ^c LLC-PK1 cells are porcine epithelial cells, and L-MDR1 (multidrug-resistance) cells are LLC-PK1 cells stably transfected with human MDR1 cDNA

3.4 Conclusions

Here we have established a dynamic *in vitro* model of the human intestine for oral bioavailability studies by using a flow-through transwell system. Firstly, cell viability and barrier integrity were examined to ensure a biological relevant barrier model. Followed by the permeability of, the well-known model compound, verapamil across a monolayer of Caco-2 and HT29-MTX-E12 cells. Verapamil permeability compared well to the golden standard the static transwell. Furthermore, results were benchmarked against *in vitro* permeability data from literature and showed similar results. In Chapter 3b, we will use the established dynamic *in vitro* model to examine the uptake of the natural mycotoxin ergotamine. Additionally, the system allows for future extension with an integrated online analysis system for semi continuous readout of absorption and biotransformation (Chapter 4).

Chapter 3b - Ergotamine

Abstract

Ergot alkaloids are mycotoxins that are produced by the fungus *Claviceps purpurea* upon infection of certain grains, like wheat and rye. Ergot alkaloids can end up in the food chain and thereby cause a harmful effect in humans. The most predominantly occurring ergot alkaloid is ergotamine and its epimer ergotaminine. However, the transport mechanism of ergotamin(in)e across the intestinal barrier is largely unknown. In this study, we examined the permeability of ergotamin(in)e across a monolayer of Caco-2 and HT29-MTX-E12 cells in a static and dynamic *in vitro* intestinal model system. A higher permeability of the epimer ergotaminine was observed compared to ergotamine in the static *in vitro* model. This difference was lost in the dynamic model experiments. Highlighting the importance of flow and flow induced shear stress on the cell monolayer and subsequently on permeability of a compound.

Keywords: Ergot alkaloids, ergotamine, stereoselective, intestinal permeability

3.5 Introduction

Examining the toxicity and bioavailability of mycotoxins in food is of great importance for risk assessment and the subsequent establishment of the maximum occurrence levels in food commodities. Mycotoxins are secondary metabolites produced by fungi that can infect crops and thereby end up in the food chain. Ergot alkaloids are a class of mycotoxins found in plants infested with the fungus of the genus *Claviceps*, with *Claviceps purpurea* being the most predominant [48]. Plants infected with these fungi belong to the *Poaceae* family, which includes grains, like wheat, rye, barley and oats. Ergot alkaloids are found in the sclerotia (ergot bodies) stage of the fungi, which are the dark purple protrusions visible in an infected plant (Figure 3.6). The ergot bodies are the overwintering stage of the *C. purpurea* fungus and can easily detach from the plant and spread across a field. In the summer and spring under cool and wet conditions the ergot bodies can germinate and form ascospores (sexual, non-motile spores), which are disseminated by rain or wind [49]. Upon infection of the plant, millions of conidia (asexual, non-motile spores) are produced and collect in the sap of the host plant, this sap is also known as honeydew. Insects are attracted to the honeydew and thereby cause a secondary spread of the fungi [50](Figure 3.6). Finally, the fungus matures inside the plant producing the ergot bodies closing the life cycle of *C. purpurea*.

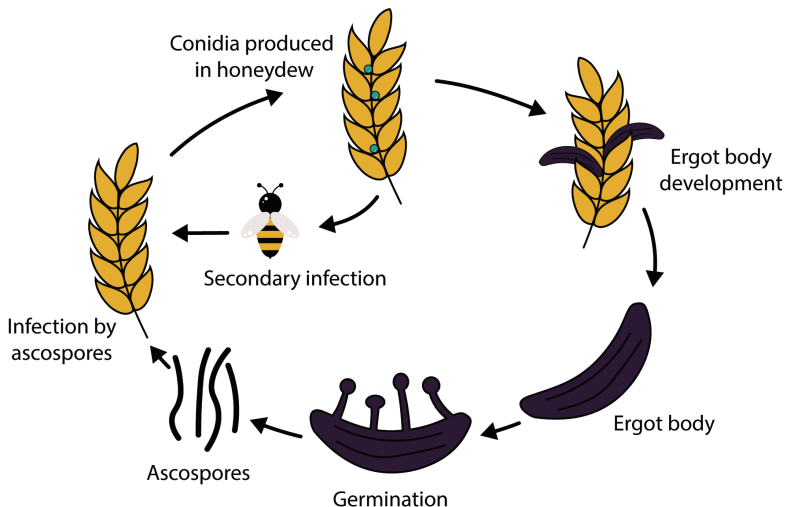


Figure 3.6: Life cycle of *Claviceps purpurea* on grains

Physical cleaning steps are undertaken to prevent ergot alkaloid contamination [51], nevertheless ergot alkaloids are still detected in several food products, mostly in cereals [52]. The toxic effects of ergot alkaloids are related to disruption of neurotransmission as ergot alkaloids are structurally similar to adrenaline, noradrenaline, dopamine and serotonin [53]. High intake of ergot alkaloids can result in ergotism also known as Saint Anthony's Fire, with symptoms such as headaches, spasms and vasoconstriction [54]. In the past couple of years an increase is seen in ergot alkaloid monitoring [52, 55-59], due to the call from the European commission to actively screen for ergot alkaloids in cereals and cereal products [60]. The European Food Safety Authority (EFSA) reported on human and animal exposure levels to ergot alkaloids and found the highest levels of ergot alkaloids in rye and rye containing products. The most predominant ergot alkaloid found was ergotamine and its epimer ergotaminine (Figure 3.7) [61]. Even though the -inine epimer is considered not biologically active, epimerization can occur under various conditions and could thus add to toxicity [62]. Human oral bioavailability of ergotamine was found to be low, only ~1% [63], however *in vitro* ergotamine intestinal permeability to elucidate its uptake mechanism has yet to be studied.

Therefore, here we examined the *in vitro* permeability of the ergot alkaloid ergotamine and its epimer ergotaminine across an intestinal barrier. A co-culture of Caco-2 and HT29-MTX-E12 cells was grown in a traditional transwell system and in a dynamic flow-through transwell system investigating the effect of flow on ergotamin(in)e permeability. Furthermore, cell viability and barrier integrity upon ergotamine exposure were evaluated.

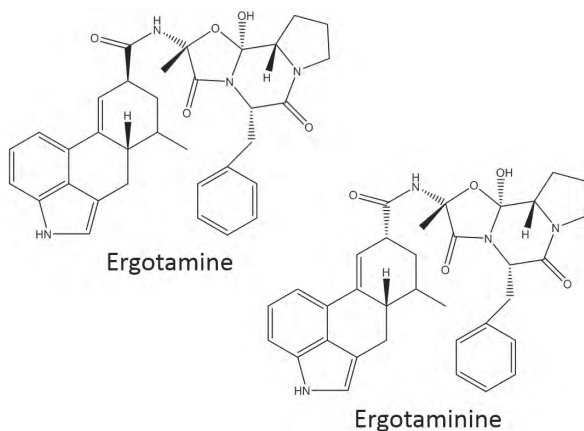


Figure 3.7: Molecular structure ergotamine and ergotaminine

3.6 Materials and Methods

Ergotamin(in)e experiments were performed as described for verapamil (Chapter 3a) with the following modifications:

3.6.1 Cell viability

Possible cytotoxic effects of ergotamin(in)e were evaluated using the cell proliferation assay WST-1. A concentration range of 0 - 20 µg/mL ergotamin(in)e was tested in cell culture medium. The viability of the cells for each concentration of ergotamin(in)e was expressed as a percentage of the negative control consisting of cell culture medium with 0.5% DMSO, as ergotamin(in)e was dissolved in cell culture medium using 0.5% DMSO. Triton-X100 (0.25%, v/v) was used as a positive control and decreased the cell viability to $4.8 \pm 2.7\%$.

3.6.2 Cell permeability experiments

For the static and dynamic cell permeability experiments ergotamin(in)e (10 µg/mL) was used suspended in HBSS (without phenol red) containing 25 mM of HEPES and 0.35 g/L NaHCO₃ as the donor solution.

3.6.3 LC-MS/MS analysis

Apical and basolateral ergotamin(in)e samples of the static transwell experiments were diluted 20 times in methanol/water 60/40 (v/v) prior to LC-MS/MS analysis, as were the apical transwell samples of the dynamic experiments. The basolateral samples of the dynamic experiments were analysed undiluted. Chromatographic separation was achieved using a Waters (Milford, MA, USA) Acquity I-Class UPLC system equipped with an Acquity UPLC BEH C18 (100 mm x 2.1 mm, 1.7 µm) column (Waters). The column temperature was kept at 50°C and the injector was kept at 10°C. A 2 µL injection volume was used. Mobile phase A consisted of 10 mM ammonium carbonate in water (pH 9) and mobile phase B consisted of acetonitrile. The mobile phase gradient started at 0% B and was linearly increased to 10% B in 1 min followed by an increase to 30% B in 10 min and returned to 0% B in 0.2 min, all at a constant flow rate of 0.4 mL/min. A mobile phase equilibration time of 2.6 min was allowed prior to the next injection. The first minute of the gradient elution was directed to waste to prevent salts from the HBSS matrix to enter the ion source of the MS. Mass spectrometric detection was performed using a Waters Xevo TQS tandem mass

spectrometer equipped with an electrospray ionisation interface (ESI) and operated in positive ion mode, with a capillary voltage of 3.0 kV, a desolvation temperature of 600 °C, a gas flow rate of 800 L/h, a source temperature of 150 °C and a cone gas flow rate of 150 L/h. For ergotamin(in)e four MRM transitions were measured (Table 3.2). For quantification of ergotamin(in)e a calibration curve was constructed. Calibration solutions were prepared in HBSS and subsequently diluted in methanol/water 60/40 (v/v) similar as the samples. Resulting in a calibration curve with the following points: 0, 0.01, 0.05, 0.1, 0.5, 1, 2.5, 5 and 10 µg/mL. LOD and LOQ were calculated as the average signal of five blank samples plus three (LOD) or ten (LOQ) times the SD of the blank samples divided by the sensitivity (slope of the calibration curve) using the transition m/z 582.4 > 208.1 resulting in a LOD of 1 ng/mL and LOQ of 1.9 ng/mL. The concentration of ergotamin(in)e in the unknown samples was then calculated using the peak area measurements in the RIC of the transition m/z 582.4 > 208.1 via interpolation of the external matrix-matched calibration curve ($r^2=0.99$).

Table 3.2. Multiple reaction monitoring (MRM) acquisition parameters for LC-MS/MS analysis of ergotamin(in)e. The reconstructed ion current (RIC) of the transitions in bold were used for quantitation using external calibration.

Compound	Precursor (m/z)	Product (m/z)	Cone (V)	Collision energy (eV)
Ergotamin(in)e	582.4	208.1	30	40
		223.1	30	35
		268.1	30	25
		277.1	30	25

3.7 Results and Discussion

We first established the Caco-2/HT29-MTX-E12 monolayer on a permeable transwell insert and examined its barrier integrity upon ergotamin(in)e exposure. We have looked at the permeability of Lucifer yellow after permeability experiments with ergotamin(in)e. Cell barrier with permeability higher than 5% of the apical concentrations were determined as leaking and discarded. In this study cell barriers used for ergotamin(in)e permeability calculations showed $0.46 \pm 0.02\%$ Lucifer yellow permeability. Furthermore, as shown in figure 3.8 a concentration of ergotamin(in)e at or below 10 µg/mL showed no toxicity. Human studies have shown overall low oral bioavailability [63, 64] of ergotamine

and therefore it has been classified to be a BCS III compound, meaning a low permeability compound [65]. Therefore, we used the highest non-toxic dose possible for the ergotamin(in)e permeability experiments (10 $\mu\text{g}/\text{mL}$).

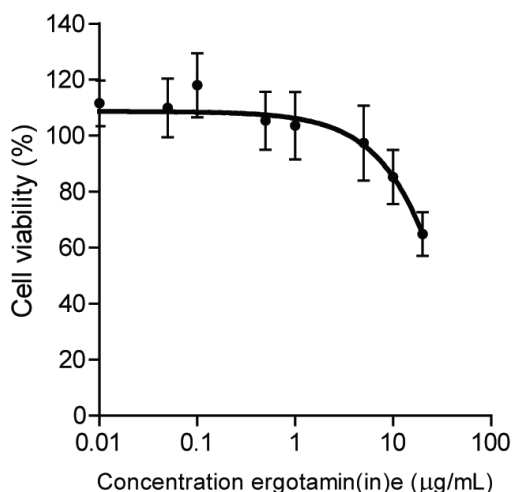


Figure 3.8: Cell viability after 24 h exposure to increasing concentrations of ergotamine. Viability is given as a percentage of the control ($\% \pm \text{SEM}$; $n=3$)

We examined the permeability of the epimers ergotamine and ergotaminine from the ergot alkaloid family, across the *in vitro* intestinal barrier. Permeability of ergotamin(in)e across the barrier of Caco-2 and HT29-MTX-E12 cells in both the static and dynamic experiments was measured by LC-MS/MS [52]. In the static experiments ergotamine permeability reached a concentration of 4.9% of the apical concentration. Interestingly, the permeability of the ergotaminine epimer reached a concentration of 32.5% after 3 hours in the static experiments (Figure 3.9a). The higher permeability of ergotaminine compared to ergotamine could be due to epimerization of ergotamine to ergotaminine either chemically in the basolateral compartment or biologically within the cells. The microenvironment surrounding the cells is kept stable during the 3 hour experiments with no changes in pH or temperature, furthermore the donor solution containing ergotamin(in)e is heated 2 hours before the start of each experiment to come to an equilibrium between the two epimers as suggested by Mulac and Humpf (2011) [66]. Another explanation could be that ergotamin(in)e is actively transported by the efflux transporter P-glycoprotein (P-gp) back into the apical compartment and has more affinity with ergotamine

than with ergotamine. Bromocriptine, another member of the ergot alkaloid family, is a known substrate for the efflux transporter P-gp [67]. For verapamil (Chapter 3a) and ergotamine we found similar permeability coefficients across the static and dynamic model systems, whereas for ergotamine, permeability is 5 times lower in the dynamic experiments compared to the static (Figure 3.9a+b). Interestingly, in the dynamic experiment measurements the large difference between the epimer permeability rates is lost. P_{app} values for the ergotamine epimer in the dynamic experiments are on the same level as for the ergotamine epimer (Figure 3.9c). This difference clearly suggests that not the microenvironment as such, but the cell layer is responsible for selective transport of the epimers and/or epimerization.

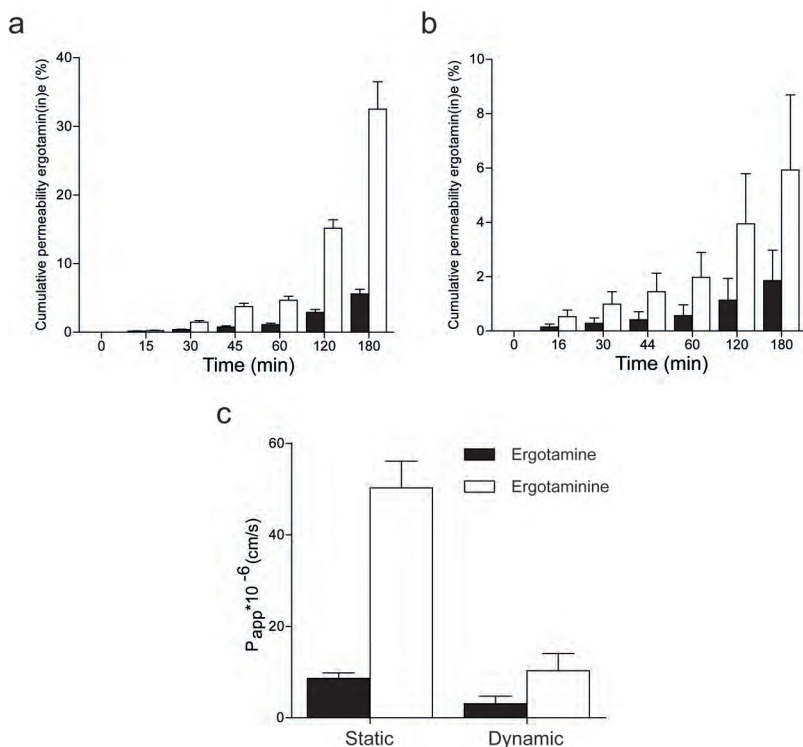


Figure 3.9: **a)** Permeability of ergotamin(in)e across a monolayer of Caco-2/HT29-MTX-E12 cells in a static transwell. Permeability is given as a percentage of the apical concentration ($\% \pm$ SEM; $n=3$). **b)** Permeability of ergotamin(in)e across a monolayer of Caco-2/HT29-MTX-E12 cells in the dynamic flow-through transwell. Permeability is given as a calculated cumulative percentage of the apical concentration ($\% \pm$ SEM; $n=3$). **c)** Apparent permeability coefficient for ergotamin(in)e in the static and dynamic transwell model ($P_{app} \times 10^{-6}$ cm/s \pm SEM; $n=3$).

3.8 Conclusions

Here we have examined for the first time the *in vitro* intestinal permeability of the epimers ergotamine and ergotamine. Cell viability and barrier integrity were evaluated upon ergotamin(in)e exposure ensuring a relevant *in vitro* model system. Ergotamin(in)e permeability was measured across a monolayer of Caco-2 and HT29-MTX-E12 cells in a static and dynamic environment, showing a clear difference in ergotamine permeability between the static and dynamic system. This clearly shows that for different compounds classes the effect of flow on the cell layer can influence the uptake of that compound. Highlighting the added value of a dynamic *in vitro* intestinal model system for permeability studies.

Acknowledgements

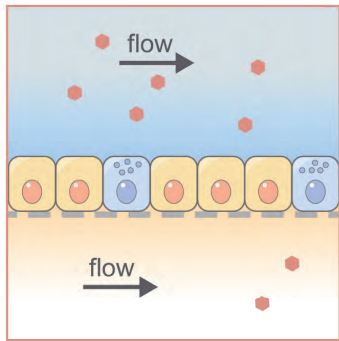
This research received funding from the Dutch Research Council (NWO) in the framework of the Technology Area PTA-COAST3 (project nr. 053.21.116) of the Fund New Chemical Innovations with Wageningen University, University of Groningen, Wageningen Food Safety Research, FrieslandCampina, Micronit Microtechnologies, Galapagos and R-biopharm as partners. We thank Patrick Mulder and Elena de Vries from Wageningen Food Safety Research for assistance with the LC-MS/MS analysis of ergotamin(in)e.

References

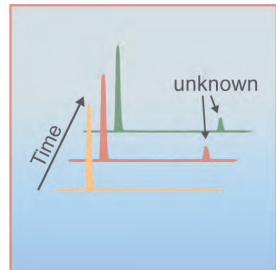
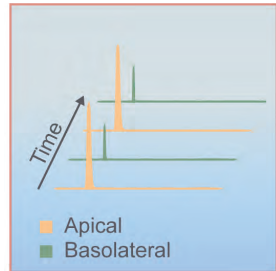
- [1] Buckley ST, Fischer SM, Fricker G, Brandl M. In vitro models to evaluate the permeability of poorly soluble drug entities: challenges and perspectives. *Eur J Pharm Sci.* 2012;45(3):235-250.
- [2] Hubatsch I, Ragnarsson EG, Artursson P. Determination of drug permeability and prediction of drug absorption in Caco-2 monolayers. *Nat Protoc.* 2007;2(9):2111-2119.
- [3] Artursson P, Palm K, Luthman K. Caco-2 monolayers in experimental and theoretical predictions of drug transport. *Adv Drug Deliv Rev.* 2001;46(1-3):27-43.
- [4] Sambuy Y, Angelis I, Ranaldi G, Scarino ML, Stammati A, Zucco F. The Caco-2 cell line as a model of the intestinal barrier: influence of cell and culture-related factors on Caco-2 cell functional characteristics. *Cell Biol Toxicol.* 2005;21(1):1-26.
- [5] Artursson P, Karlsson J. Correlation between oral-drug absorption in humans and apparent drug permeability coefficients in human intestinal epithelial (Caco-2) cells. *Biochem Biophys Res Commun.* 1991;175(3):880-885.
- [6] Sun H, Chow ECY, Liu S, Du Y, Pang KS. The Caco-2 cell monolayer: usefulness and limitations. *Expert Opin Drug Met.* 2008;4(4):395-411.
- [7] Cheng KC, Li C, Uss AS. Prediction of oral drug absorption in humans - from cultured cell lines and experimental animals. *Expert Opin Drug Met.* 2008;4(5):581-590.
- [8] Hilgendorf C, Spahn-Langguth H, Regardh CG, Lipka E, Amidon GL, Langguth P. Caco-2 versus Caco-2/HT29-MTX co-cultured cell lines: Permeabilities via diffusion, inside- and outside-directed carrier-mediated transport. *J Pharm Sci.* 2000;89(1):63-75.
- [9] Behrens I, Stenberg P, Artursson P, Kissel T. Transport of lipophilic drug molecules in a new mucus-secreting cell culture model based on HT29-MTX cells. *Pharm Res.* 2001;18(8):1138-1145.
- [10] Pan F, Han L, Zhang Y, Yu Y, Liu J. Optimization of Caco-2 and HT29 co-culture in vitro cell models for permeability studies. *Int J Food Sci Nutr.* 2015;66(6):680-685.
- [11] Billat PA, Roger E, Faure S, Lagarce F. Models for drug absorption from the small intestine: where are we and where are we going? *Drug Discov Today.* 2017;22(5):761-775.
- [12] Zheng FY, Fu FF, Cheng Y, Wang CY, Zhao YJ, Gu ZZ. Organ-on-a-chip systems: Microengineering to biomimic living systems. *Small.* 2016;12(17):2253-2282.
- [13] Ergir E, Bachmann B, Redl H, Forte G, Ertl P. Small Force, Big Impact: Next generation organ-on-a-chip systems incorporating biomechanical cues. *Front Physiol.* 2018;9:1417.
- [14] Sosa-Hernandez JE, Villalba-Rodríguez AM, Romero-Castillo KD, Aguilar-Aguila-Isaias MA, Garcia-Reyes IE, Hernandez-Antonio A, et al. Organs-on-a-chip module: A review from the development and applications perspective. *Micromachines-Basel.* 2018;9(10):536.
- [15] Rothbauer M, Rosser JM, Zirath H, Ertl P. Tomorrow today: organ-on-a-chip advances towards clinically relevant pharmaceutical and medical in vitro models. *Curr Opin Biotech.* 2019;55:81-86.
- [16] Bein A, Shin W, Jalili-Firoozinezhad S, Park MH, Sontheimer-Phelps A, Tovaglieri A, et al. Microfluidic organ-on-a-chip models of human intestine. *Cell Mol Gastroenterol.* 2018;5(4):659-668.
- [17] Esch MB, Mahler GJ, Stokol T, Shuler ML. Body-on-a-chip simulation with gastrointestinal tract and liver tissues suggests that ingested nanoparticles have the potential to cause liver injury. *Lab Chip.* 2014;14(16):3081-3092.
- [18] Pocock K, Delon L, Bala V, Rao S, Priest C, Prestidge C, et al. Intestine-on-a-chip microfluidic model for efficient in vitro screening of oral chemotherapeutic uptake. *ACS Biomater Sci Eng.* 2017;3(6):951-959.
- [19] Ramadan Q, Jafarpoorchehab H, Huang CB, Silacci P, Carrara S, Koklu G, et al. NutriChip: nutrition analysis meets microfluidics. *Lab Chip.* 2013;13(2):196-203.
- [20] Shim KY, Lee D, Han J, Nguyen NT, Park S, Sung JH. Microfluidic gut-on-a-chip with three-dimensional villi structure. *Biomed Microdevices.* 2017;19(2):37.
- [21] Kim HJ, Huh D, Hamilton G, Ingber DE. Human gut-on-a-chip inhabited by microbial flora that experiences intestinal peristalsis-like motions and flow. *Lab Chip.* 2012;12(12):2165-2174.
- [22] Imura Y, Asano Y, Sato K, Yoshimura E. A Microfluidic System to Evaluate Intestinal Absorption. *Anal Sci.* 2009;25(12):1403-1407.

- [23] Kasendra M, Tovaglieri A, Sontheimer-Phelps A, Jalili-Firoozinezhad S, Bein A, Chalkiadaki A, et al. Development of a primary human small intestine-on-a-chip using biopsy-derived organoids. *Sci Rep-Uk*. 2018;8(1):2871.
- [24] Tan HY, Trier S, Rahbek UL, Dufva M, Kutter JP, Andresen TL. A multi-chamber microfluidic intestinal barrier model using Caco-2 cells for drug transport studies. *Plos One*. 2018;13(5):e0197101.
- [25] Trietsch SJ, Naumovska E, Kurek D, Setyawati MC, Vormann MK, Wilschut KJ, et al. Membrane-free culture and real-time barrier integrity assessment of perfused intestinal epithelium tubes. *Nat Commun*. 2017;8(1):262.
- [26] Santbergen MJC, van der Zande M, Bouwmeester H, Nielen MWF. Online and in situ analysis of organs-on-a-chip. *Trac-Trend Anal Chem*. 2019;115:138-146.
- [27] Giusti S, Sbrana T, La Marca M, Di Patria V, Martinucci V, Tirella A, et al. A novel dual-flow bioreactor simulates increased fluorescein permeability in epithelial tissue barriers. *Biotechnol J*. 2014;9(9):1175-1184.
- [28] Yeon JH, Park JK. Drug permeability assay using microhole-trapped cells in a microfluidic device. *Anal Chem*. 2009;81(5):1944-1951.
- [29] Chen ML, Sundrud MS. Xenobiotic and endobiotic handling by the mucosal immune system. *Curr Opin Gastroen*. 2018;34(6):404-412.
- [30] Hooper LV. Epithelial cell contributions to intestinal immunity. *Adv Immunol*. 2015;126:129-172.
- [31] Vancamelbeke M, Vermeire S. The intestinal barrier: a fundamental role in health and disease. *Expert Rev Gastroent*. 2017;11(9):821-834.
- [32] Turner JR. Molecular basis of epithelial barrier regulation - From basic mechanisms to clinical application. *Am J Pathol*. 2006;169(6):1901-1909.
- [33] Hidalgo IJ, Raub TJ, Borchardt RT. Characterization of the human-colon carcinoma cell-line (Caco-2) as a model system for intestinal epithelial permeability. *Gastroenter*. 1989;96(3):736-749.
- [34] Kulthong K, Duivenvoorde L, Mizera BZ, Rijkers D, ten Dam G, Oegema G, et al. Implementation of a dynamic intestinal gut-on-a-chip barrier model for transport studies of lipophilic dioxin congeners. *Rsc Adv*. 2018;8(57):32440-32453.
- [35] Galkin A, Fallarero A, Vuorela PM. Coumarins permeability in Caco-2 cell model. *J Pharm Pharmacol*. 2009;61(2):177-184.
- [36] Engman H, Tannergren C, Artursson P, Lennernas H. Enantioselective transport and CYP3A4-mediated metabolism of R/S-verapamil in Caco-2 cell monolayers. *Eur J Pharm Sci*. 2003;19(1):57-65.
- [37] Tubic-Grozdanis M, Bolger MB, Langguth P. Application of gastrointestinal simulation for extensions for biowaivers of highly permeable compounds. *AAPS J*. 2008;10(1):213-226.
- [38] Manson SM. Simplifying complexity: a review of complexity theory. *Geoforum*. 2001;32(3):405-414.
- [39] Winiwarter S, Bonham NM, Ax F, Hallberg A, Lennernas H, Karlen A. Correlation of human jejunal permeability (in vivo) of drugs with experimentally and theoretically derived parameters. A multivariate data analysis approach. *J Med Chem*. 1998;41(25):4939-4949.
- [40] Sun DX, Lennernas H, Welage LS, Barnett JL, Landowski CP, Foster D, et al. Comparison of human duodenum and Caco-2 gene expression profiles for 12,000 gene sequences tags and correlation with permeability of 26 drugs. *Pharmaceut Res*. 2002;19(10):1400-1416.
- [41] Gao D, Liu HX, Lin JM, Wang YN, Jiang YY. Characterization of drug permeability in Caco-2 monolayers by mass spectrometry on a membrane-based microfluidic device. *Lab Chip*. 2013;13(5):978-985.
- [42] Pauli-Magnus C, von Richter O, Burk O, Ziegler A, Mettang T, Eichelbaum M, et al. Characterization of the major metabolites of verapamil as substrates and inhibitors of P-glycoprotein. *J Pharmacol Exp Ther*. 2000;293(2):376-382.
- [43] Fossati L, Dechaume R, Hardillier E, Chevillon D, Prevost C, Bolze S, et al. Use of simulated intestinal fluid for Caco-2 permeability assay of lipophilic drugs. *Int J Pharm*. 2008;360(1-2):148-155.
- [44] Faasen F, Vogel G, Spanjns H, Vromans H. Caco-2 permeability, P-glycoprotein transport ratios and brain penetration of heterocyclic drugs. *Int J Pharm*. 2003;263(1-2):113-122.
- [45] Westerhout J, de Steeg EV, Gossouw D, Zeijdner EE, Krul CAM, Verwei M, et al. A new approach to predict human intestinal absorption using porcine intestinal tissue and biorelevant matrices. *Eur J Pharm Sci*. 2014;63:167-177.

- [46] Turco L, Catone T, Caloni F, Di Consiglio E, Testai E, Stammati A. Caco-2/TC7 cell line characterization for intestinal absorption: how reliable is this in vitro model for the prediction of the oral dose fraction absorbed in human? *Toxicol In Vitro*. 2011;25(1):13-20.
- [47] Lozoya-Agullo I, Araujo F, Gonzalez-Alvarez I, Merino-Sanjuan M, Gonzalez-Alvarez M, Bermejo M, et al. Usefulness of Caco-2/HT29-MTX and Caco-2/HT29-MTX/Raji B coculture models to predict intestinal and colonic permeability compared to Caco-2 monoculture. *Mol Pharm*. 2017;14(4):1264-1270.
- [48] Haarmann T, Rolke Y, Giesbert S, Tudzynski P. Ergot: from witchcraft to biotechnology. *Mol Plant Pathol*. 2009;10(4):563-577.
- [49] Mitchell DT, Cooke RC. Some Effects of Temperature on Germination and Longevity of Sclerotia in *Claviceps Purpurea*. *T Brit Mycol Soc*. 1968;51(5):721-729.
- [50] Schiff PL. Ergot and its alkaloids. *Am J Pharm Educ*. 2006;70(5):98.
- [51] Franzmann C, Schroder J, Mupsilonnzing K, Wolf K, Lindhauer MG, Humpf HU. Distribution of ergot alkaloids and ricinoleic acid in different milling fractions. *Mycotoxin Res*. 2011;27(1):13-21.
- [52] Mulder PPJ, Pereboom-de Fauw DPKH, Hoogenboom RLAP, de Stoppelaar J, de Nijs M. Tropane and ergot alkaloids in grain-based products for infants and young children in the Netherlands in 2011-2014. *Food Addit Contam B*. 2015;8(4):284-290.
- [53] Klotz JL. Activities and Effects of ergot alkaloids on livestock physiology and production. *Toxins*. 2015;7(8):2801-2821.
- [54] EFSA. Scientific opinion on ergot alkaloids in food and feed. *EFSA J*. 2012;10(7):2798.
- [55] Tittlemier SA, Drul D, Roscoe M, McKendry T. Occurrence of ergot and ergot alkaloids in western canadian wheat and other cereals. *J Agr Food Chem*. 2015;63(29):6644-6650.
- [56] Bryla M, Ksieniewicz-Wozniak E, Podolska G, Waskiewicz A, Szymczyk K, Jedrzejczak R. Occurrence of ergot and its alkaloids in winter rye harvested in Poland. *World Mycotoxin J*. 2018;11(4):635-646.
- [57] Topi D, Jakovac-Strajn B, Pavsic-Vrtac K, Tavcar-Kalcher G. Occurrence of ergot alkaloids in wheat from Albania. *Food Addit Contam A*. 2017;34(8):1333-1343.
- [58] Orlando B, Maumene C, Piraux F. Ergot and ergot alkaloids in French cereals: occurrence, pattern and agronomic practices for managing the risk. *World Mycotoxin J*. 2017;10(4):327-338.
- [59] Debegnach F, Patriarca S, Brera C, Gregori E, Sonogo E, Moracci G, et al. Ergot alkaloids in wheat and rye derived products in Italy. *Foods*. 2019;8(5).
- [60] Recommendation C. 2012/154/EU on the monitoring of the presence of ergot alkaloids in feed and food. *O J EU*. 2012. p. 20-21.
- [61] Arcella D, Ruiz JAG, Innocenti ML, Roldan R, Authority EFSA. Human and animal dietary exposure to ergot alkaloids. *EFSA J*. 2017;15(7).
- [62] Hafner M, Sulyok M, Schuhmacher R, Crews C, Krska R. Stability and epimerisation behaviour of ergot alkaloids in various solvents. *World Mycotoxin J*. 2008;1(1):67-78.
- [63] Little PJ, Jennings GL, Skews H, Bobik A. Bioavailability of dihydroergotamine in man. *Br J Clin Pharmacol*. 1982;13(6):785-790.
- [64] Sanders SW, Haering N, Mosberg H, Jaeger H. Pharmacokinetics of ergotamine in healthy volunteers following oral and rectal dosing. *Eur J Clin Pharmacol*. 1986;30(3):331-334.
- [65] Sun L, Liu X, Xiang R, Wu C, Wang Y, Sun Y, et al. Structure-based prediction of human intestinal membrane permeability for rapid in silico BCS classification. *Biopharm Drug Dispos*. 2013;34(6):321-335.
- [66] Mulac D, Humpf HU. Cytotoxicity and accumulation of ergot alkaloids in human primary cells. *Toxicol*. 2011;282(3):112-121.
- [67] Vautier S, Lacomblez L, Chacun H, Picard V, Gimenez F, Farinotti R, et al. Interactions between the dopamine agonist, bromocriptine and the efflux protein, P-glycoprotein at the blood-brain barrier in the mouse. *Eur J Pharm Sci*. 2006;27(2-3):167-174.



Dynamic In Vitro
Intestinal Barrier Model



Chapter 4

Dynamic *in vitro* intestinal barrier model coupled to chip-based liquid chromatography mass spectrometry for oral bioavailability studies

This chapter was adapted from
M.J.C. Santbergen, M. van der Zande, A. Gerssen, H. Bouwmeester and M.W.F. Nielen. Dynamic *in vitro* intestinal barrier model coupled to chip-based liquid chromatography mass spectrometry for oral bioavailability studies. *Analytical and Bioanalytical Chemistry* (2020);412:1111-1122

Abstract

In oral bioavailability studies, evaluation of the absorption and transport of drugs and food components across the intestinal barrier is crucial. Advances in the field of organ-on-a-chip technology have resulted in a dynamic gut-on-a-chip model that better mimics the *in vivo* microenvironment of the intestine. Despite a few recent integration attempts, ensuring a biological relevant microenvironment while coupling with a fully online detection system still represents a major challenge. Herein, we designed an online technique to measure drug permeability and analyse (un)known product formation across an intestinal epithelial layer of Caco-2 and HT29-MTX cells cultured on a flow-through transwell system, while ensuring the quality and relevance of the biological model. Chip-based ultra-performance liquid chromatography quadrupole time-of-flight mass spectrometry (UPLC-QTOF-MS) was coupled to the dynamic transwell via a series of switching valves, thus allowing alternating measurements of the apical and basolateral side of the *in vitro* model. Two trap columns were integrated for online sample pre-treatment and compatibility enhancement. Temporal analysis of the intestinal permeability was successfully demonstrated using verapamil as a model drug and ergotamine epimers as a model for natural mycotoxins present in foods. Evidence was obtained that our newly developed dynamic online analysis system provides reliable results versus offline analysis. Finally, initial experiments with the drug granisetron suggest that metabolic activity can be studied as well, thus highlighting the versatility of the bio-integrated online analysis system developed.

Keywords: Gut-on-a-chip, chip-based liquid chromatography, mass spectrometry, intestinal barrier, oral bioavailability

4.1 Introduction

Human oral bioavailability is defined as the fraction of a compound that reaches the systemic circulation after oral ingestion [1]. Before a compound reaches its activation site it undergoes digestion, absorption and metabolism both in the intestine and the liver. Currently, animals and static *in vitro* cell culture models are used to capture these complex processes and predict the human response [2, 3]. However, with the rise of techniques such as soft-lithography [4], thermal moulding [5], 3D printing [6] and laser machining [7] more complex *in vitro* cell culture models have become available, the so called organs-on-a-chip. These dynamic cell culture models can integrate the biochemical and mechanical triggers that are present in the human body, like fluid shear stresses, biochemical gradients and mechanical strain [4, 8, 9]. Capturing these key features in an *in vitro* cell culture model can significantly improve the predictive power of these models [10]. In Chapter 3, we have discussed the development and evaluation of a dynamic *in vitro* intestinal barrier model for predicting uptake of chemicals by the human intestine. We have shown a biologically relevant *in vitro* cell culture model suited for permeability studies. Besides that dynamic model systems better represent the *in vivo* microenvironment they also provide the possibility to fully automate the system by integration with an analytical detection system [11]. This however, implies serious compatibility challenges for measurements in the highly complex chemical composition of cell culture media that typically contains very high concentrations of salts, proteins, dyes and antibiotic drugs.

Theoretically, electrospray ionization mass spectrometry (ESI-MS) would be the technique of choice for integration with a dynamic *in vitro* cell culture system, as ionization takes place in the liquid phase [12]. Furthermore, MS is well suited for multi-analyte detection and apart from analyte transport across the cellular barrier also (un)known product formation (e.g. metabolites) can be monitored. However, due to the complex chemical composition of the cell culture medium integration of dynamic *in vitro* models with ESI-MS requires extensive sample preparation to ensure system compatibility [11]. Several semi-integrated systems have been reported, in which solid phase extraction (SPE) columns were used as a sample pre-treatment step [13-17]. In these reports, the sample pre-treatment steps required manual operations to flush

the SPE column, hampering full automation and compromising robustness of the system. Few online integrations have been described in literature [18, 19], but unfortunately, they did not report on biological integrity for assuring a relevant organ-on-a-chip model. A complete online integration featuring an evidence-based biologically relevant dynamic *in vitro* intestinal barrier system and ESI-MS detection, has not been described yet in literature.

In this study, we uniquely integrated a dynamic *in vitro* model of the intestine with a chip-based ultra-performance liquid chromatography quadrupole time-of-flight (UPLC-QTOF) MS analysis system for oral bioavailability and biotransformation studies. This combines a dynamic cell barrier system together with automated and continuous analytical read out of translocation processes and cell induced product formation while maintaining full biological integrity and without compromising the analytical performance. For this a co-culture of Caco-2 and HT29-MTX cells was grown in a flow-through transwell system, connected to the UPLC-QTOF-MS via a series of switching valves. The switching valves allow for alternating UPLC-QTOF-MS measurements of the apical and basolateral side of the flow-through transwell system. Prior to chromatographic separation two nanotrap columns are integrated in the series of switching valves for sample pre-treatment. To benchmark the online total analysis system for absorption studies, the permeability of two model compounds is examined (i.e. verapamil and ergotamine) and compared to offline analysis. Some initial experiments have been performed with the drug granisetron to show future application of the system for biotransformation studies.

4.2 Experimental Section

4.2.1 Chemicals and reagents

Verapamil hydrochloride, ergotamin(in)e d-tartrate, penicillin-streptomycin, formic acid, Lucifer yellow, 4-(2-hydroxyethyl)-1-piperazineethanesulfonic acid (HEPES), sodium bicarbonate (NaHCO_3), ammonium carbonate, Triton-X100 and Hank's balanced salt solution (HBSS), with and without phenol red, were purchased from Sigma-Aldrich/Merck (Steinback, Germany). Dulbecco's Modified Eagle Medium (DMEM) with 4.5 g/L glucose and L-glutamine with and without phenol red, bovine serum albumin (BSA) and heat-inactivated fetal

bovine serum (FBS) were purchased from Gibco (Bleiswijk, the Netherlands). Dimethyl sulfoxide (DMSO), phosphate buffered saline (PBS) and non-essential amino acids (NEAA) were obtained from Thermo Fisher Scientific (Landsmeer, the Netherlands). Acetonitrile and methanol were purchased from Actua-chemicals (Oss, the Netherlands). Granisetron was purchased from TCI Europe (Zwijndrecht, Belgium), paraformaldehyde from VWR (Amsterdam, the Netherlands), WST-1 reagent from Roche Diagnostics GmbH (Mannheim, Germany) and water was daily prepared using a Milli-Q Reference Water Purification System from Millipore (Burlington, MA, USA).

4.2.2 Cell culturing

The human colonic adenocarcinoma Caco-2 cell line was obtained from the American Type Culture Collection (ATCC, Manassas, VA, USA) and the human colon adenocarcinoma mucus secreting HT29-MTX-E12 cell line was obtained from the European Collection of Authenticated Cell Cultures (ECACC, Salisbury, UK). Caco-2 cells were used at passage numbers 29-40 and HT29-MTX-E12 cells were used at passage numbers 52-70 for all experiments. Cells were cultured in DMEM containing 10% FBS, 1% NEAA and 1% penicillin-streptomycin and maintained at 37°C in a 5% CO₂-humidified air atmosphere and subcultured every 2 to 3 days. For permeability experiments cells were seeded at a density of 40,000 cells/cm² on a polycarbonate transwell insert (area 0.6 cm², 0.4 μm pore size, Millipore) as follows: Caco-2 and HT29-MTX-E12 cells were seeded in a 3:1 ratio on the apical side of the transwell and allowed to attach for 24 hours. After 24 hours, cell culture medium was refreshed every 2-3 days and transwells were used for permeability experiments after 21 days of culturing. All dynamic online cellular experiments were conducted using the flow-through transwell system (discussed in Chapter 3).

4.2.3 Cell viability

Possible cytotoxic effects of granisetron were evaluated using the cell proliferation assay WST-1, as follows: Caco-2 and HT29-MTX-E12 cells (ratio 3:1) were seeded in Greiner bio-one (Alphen aan den Rijn, the Netherlands) flat bottom 96-well plates at a concentration of 1 x 10⁵ cells/mL in cell culture medium (100 μL/well). Plates were incubated for 24 hours at 37°C under 5% CO₂. Cell culture medium was removed and subsequently the cells were exposed to 100 μL/well serial dilutions of granisetron (0 – 1000 μg/mL) in cell

culture medium for 24 hours, at 37°C. Then, the exposure media containing the compounds was discarded and the cells were washed with pre-warmed HBSS. Subsequently, WST-1 reagent (in cell culture medium without phenol red) was added to the cells (1:10, 100 µL/well). After 1.5 hour of incubation at 37°C, the absorbance of each well was measured at 440nm using a Bio-Tek (Winooski, VT, USA) Synergy HT Multi-Mode microplate reader. The viability of the cells for each concentration of granisetron was expressed as a percentage of the negative control consisting of cell culture medium. Triton-X100 (0.25%, v/v) was used as a positive control and decreased the cell viability to 0.0±0.4%.

4.2.4 Flow-through transwell coupled online with chip UPLC-QTOFMS

A series of three 2 position/10-port UltraLife switching valves (IDEX Health & Science, Oak Harbor, WA, US) with 1/16" fittings were used to interface the flow-through transwell to the chip UPLC-QTOFMS. Apical and basolateral effluents from the flow-through transwell were alternatingly loaded onto 5 µL stainless steel sample loops, mounted on the first and second switching valve (Figure 4.1). Each sample loop was loaded for 15 min at 200 µL/min (apical) and 100 µL/min (basolateral), the detailed valve switching program is listed in Table 4.1. After 15 min of sample collection the sample loop was flushed for 4 minutes towards an Optimize Technologies (Oregon City, OR, USA) C8 nanotrap column (180 µm i.d. x 5 mm, particle size 2.7 µm) using an aqueous solvent (H₂O with 1% acetonitrile) at a flow rate of 20 µL/min. Following the clean-up, the nanotrap column was eluted towards a chip-based iKey BEH C18 analytical column (150 µm i.d. x 50 mm, particle size 1.7 µm) (Waters). The 3 µL/min microflow gradient for verapamil and granisetron experiments consisted of mobile phase A, water with 1% acetonitrile and mobile phase B, acetonitrile with 1% water, both containing 0.1% formic acid. The gradient started at 0% B and after 4 min was linearly increased to 100% B in 4 min. This composition was kept for 3 min and returned to 0% B in 0.1 min. An equilibration time of 3.9 min was allowed prior to the next injection. For ergotamin(in)e experiments the gradient consisted of mobile phase A, water with 10 mM ammonium carbonate (pH 9) and mobile phase B, acetonitrile. The gradient started at 30% B and after 4 min was linearly increased to 70% B in 6 min. This composition was kept for 1 min and returned to 30% B in 0.2 min. An equilibration time of 3.8 min was allowed prior to the next injection. The complete process is illustrated in Figure 4.1. Data were collected using MassLynx v4.1 software, yielding a separate data

file for each nanotrap analysis, or in other words alternatingly for the apical and basolateral sides of the dynamic *in vitro* model. Mass spectrometric detection was performed with a Waters Xevo QTOF mass spectrometer equipped with an iKey nano electrospray ionisation interface. The mass spectrometer was operated in positive ion mode, with a capillary voltage of 3.9 kV, a desolvation temperature of 350 °C, a gas flow rate of 400 L/h, a source temperature of 80 °C and a cone gas flow rate of 10 L/h.

Table 4.1 Valve switching program for online coupling of dynamic flow through transwell effluents with iKey-UPLC-QTOFMS

Apical Sample			Basolateral Sample		
Time (min)	Switching valve	Action	Time (min)	Switching valve	Action
Initial	1	Off	Initial	1	On
Initial	2	On	Initial	2	Off
Initial	3	On	Initial	3	Off
0.1	1	On	0.1	1	Off
0.1	2	Off	0.1	2	On
4.10	3	Off	4.10	3	On

4.2.5 Evaluation of carry-over in the online chip-based UPLC-QTOFMS analysis system

Carry-over for the online chip-based UPLC-QTOFMS analysis system was assessed for the initial (Figure 4.2) and final (Figure 4.1) systems by removing the flow-through transwell model and instead connecting two syringes directly at the valve inlets for the apical and basolateral effluent. First, the syringe connected at the apical inlet contained 5 µg/mL of verapamil in HBSS and the syringe connected at the basolateral inlet contained HBSS only. The online analysis system was run for 6-8 measurements, and any appearance of a verapamil peak in the basolateral measurements was a sign of carry over. This experiment was repeated, but then with the syringe containing 5 µg/mL of verapamil attached at the basolateral valve inlet.

4.2.6 Data analysis

The apparent permeability coefficient (P_{app} , cm/s) was calculated as described by Yeon and Park (2009) [20], according to the following equation:

$$P_{app} = \frac{dQ}{dt} \frac{1}{A C_0}$$

Where dQ/dt is the cumulative transport rate in the basolateral compartment ($\mu\text{mol/s}$), A is the surface area of the cell layer (0.6 cm^2) and C_0 is the initial concentration of the compounds in the apical compartment ($\mu\text{mol}/\text{cm}^3$).

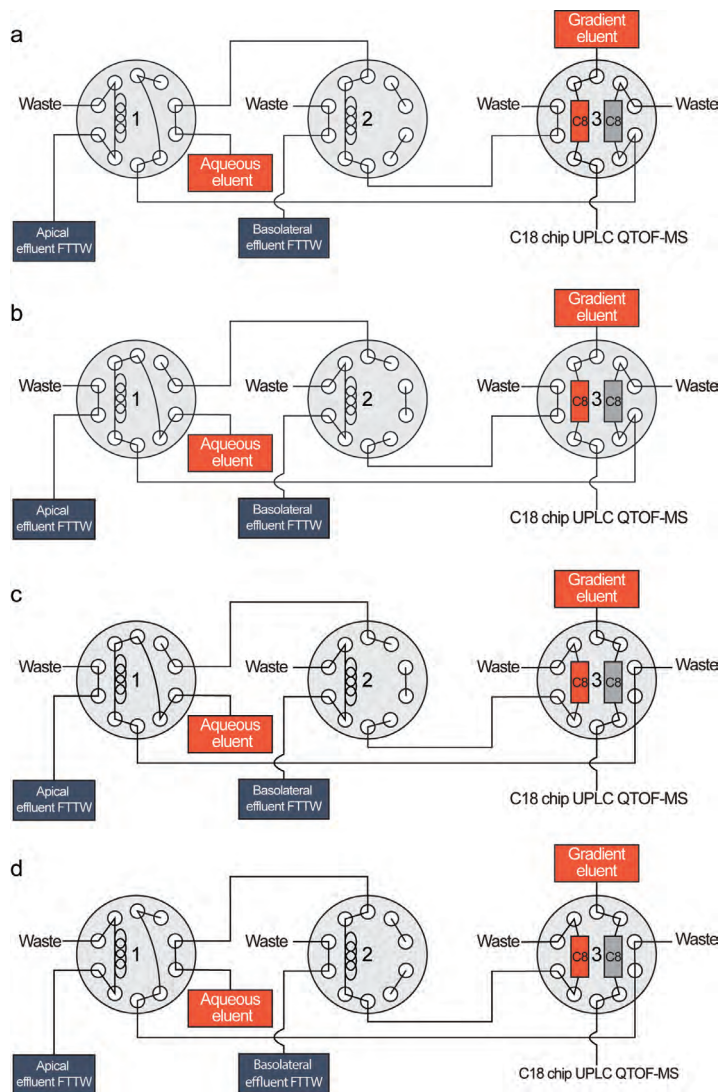


Figure 4.1: Schematic depiction of the final flow-through transwell (FTTW) to chip-UPLC-QTOFMS coupling using parallel trap columns as interface. The setup consists of three switching valves, two sample loops, two C8 trap columns and a chip-based C18 analytical column. **a)** Sample effluent from the apical side of the FTTW fills the sample loop in the first switching valve for 15 minutes, while aqueous effluent flows through the second sample loop to the waste. **b)** After 15 minutes sample collection the first valve switches and aqueous effluent flows through the first sample loop towards the C8 trap column in the third switching valve. The aqueous effluent loads the sample onto the trap column and

rinses away the salts. At the same time, the second valve switches to collect effluent from the basolateral side of the FTTW. c) Subsequently, a gradient from aqueous to organic solvent runs through the trap column in the third valve, through the analytical column and to the MS. d) The next valve switch flushes the sample collected from the basolateral side of the FTTW to the trap column. The analytes captured on the trap column are eluted by the gradient from aqueous to organic solvent onto the analytical column and to the MS (a). Total analysis from the trap column to the analytical column takes 15 min. The pattern repeats until the *in vitro* biological experiment is completed.

4.3 Results and Discussion

4.3.1 Online flow-through transwell analysis system, design and performance

Initial designs of the online total analysis system consisted of different configurations of the switching valves (Figure 4.2), providing shorter run times and the possibility to select which effluent stream to measure. However, these configurations experienced severe analyte carry over between the two effluent streams, due to shared capillary tubing. We have tried different concentrations of methanol in the eluent that flushes the sample to the C8 trap column, but no optimal concentration could be found without carry over and proper analyte retaining on the nanotrapp column.

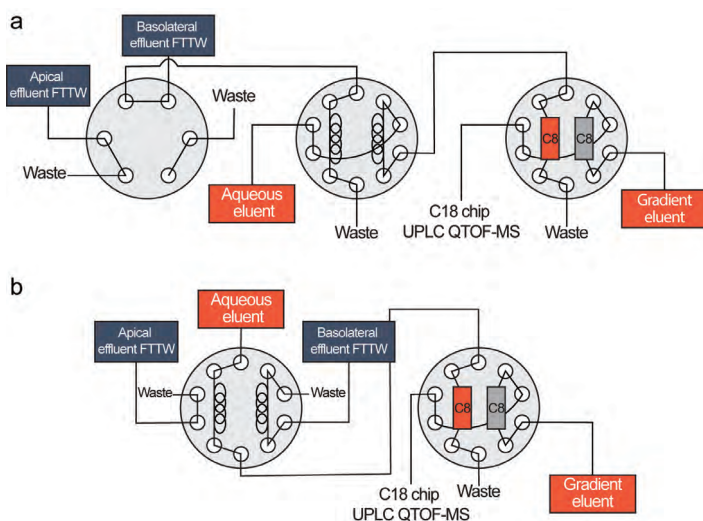


Figure 4.2: Initial configurations of the switching valves. **a)** Series of three switching valves with the possibility to choose the effluent stream to be measured in the first valve, sample collection in the second valve and analyte trapping in the third valve. **b)** Two switching valves, for alternating apical and basolateral sample analysis. In the first valve sample was collected and in the second valve the analyte was trapped on a nanotrapp column.

Finally, the *in vitro* model of the human intestinal epithelium could be successfully integrated with chip-based UPLC-QTOF-MS, using the set-up as shown in figure 4.1, thanks to the separate tubing and trap columns for apical and basolateral effluents, having high and (very) low concentrations of analytes, respectively. A flow-through transwell containing a co-culture of Caco-2 and HT29-MTX cells was operated upstream by a syringe pump equipped with a syringe heater to maintain a physiological relevant temperature of the cell culture medium. HEPES was added to the cell culture medium as a pH buffer to maintain the physiological relevant microenvironment. After starting the exposure, 15 minutes of apical effluent was collected in the sample loop of the first switching valve (Figure 4.1a). The sample was subsequently directed to a C8 nanotrap column integrated on the third switching valve, allowing for analyte trapping and desalting (Figure 4.1b). After trapping, the analyte was separated on a chip-based reversed phase C18 column having an integrated nano electrospray ionization emitter and analysed by QTOF-MS (Figure 4.1c). Total analysis time including sample trapping, desalting and MS measurement was 15 minutes. During these 15 minutes the sample loop in the second switching valve was filled with the basolateral effluent for the next measurement (Figure 4.1b-c) following the same trapping and desalting steps (Figure 4.1d), but in a fully independent fluidic part of the set-up in order to exclude any carry-over. Thus, every 15 min there was a switch between the apical and basolateral channel and this process repeated until the end of the biological experiment. This final design turned out to be the best compromise with regards to lack of carry-over, analysis time, frequency of sampling and analytical robustness. System stability was proven by introducing 5 µg/mL verapamil in HBSS for three hours into the automated total analysis system by a syringe pump. During the complete run time of the experiment retention time for the verapamil peak at 6.8 min was found to be stable (Figure 4.3a). Also, the pressure profile of the UPLC gradient pump attached to the third switching valve that runs over the trap columns and the analytical column confirmed no increase (column clogging) or decrease of pressure during the three-hour measurements (Figure 4.3b), thus demonstrating adequate removal of the very high level of salts in the medium.

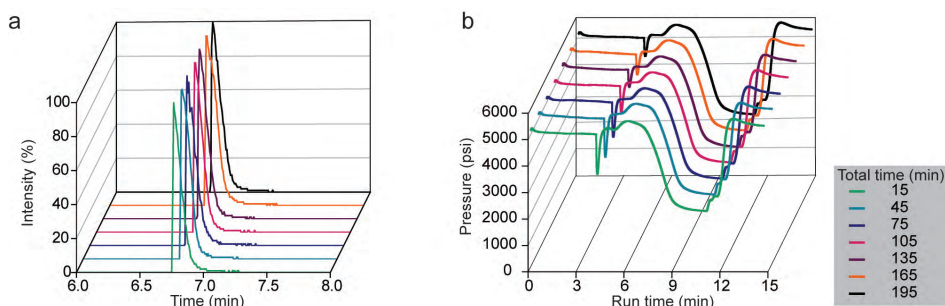


Figure 4.3: a) Peak stability of verapamil during three hours of measurements. b) Pressure stability gradient pump running through the nanotrap column and analytical column for three hours of measurements

4.3.2 Temporal analysis of intestinal permeability

To demonstrate the feasibility of the flow-through transwell coupled to chip-based UPLC QTOF-MS for permeability studies, the apparent permeability coefficients (P_{app}) were calculated for verapamil and ergotamin(in)e and compared to the P_{app} values obtained with offline analysis in chapter 3. Online mass spectrometry analysis systems are intrinsically more complex than offline analysis system, as they require online sample collection, sample clean-up (due to the cellular matrix) and analysis [18, 19, 21]. Nevertheless, both the offline and the newly developed online analysis system show similar P_{app} values for verapamil (Figure 4.4). Confirming that the increased complexity in the online analysis system does not affect the biological outcome for verapamil. For ergotamin(in)e the differences between the offline and online analysis are larger, deviation between individual biological samples is also greater (Figure 4.4). Recalling the static versus dynamic data from chapter 3 regarding ergotamin(in)e flow seems to influence the uptake of the ergotaminine epimer and to a lesser extent the ergotamine epimer. Therefore, larger deviations between biological samples in the dynamic analysis are to be expected, this might explain the larger differences for the ergotamin(in)e experiments. Our online analysis system allows for automated and non-invasive read-out of the dynamic responses of the *in vitro* intestinal model to chemicals in semi real-time. This is highly coveted for kinetic studies and long-term exposure experiments. Moreover, it eliminates most of the manually handling reducing the chance of human error. Furthermore, our system is flexible in the sense that sample loops, nanotrap columns and analytical columns can easily be changed

to suite different analytes. Which is more complex in systems that use on chip sample loops or SPE columns [14, 16, 18]. From a biological standpoint, shorter analysis times might be preferred as rapidly transporting compounds already reach their permeability equilibrium within 15 minutes [22]. In literature, only a few organ-on-a-chip system integrated with MS have shorter analysis times [16, 19], but not shorter than 9 minutes.

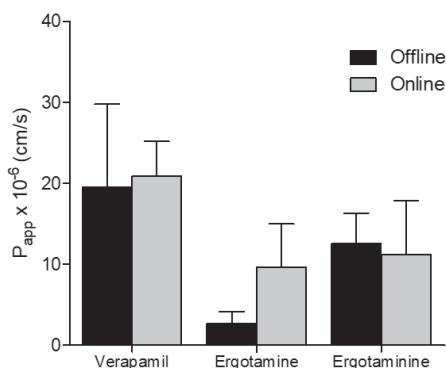


Figure 4.4: Apparent permeability coefficient of verapamil, ergotamine and ergotaminine offline (data taken from chapter 3, black) versus online analysis (grey) (\pm SEM; n=3).

4.3.3 Potential for online analysis of cell-induced product formation

With the analysis of verapamil and ergotamin(in)e we have demonstrated the robustness of the online analysis system to measure intestinal absorption in time. Besides temporal permeability analysis the system could be suited for the detection of cell-induced product formation as well. For an initial feasibility experiment we selected the compound granisetron (Figure 4.5a), which is a serotonin 5-HT₃ receptor antagonist [23] as a model substrate for metabolism in our intestinal barrier model. Granisetron is an oral drug that is used against nausea as a result of chemotherapy [24] and is metabolized by the enzymes CYP1A1 and CYP3A4, resulting in 7-hydroxygranisetron and 9-desmethylgranisetron, respectively [25]. Caco-2 cells express the CYP1A1 enzyme, suggesting that granisetron might be metabolised in our Caco-2/HT29-MTX model [26]. First a non-toxic concentration of 10 μ g/ml granisetron was established (Figure 4.5b). Next, an initial experiment was conducted using the newly developed dynamic online analysis system. After 3 hours of exposure 13.1% of granisetron translocated the *in vitro* intestinal barrier (Figure 4.5c), but unfortunately no metabolites were detected on the basolateral side

of the cell barrier. Nevertheless, an additional ion with m/z 309 appeared on the apical side of the membrane (Figure 4.5d). It was confirmed that the formation of this unknown compound was due to the presence of the cells, as the ion at m/z 309 was not detected after 24 hours incubation in the same matrix at 37°C without cells (Figure S4.1, Supplemental information). In other words, we can exclude chemical degradation as the cause of the product formation and therefore the formation of this unknown compound is due to the biologically active cells through either metabolism of granisetron itself or excretion of an unknown cell metabolite. More research is needed to elucidate the structure of this compound. Nevertheless, these results demonstrate the applicability and robustness of the automated online analysis system for measuring unknown product formation in the *in vitro* intestinal model.

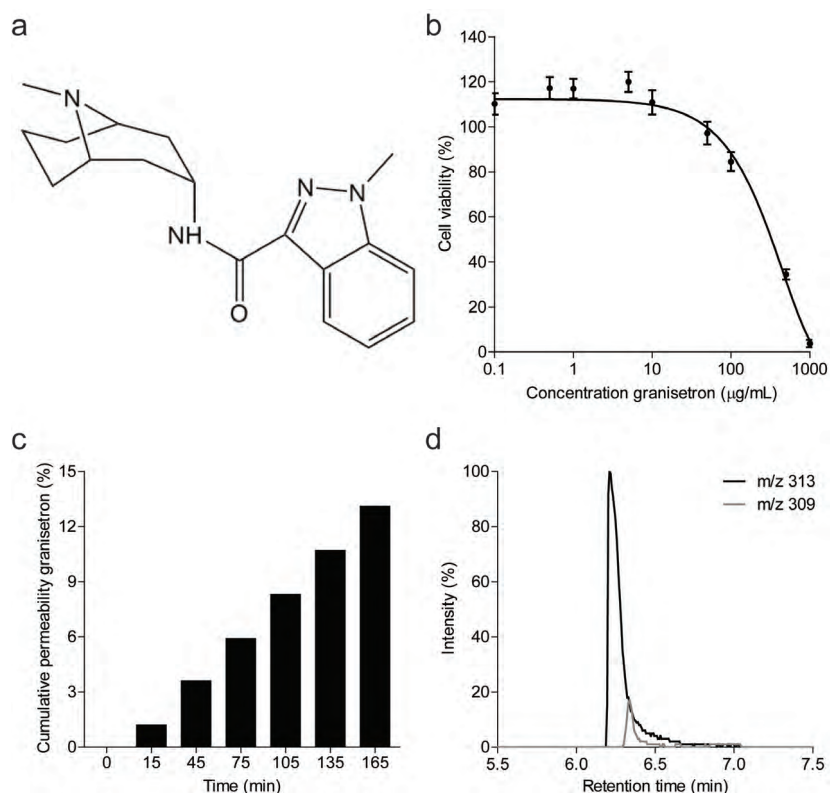


Figure 4.5: **a)** Chemical structure granisetron. **b)** Cell viability after 24 h exposure to increasing concentrations of granisetron. Viability is given as a percentage of the control (% \pm SEM; $n=3$). **c)** Cumulative permeability of granisetron across a monolayer of Caco-2/HT29-MTX cells in the dynamic flow-through transwell with online analysis. Permeability is given as a calculated cumulative percentage of the apical concentration ($n=1$). **d)** reconstructed-ion chromatogram of m/z 313 ($[M+H]^+$ ion of granisetron) and an unknown ion m/z 309 at time point 30 minutes on the apical side.

4.4 Conclusions

Here we developed an integrated online analysis system for the detection of intestinal absorption and unknown product formation by using a flow-through transwell and mass spectrometry while ensuring full bio-integrity. The biggest strength of the online analysis system is the combination of a relevant dynamic biological model of the intestine with semi continuous online analytical detection. The permeability of verapamil and ergotamin(in)e across a monolayer of Caco-2 and HT29-MTX cells was successfully studied in a time resolved manner without the need for any manual handling. Furthermore, we were able to detect an unknown product upon stimulating the intestinal cell layer with granisetron. While this work should be considered as a proof of concept a wide range of different drugs, toxins or dietary compounds can be easily evaluated using this system, even other cell types can be easily incorporated into the flow-through transwell system for more complex biological studies looking at the interaction of different cell types. Finally, the system easily allows future extension with a dynamic *in vitro* oral digestion system to provide a full oral bioavailability system with semi continuous readout of absorption and biotransformation (Chapter 5).

Acknowledgements

This research received funding from the Dutch Research Council (NWO) in the framework of the Technology Area PTA-COAST3 (project nr. 053.21.116) of the Fund New Chemical Innovations with Wageningen University, University of Groningen, Wageningen Food Safety Research, FrieslandCampina, Micronit Microtechnologies, Galapagos and r-Biopharm as partners.

References

- [1] Musther H, Olivares-Morales A, Hatley OJD, Liu B, Hodjegan AR. Animal versus human oral drug bioavailability: Do they correlate? *Eur J Pharm Sci.* 2014;57:280-291.
- [2] Harloff-Helleberg S, Nielsen LH, Nielsen HM. Animal models for evaluation of oral delivery of biopharmaceuticals. *J Control Release.* 2017;268:57-71.
- [3] Butler J, Hens B, Vertzoni M, Brouwers J, Berben P, Dressman J, et al. In vitro models for the prediction of in vivo performance of oral dosage forms: Recent progress from partnership through the IMI OrBiTo collaboration. *Eur J Pharm Biopharm.* 2019;136:70-83.
- [4] Kim HJ, Huh D, Hamilton G, Ingber DE. Human gut-on-a-chip inhabited by microbial flora that experiences intestinal peristalsis-like motions and flow. *Lab Chip.* 2012;12(12):2165-2174.
- [5] Jeon JS, Chung S, Kamm RD, Charest JL. Hot embossing for fabrication of a microfluidic 3D cell culture platform. *Biomed Microdevices.* 2011;13(2):325-333.
- [6] Knowlton S, Yenilmez B, Tasoglu S. Towards single-step biofabrication of organs on a chip via 3D printing. *Trends Biotechnol.* 2016;34(9):685-688.
- [7] Pensabene V, Costa L, Terekhov AY, Gnecco JS, Wikswo JP, Hofmeister WH. Ultrathin polymer membranes with patterned, micrometric pores for organs-on-chips. *ACS Appl Mater Interfaces.* 2016;8(34):22629-22636.
- [8] Zheng FY, Fu FF, Cheng Y, Wang CY, Zhao YJ, Gu ZZ. Organ-on-a-chip systems: Microengineering to biomimic living systems. *Small.* 2016;12(17):2253-2282.
- [9] Huh D, Matthews BD, Mammoto A, Montoya-Zavala M, Hsin HY, Ingber DE. Reconstituting organ-level lung functions on a chip. *Science.* 2010;328(5986):1662-1668.
- [10] Bhatia SN, Ingber DE. Microfluidic organs-on-chips. *Nat Biotechnol.* 2014;32(8):760-772.
- [11] Santbergen MJC, van der Zande M, Bouwmeester H, Nielen MWF. Online and in situ analysis of organs-on-a-chip. *Trac-Trend Anal Chem.* 2019;115:138-146.
- [12] Jie MS, Mao SF, Li HF, Lin JM. Multi-channel microfluidic chip-mass spectrometry platform for cell analysis. *Chinese Chem Lett.* 2017;28(8):1625-1630.
- [13] Gao D, Li H, Wang N, Lin JM. Evaluation of the absorption of methotrexate on cells and its cytotoxicity assay by using an integrated microfluidic device coupled to a mass spectrometer. *Anal Chem.* 2012;84(21):9230-9237.
- [14] Gao D, Liu H, Lin JM, Wang Y, Jiang Y. Characterization of drug permeability in Caco-2 monolayers by mass spectrometry on a membrane-based microfluidic device. *Lab Chip.* 2013;13(5):978-985.
- [15] Wei H, Li H, Gao D, Lin JM. Multi-channel microfluidic devices combined with electrospray ionization quadrupole time-of-flight mass spectrometry applied to the monitoring of glutamate release from neuronal cells. *Analyst.* 2010;135(8):2043-2050.
- [16] Mao S, Zhang J, Li H, Lin JM. Strategy for signaling molecule detection by using an integrated microfluidic device coupled with mass spectrometry to study cell-to-cell communication. *Anal Chem.* 2013;85(2):868-876.
- [17] Wei H, Li H, Mao S, Lin JM. Cell signaling analysis by mass spectrometry under coculture conditions on an integrated microfluidic device. *Anal Chem.* 2011;83(24):9306-9313.
- [18] Dugan CE, Grinias JP, Parlee SD, El-Azzouny M, Evans CR, Kennedy RT. Monitoring cell secretions on microfluidic chips using solid-phase extraction with mass spectrometry. *Anal Bioanal Chem.* 2017;409(1):169-178.
- [19] Marasco CC, Enders JR, Seale KT, McLean JA, Wikswo JP. Real-time cellular exometabolome analysis with a microfluidic-mass spectrometry platform. *Plos One.* 2015;10(2):e0117685.
- [20] Yeon JH, Park JK. Drug permeability assay using microhole-trapped cells in a microfluidic device. *Anal Chem.* 2009;81(5):1944-1951.
- [21] Mao SF, Li WW, Zhang Q, Zhang WL, Huang QS, Lin JM. Cell analysis on chip-mass spectrometry. *Trac-Trend Anal Chem.* 2018;107:43-59.
- [22] Hubatsch I, Ragnarsson EGE, Artursson P. Determination of drug permeability and prediction of drug absorption in Caco-2 monolayers. *Nat Protoc.* 2007;2(9):2111-2119.

Chapter 4

- [23] Gan TJ. Selective serotonin 5-HT₃ receptor antagonists for postoperative nausea and vomiting - Are they all the same? *Cns Drugs*. 2005;19(3):225-238.
- [24] Plosker GL, Goa KL. Granisetron - a review of its pharmacological properties and therapeutic use as an antiemetic. *Drugs*. 1991;42(5):805-824.
- [25] Boppana VK, Miller-Stein C, Schaefer WH. Direct plasma liquid chromatographic-tandem mass spectrometric analysis of granisetron and its 7-hydroxy metabolite utilizing internal surface reversed-phase guard columns and automated column switching devices. *J Chromatogr B*. 1996;678(2):227-236.
- [26] Sergentengelen T, Delistrie V, Schneider YJ. Phase-I and phase-II biotransformations in living Caco 2 cells cultivated under serum-free conditions - selective apical excretion of reaction-products. *Biochem Pharmacol*. 1993;46(8):1393-1401.

Supplemental information

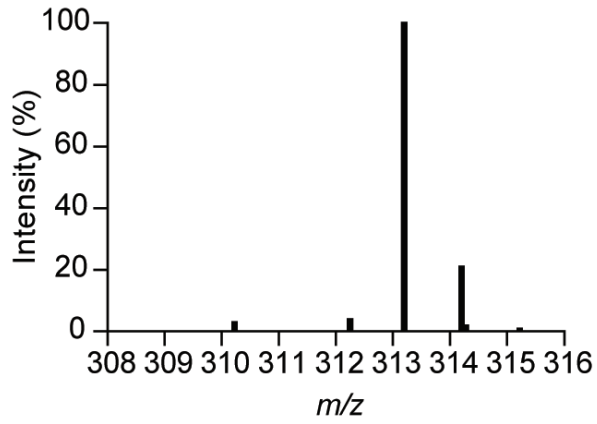


Figure S4.1: Centroided mass spectrum upon positive electrospray ionization of granisetron after 24 hour exposure of exposure to 37°C without the presence of cells in a transwell

Chapter 5

An integrated, modular, *in vitro* gastrointestinal tract total analysis system for oral bioavailability studies

This chapter was adapted from

P. de Haan*, M.J.C. Santbergen*, M. van der Zande, H. Bouwmeester, M.W.F. Nielen and E. Verpoorte. An integrated, modular, *in vitro* gastrointestinal tract – total analysis system for oral bioavailability studies. (*Submitted*)

* These authors contributed equally to this work

Abstract

A novel, integrated, *in vitro* gastrointestinal system is presented to study oral bioavailability of small molecules. Three modules were combined into one hyphenated set-up. In the first module, a compound was exposed dynamically to enzymatic digestion in three consecutive microreactors, mimicking the processes of the mouth, stomach, and intestine. The resulting solution (chyme), continued to the second module, a flow-through barrier model of the intestine allowing translocation of the compound and metabolites thereof. The final module analysed the composition of both effluents from the barrier model by chip-based electrospray ionization mass spectrometry. Apart from technical challenges interfacing the modules, a key challenge is ensuring proper barrier integrity of the intestinal layer under these hyphenated conditions. Two model drugs were used to test the integrated model, omeprazole and verapamil. Omeprazole was shown to be broken down upon treatment with gastric acid, but reached the cell barrier unharmed when emulating an enteric-coated formulation. In contrast, verapamil was unaffected by digestion. Finally, a simple food matrix, apple juice, was introduced into the system resulting in a reduced uptake of verapamil. It is envisaged that this integrated modular gastrointestinal system has great potential for future research in the fields of pharmacology, toxicology, and nutrition.

Keywords: oral bioavailability, digestion-on-a-chip, total analysis system, gastrointestinal tract, gut-on-a-chip, mass spectrometry

5.1 Introduction

The oral bioavailability of ingested compounds is both of pharmacological and toxicological interest. It is a crucial factor, for example, for drug dosing in pharmacotherapy, in the occurrence of oral intoxications, and in nutrition studies. Oral bioavailability is determined by three processes, namely bioaccessibility, absorption and metabolism. A chemical is considered to be bioaccessible if it is released from the matrix (either food or a drug formulation) into the gastrointestinal tract in a form that can be absorbed by the intestinal wall [1]. Parameters in the gastrointestinal tract, such as pH and residence time, are of great influence on bioaccessibility, and there are several *in vitro* digestion models available to study these effects. These models mimic the chemical and enzymatic reactions that take place in the mouth, stomach and small intestine [2, 3]. In the mouth phase, the main process involved in digestion can be ascribed to the enzyme amylase [4]. In the stomach phase, a low pH causes denaturation of proteins, which are then hydrolysed into smaller peptides by the enzyme, pepsin [5]. In the small intestine, the pH is neutralized by the addition of bicarbonate. Enzymes from the pancreas, including proteases and lipases, are introduced [6], as is bile from the gallbladder to emulsify fats [7].

The next processes involved in determining oral bioavailability are absorption and metabolism by the intestinal wall. Absorption of a compound through the intestinal wall may occur via one or more of four mechanisms: 1) active carrier-mediated transport, with membrane transport proteins shuttling compounds over the cell membrane into and out of the cell; 2) transcytosis, a mechanism by which macromolecules are taken up in vesicles along one side of the cell, to then be transported across the cell interior and ejected from the cell at another location; 3) transcellular diffusion, a passive mechanism by which molecules are transported through cells; or 4) paracellular diffusion, passive diffusion of molecules in-between cells to cross the intestinal wall [8]. For small lipophilic drug molecules transcellular diffusion is the most common way of translocation [9]. The third parameter of oral bioavailability is first-pass metabolism of drug compounds by the liver (from portal vein blood) before reaching the central circulation. Currently, animal models and static *in vitro* cell culture models are used to predict oral bioavailability. Besides the obvious ethical issues, animal experiments are expensive and time-consuming and

extrapolation from animal data to predict human oral bioavailability has been shown to be difficult [10]. Static *in vitro* cell culture models of the intestine, based on immortalized human cell lines such as Caco-2 cells, have been used in the past to provide predictive data for human intestinal uptake [11, 12]. However, they do not capture the dynamic features in the intestine, such as peristaltic motion and flow-induced shear stress.

With the rise of microfluidic technology and organ-on-a-chip devices, most cell culture systems involved in oral bioavailability can be miniaturized and automated. One example is the recent development of a three-stage digestion-on-a-chip model where chemical and enzymatic breakdown in the mouth, stomach and intestinal phase is recapitulated [13]. Moreover, a range of different dynamic cell culture systems has been developed, which mimic the intestinal epithelial barrier and are suited for permeability studies [14-20]. These dynamic cell culture systems consist of two chambers separated by a porous membrane containing cells of human intestinal origin. The cells used are either from cell lines, or less frequently, are primary human cells or cells derived from human stem cells. The cells inside the devices are subjected to flow, resulting in a better representation of the *in vivo* intestinal microenvironment by inducing shear stress on the cells [19, 21]. Furthermore, some of these dynamic cell culture systems have been integrated with analytical detection platforms allowing for automated real-time measurements and identification of (un) known metabolites [18, 22-24].

Ideally, a digestion-on-a-chip and a dynamic *in vitro* flow-through intestinal cell culture model with mass spectrometry (MS) detection are hyphenated to study oral bioavailability in one automated system. However, this is highly challenging for several reasons: 1) The digested material, or chyme, produced in the digestive processes contains active enzymes and bile salts, which are known to be harmful to cells in the *in vitro* dynamic intestinal model, thus compromising the integrity of the intestinal barrier module. Also, the chyme does not contain the right nutrients such as glucose in sufficient concentrations for the cells to stay alive even in short-term experiments of about 3 h. 2) The flow rates in all modules should be matched in order to expose the living cells continuously to the chyme, and the drug or metabolite molecules therein, at a constant, physiological shear stress. The fact that the different modules

have significantly different internal volumes means that they are operated in different flow rate ranges. This innate incompatibility requires attention especially in the design of the interfaces between modules. 3) The presence of compounds like the added proteins and salts found in the chyme interfere with the MS analysis due to ion suppression [25]. Thus, there is an increased demand placed on the sample preparation protocol for MS analysis, whose purpose it is to largely remove these background compounds to minimise background chemical noise in the analysis.

In this work, we have successfully combined, for the first time, a microfluidic digestion-on-a-chip with a dynamic, flow-through cell culture model of the intestinal barrier and online MS analysis to study and predict the fate of compounds of interest upon ingestion. In doing so, we have addressed the challenges related to the introduction of chyme to the intestinal cell culture, inherent internal-volume incompatibility between modules, and sample preparation of chyme-medium samples for MS analysis. An automated multi-modular system has been obtained, featuring both enzymatic digestion in the mouth, stomach and intestine, and cellular uptake by the intestinal barrier. Thereby, it enables us to model all the important parameters for oral bioavailability, except for the first-pass metabolism by the liver (which would obviously require another organ model) [26]. We confirmed adequate biological integrity of the Caco-2 and HT29-MTX-E12 cell barrier in the dynamic cell culture system upon exposure to digestive juices using confocal microscopy, and by evaluating cell-barrier permeation by the fluorescent dye, lucifer yellow. The fate of a model drug, omeprazole, known to be sensitive to degradation in the stomach, was studied using either the complete digestion module (*i.e.* mouth, stomach, and intestine) or a simplified, intestinal-digestion-only module coupled to the cell barrier module. The latter experiment mimicked the behaviour of an enteric-coated formulation of omeprazole, which reaches the intestine unaffected by conditions in the mouth and stomach [27]. Next, we coupled the digestion-on-a-chip and dynamic, flow-through intestinal cell culture model with online MS analysis, and measured the uptake of another model drug, verapamil, known not to be influenced by digestive processes. Finally, the impact of a simple food matrix on the *in vitro* bioavailability of verapamil was studied.

5.2 Materials and Methods

5.2.1 Chemicals

Verapamil hydrochloride, omeprazole, penicillin-streptomycin, formic acid, lucifer yellow, 4-(2-hydroxyethyl)-1-piperazineethanesulfonic acid (HEPES), sodium bicarbonate, Triton-X100 and Hank's balanced salt solution (HBSS), with and without phenol red, were all purchased from Sigma-Aldrich/Merck (Zwijndrecht, the Netherlands). Dulbecco's Modified Eagle Medium (DMEM) with 4.5 g/L glucose and L-glutamine with and without phenol red, bovine serum albumin (BSA) and heat-inactivated fetal bovine serum (FBS) were obtained from Gibco (Bleiswijk, the Netherlands). Rabbit polyclonal antibody ZO-1/TJP1 conjugated to Alexa fluor 594, Prolong Diamond Antifade Mountant, dimethyl sulfoxide (DMSO), phosphate-buffered saline (PBS) and non-essential amino acids (NEAA) were bought from Thermo Fisher Scientific (Landsmeer, the Netherlands). All chemicals for digestive juices, including enzymes, came from Sigma-Aldrich/Merck, except sodium dihydrogen phosphate monohydrate and hydrochloric acid (Acros, Geel, Belgium), and potassium chloride and sodium chloride (Duchefa, Haarlem, the Netherlands). Acetonitrile was purchased from Actu-All Chemicals (Oss, the Netherlands), and UPLC-MS grade water from Biosolve (Valkenswaard, the Netherlands). Paraformaldehyde was obtained from VWR (Amsterdam, the Netherlands), polydimethylsiloxane (PDMS) from Dow Corning (Sylgard, Midland, Michigan, USA), and WST-1 reagent from Roche Diagnostics GmbH (Mannheim, Germany). Water was prepared fresh daily using a Milli-Q Reference Water Purification System from Millipore (Burlington, Massachusetts, USA).

5.2.2 Cell culture

The human colorectal adenocarcinoma cell line, Caco-2, was obtained from the American Type Culture Collection (ATCC, Manassas, Virginia, USA) and co-cultured with the human colon adenocarcinoma mucus secreting cell line HT29-MTX-E12 obtained from the European Collection of Authenticated Cell Cultures (ECACC, Salisbury, UK). Cells were used at passage numbers 29-40 and 52-70, respectively. Cell lines were cultured in separate 75 cm² cell culture flasks (Corning, Corning, New York, USA) in cell culture medium (DMEM containing 10% FBS, penicillin-streptomycin (100 U/mL and 100 µg/mL) and 1% NEAA). Cells were maintained in a humidified 5% CO₂ atmosphere at 37°C

and subcultured every 2 to 3 days. The cells were seeded at a density of 40,000 cells/cm² on a polycarbonate 24-well transwell insert (0.4 µm pore size, 0.6 cm² surface area, Millipore) in cell culture medium. Caco-2 and HT29-MTX-E12 cells were seeded on the apical side of the insert at a 3:1 ratio; cell culture medium was replaced every other day. For permeability experiments, transwell inserts were placed into the QV600 system from Kirkstall (Rotherham, UK), henceforth referred to as a flow-through transwell, at day 20 of culture. The apical and basolateral compartments of the flow-through transwell each had internal volumes of 2 mL. Cell culture medium containing 25 mM HEPES was introduced into the apical compartment (200 µL/min, maximum shear stress 6×10^{-3} dyne/cm² [28]) and basolateral compartment (100 µL/min) of the flow-through transwell system using a separate syringe pump (New Era Pump Systems, Farmingdale, New York, USA) for each compartment. Medium was maintained at 37°C and perfusion continued for 24 h, as described by Giusti et al. (2014) [28]. After 24 hours, the apical and basolateral syringes were both replaced by syringes containing HBSS with 25 mM HEPES 0.35 g/L NaHCO₃ added. To assure a biologically relevant environment, syringe heaters (New Era Pump Systems) were used to heat the medium and keep the cells at 37°C without the need for an additional incubator.

5.2.3 Cell viability

Possible cytotoxic effects of omeprazole and chyme were evaluated using the WST-1 cell viability assay. First, Caco-2 and HT29-MTX-E12 cells (ratio 3:1) were seeded in flat bottom 96-well plates (Greiner Bio-One, Alphen aan den Rijn, the Netherlands) at a concentration of 1×10^5 cells/mL in cell culture medium (100 µL/well). Plates were incubated at 37°C under 5% CO₂ for 24 hours. Cell culture medium was removed, and the cells were subsequently exposed for 24 h to 100 µL/well volumes of serial dilutions of omeprazole (0 - 50 µg/mL) or chyme (0 - 100%) in cell culture medium at 37°C. Then, the exposure media containing the compounds was discarded and the cells were washed with pre-warmed HBSS. Subsequently, WST-1 reagent (in cell culture medium without phenol red, as this interferes with absorbance measurements) was added to the cells (1:10, 100 µL/well). After 1.5 hour of incubation at 37°C, the absorbance of each well was measured at 440 nm using a Synergy HT Multi-Mode microplate reader (Bio-Tek, Winooski, Vermont, USA). The viability of the cells for each concentration of chyme was expressed as a percentage of the

negative control consisting of only cell culture medium. For omeprazole, the negative control consisted of cell culture medium with 0.5% DMSO added to match the concentration of DMSO in the samples. Triton-X100 (0.25%, v/v) was used as a positive control and decreased the cell viability to $0.0\pm 0.4\%$.

5.2.4 Evaluation of cell barrier integrity

Barrier integrity was evaluated after cells had been cultured on a transwell membrane for 21 days and subsequently stained for tight junction protein, ZO-1. Just before staining, the cells were washed with PBS and fixed with 4% paraformaldehyde (w/v) for 15 min, permeabilized with 0.25% Triton-X100 (v/v) and blocked with 1% BSA (w/v). The cells were then incubated with 100 μL of solution containing 10 $\mu\text{g}/\text{mL}$ of the conjugated antibody ZO-1/TJP1-Alexa Fluor 594 for 45 min. Between steps, cells were washed with PBS three times. Cells were mounted in a 120 μm spacer (Sigma-Aldrich) on a microscope slide (Thermo Scientific) with ProLong Diamond Antifade Mountant. Slides were then examined using a confocal microscope (LSM 510-META, Zeiss, Jena, Germany), with samples excited with a 543 nm laser at a magnification of 40 X. Cell layer integrity was also evaluated using the transport marker, lucifer yellow. Following drug permeability experiments, the cells were incubated with lucifer yellow at an apical concentration of 500 $\mu\text{g}/\text{mL}$ in HBSS for 30 minutes. HBSS was collected from the apical and basolateral side at $t=0$ and $t=30$ minutes and analysed for fluorescence at 458/530 nm (excitation/emission) using a microplate reader. Cell layers that transported more than 5% of lucifer yellow to the basolateral compartment were judged as leaky and were discarded.

5.2.5 Artificial digestive juices

Artificial saliva, stomach juice, duodenal juice and bile were prepared as described by de Haan et al. [13]; a detailed composition of the juices can be found in Table S1 of the supplementary information (SI). In short, all chemicals except the enzymes were dissolved in ultrapure water and the pH was evaluated using a pH meter (Metrohm 713, Barendrecht, the Netherlands) and adjusted if necessary using HCl or NaOH. After setting the right pH (leading to local pH values of 7.0, 3.0 and 7.0 in the mouth, stomach, and intestine compartment (respectively), the enzymes were added to the juices in order to prevent inactivation or denaturation of enzymes if added to a solution with an aberrant pH.

5.2.6 Modular system design and operation

Fabrication of the digestion-on-a-chip system shown in Fig. 5.1a has been previously described [13]. In short, identical micromixer devices for the three phases of digestion were fabricated by micromolding PDMS on molds made by photolithography in SU-8 photoresist layers deposited on 0.7-mm-thick, polished glass substrates. Mixing channels were 300 μm wide and 51.5 mm long and contained 16 sequential arrays of 12 herringbone-shaped grooves each. Channels were 60 μm deep and 50 μm deeper in the groove regions. Grooves were 110 μm wide and spaced 60 μm apart. The total internal volume of each micromixer was 1.48 μL including inlet channels leading to the groove arrays. The grooves perturb the profile of side-by-side laminar flows entering the mixing channel to generate 'chaotic' flow patterns that result in larger contact areas between solutions. In this way, diffusion distances are shortened substantially, and diffusional mixing times dramatically reduced. The different phases of digestion were connected to each other via polytetrafluoroethylene (PTFE) tubing (0.8/1.6 mm inner/outer diameter, Polyflor Plastics, Breda, the Netherlands) (Fig. 5.1a). Flow for the digestion-on-a-chip was regulated by a pressure-driven flow control system [29]. Pressurized air was passed through a microfilter (PTFE, 0.45 μm pore size, Boom B.V., Meppel, the Netherlands) and distributed to the four glass bottles into which 15 mL tubes (Greiner Bio-One, Frickenhausen, Germany) were placed containing the digestive juices and the sample. Digestive juices in each of the containers were kept at a constant pressure of 500 mbar. PTFE tubing was used to connect the liquid containers to the Coriolis-based mass flow controllers (ML120 and BL100, Bronkhorst High-Tech, Ruurlo, The Netherlands), using blunt Fine-Ject 21G needles (HenkeSassWolf, Tuttlingen, Germany) to connect the tubing. The micro-Coriolis-based mass flow sensors were used to regulate the flow of juices and samples with a far greater stability and accuracy than would be possible with syringe pumps and other flow sensors [29]. A Bronkhorst software package was used to change flow controller settings and to take measurements of mass flow and density. A fourth micromixer (Fig. 5.1b) was incorporated to dilute the chyme from the digestion-on-a-chip with the exposure medium (HBSS) required for permeability experiments, to prevent any cytotoxic effect of chyme on the cells. The effluent from this last micromixer was connected to the apical side of the flow-through transwell (Fig. 5.1b). Subsequently, the flow-through transwell was coupled to either a fraction collector, collecting one sample

every minute in a 96-well plate or microfluidic chip-based UPLC-QTOF-MS via a series of three switching valves (Fig. 5.1c) as described by Santbergen et al. [24]. In short, apical and basolateral effluents from the flow-through transwell were alternately loaded onto 5 μL stainless steel sample loops, mounted on the first and second switching valve (Fig. 5.1c). Each sample loop was loaded for 15 min. After sample collection, the content of each sample loop was depleted of proteins and bile salts by flushing for 4 minutes towards an Optimize Technologies (Oregon City, Oregon, USA) C8 nanotrap column (180 μm x 5 mm, 2.7 μm) using an aqueous solvent (H_2O with 1% acetonitrile) at a flow rate of 20 $\mu\text{L}/\text{min}$. Following the clean-up, the trap column was eluted with a microflow gradient at 3 $\mu\text{L}/\text{min}$ towards a microfluidic iKey chip BEH C18 analytical column for UPLC-QTOF-MS analysis (see below for more details on MS analysis).

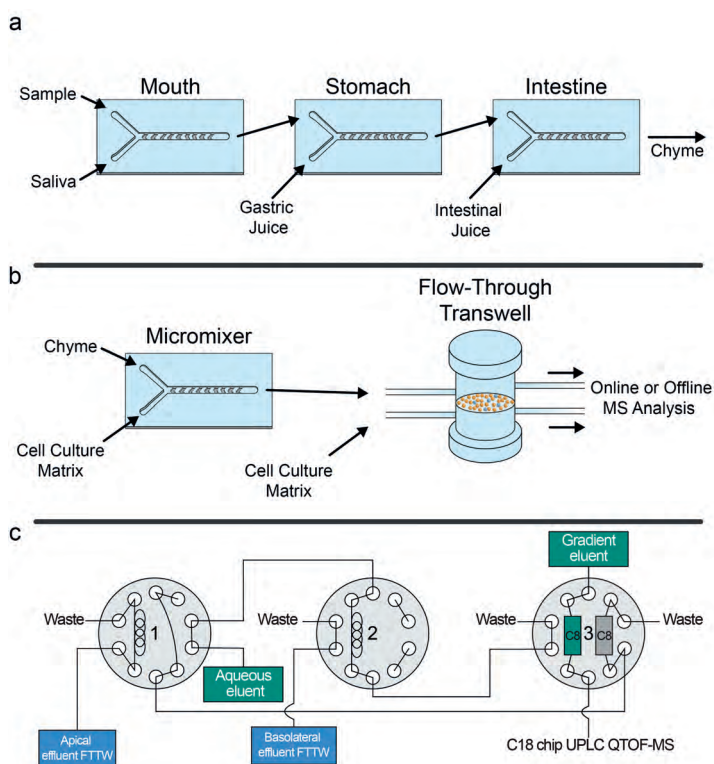


Figure 5.1: Schematic overview of the different components used throughout experiments. **a)** Three chaotic micromixers representing the mouth, stomach and intestinal phase of digestion are coupled to one another using PTFE tubing. Conditions are individually controlled by addition of appropriate artificial juices to each micromixer. **b)** A fourth micromixer is used to mix the chyme from the digestion-

on-a-chip with cell culture matrix needed for the cells, in order to dilute the chyme before exposing cells to it. Effluent was connected to the apical side of the flow-through transwell (FTTW) system containing a co-culture of Caco-2 and HT29-MTX-E12 cells, followed by either fraction collection and offline analysis or c) online analysis that automatically collected sample from the apical and basolateral side in the first and second switching valve, respectively. In the third switching valve, two nanotraps were integrated to retain the analyte of interest and wash away unwanted sugars and salts from the cell matrix. Subsequently, the analyte of interest was eluted to a microfluidic C18 chip-based column and analysed by QTOF-MS. The current state of the valves indicates the initial configuration at the start of the experiment where the apical effluent is collected in the sample loop.

5.2.7 Offline and online UPLC-QTOF-MS analysis

Offline analysis of omeprazole

For the static cell permeability experiments (in transwells), 5 µg/mL omeprazole was suspended in HBSS (without phenol red) containing 25 mM HEPES and 0.35 g/L NaHCO₃ as the donor solution. At day 21 of culture, the donor solution was directly applied to the apical side of the cells (400 µL/insert). The basolateral side was filled with 600 µL of HBSS per insert. Samples were taken (100 µL) from the basolateral side at 15, 30, 45, 60, 120 and 180 minutes, after which the sampled medium was replenished with 100 µL fresh medium. At t=0 and t=180 minutes apical samples were taken. For dynamic experiments (in the flow-through device) including the complete integrated modular gastrointestinal tract (Fig. 5.1a+b), omeprazole was introduced into the digestion-on-a-chip at a concentration of 1 mg/mL in DMSO (1 µL/min). When intestinal digestion only was desired, omeprazole was dissolved in the combined digestive juices from the mouth, stomach and intestine at a concentration of 40 µg/mL before introduction to the micromixer in which chyme was diluted with HBSS. In both cases, the final omeprazole concentration on the apical side of the flow-through transwell was 5 µg/mL. The apical and basolateral effluent flows of the flow-through transwell were directed to a Gilson 234 autosampler (Villiers-le-Bel, France), which was used as a fraction collector in this case to collect samples every minute in a 96-well plate. All samples were analysed undiluted by UPLC-QTOF-MS, using the procedure that is described next. One 2-position/10-port Ultralife switching valve (IDEX Health & Science, Oak Harbor, Washington, USA) with 1/16" fittings was used to incorporate online sample preparation with the microfluidic chip UPLC-QTOF-MS. A nano Acquity autosampler (Waters) set at 10°C and with a 2 µL injector was used. The sample loop was flushed for 4 min with mobile phase A (water with 1% acetonitrile and 0.1% formic acid) at a flow rate of 3 µL/min towards a C8 nanotrap column (Optimize Technologies) (180

μm I.D. x 5 mm, 2.7 μm particles). Following the clean-up, the nanotrap column was eluted towards a microfluidic chip-based iKey BEH C18 analytical column (150 μm I.D. x 50 mm, particle size 1.7 μm) (Waters) by switching the valve. The 3 $\mu\text{L}/\text{min}$ microflow gradient elution consisted of mobile phase A (*cf.* above) and mobile phase B consisting of acetonitrile with 1% water and 0.1% formic acid. The gradient started at 0% B and after 1 min was increased to 50% B in 0.1 min. This composition was maintained for 3.9 minutes, and then increased to 90% in 0.1 min, to be kept constant for 3.9 min. The composition was returned to 0% in 0.1 min and an equilibration time of 3.9 min was allowed prior to the next injection. MS detection was performed with a Waters Xevo QTOF MS equipped with an iKey nano electrospray ionisation source operated in the positive ion mode, with a capillary voltage of 3.9 kV, desolvation temperature of 350 °C, gas flow rate 400 L/h, source temperature of 80 °C and cone gas flow rate of 10 L/h. Data were acquired and processed using MassLynx v4.1 (Waters) software.

Online analysis of verapamil

Verapamil was introduced into the integrated, modular, microfluidic-gastrointestinal-tract total- analysis system at a concentration of 1 mg/mL (Fig. 5.1a) in either ultrapure water or apple juice sample matrices (1 $\mu\text{L}/\text{min}$). Final concentration of verapamil on the apical side of the flow-through transwell was 5 $\mu\text{g}/\text{mL}$. The automated sample clean-up and trapping was described above in the section "Modular system design and operation". In the case of verapamil analysis, the C8 nanotrap column is eluted towards a microfluidic chip-based iKey BEH C18 analytical column using the following gradient. The 3 $\mu\text{L}/\text{min}$ microflow gradient consisted of mobile phase A (water with 1% acetonitrile) and mobile phase B (acetonitrile with 1% water), both containing 0.1% formic acid. The gradient started at 10% B and, after 4 min, was linearly increased to 100% B in 4 min. This composition was kept constant for 3 min, and then reverted to 10% B in 0.1 min. An equilibration time of 3.9 min was allowed prior to the next injection. Mass spectrometric detection was performed with a Waters Xevo QTOF mass spectrometer with the same settings as for the offline analysis of omeprazole. Data were collected using MassLynx, yielding a separate data file for each trap-column analysis.

5.2.8 Permeability calculations

The apparent permeability coefficient (P_{app} , cm/s) was calculated as described by Yeon and Park [30], according to the following equation:

$$P_{app} = \frac{dQ}{dt} \frac{1}{A C_0}$$

In this equation, dQ/dt is the transport rate into the basolateral compartment ($\mu\text{mol/s}$), A is the surface area of the cell layer (0.6 cm^2) and C_0 is the initial concentration of the compounds in the apical compartment ($\mu\text{mol/cm}^3$).

5.3 Results and Discussion

5.3.1 General considerations

Our aim in this study was to develop a modular *in vitro* model of the gastrointestinal tract to investigate the oral bioavailability of orally consumed compounds. Our system is unique as it combines a microfluidic digestion-on-a-chip, an *in vitro* intestinal barrier model and online MS analysis in one automated total analysis system. In the past, these processes have been performed singly and offline, even if they were employed in a combined fashion to carry out digestion and absorption studies. Moreover, static cell culture systems have generally been applied for absorption studies, which may not always be optimal for predicting *in vivo* absorption behaviour [8, 11]. We faced three challenges in the construction and demonstration of our system, namely: 1) the coupling of the different modules to one another, with particular attention needed to design around the significant differences in internal volumes and required flow rates in the different modules. 2) Analysis of solutions that have been processed in the digestion-on-a-chip by MS requires significant sample clean-up (removal of proteins and bile salts) before MS analysis. 3) The co-culture of Caco-2 and HT29-MTX-E12 cells is subjected to damage if exposed to solutions coming from the digestion module. However, maintaining a relevant biological barrier is essential for studying the uptake of compounds. How we addressed these three challenges is described in the next three sections.

In Fig. 5.1, a schematic representation is given of our hyphenated modules. Figure 5.1a depicts the microfluidic digestion-on-a-chip system, consisting

of three 'chaotic' micromixers representing the three phases of digestion, the mouth, stomach and intestine. In the first micromixer, the sample containing the compound of interest (1 $\mu\text{L}/\text{min}$) and the saliva (4 $\mu\text{L}/\text{min}$) were mixed, resulting in an effluent flow of 5 $\mu\text{L}/\text{min}$ from the mouth phase. The mouth phase was connected to the stomach phase by PTFE tubing, creating an incubation time in the oral phase of 2 min resulting from the internal volume of the tubing. In the second micromixer gastric juice (8 $\mu\text{L}/\text{min}$) was mixed with the 5 $\mu\text{L}/\text{min}$ effluent from the mouth, with a gastric incubation time of 120 min determined by the volume of tubing used. Finally, the 13 $\mu\text{L}/\text{min}$ effluent from the gastric phase was mixed with the intestinal juices (12 $\mu\text{L}/\text{min}$) in the third micromixer, resulting in a final chyme flow rate of 25 $\mu\text{L}/\text{min}$ from the digestion-on-a-chip. The incubation time of chyme in the intestinal phase was also 120 min, before reaching the cell culture barrier module. All microfluidic chips were kept at a constant temperature of 37 °C for optimal enzymatic activity. The selected flow rates and residence times in the different compartments were based on average values that are relevant for *in vivo* human physiology [31, 32]. Also, the ratios between the respective flow rates represent the volumetric ratios *in vivo*. Whereas the cells of the intestinal epithelium are exposed to pure (undiluted) chyme *in vivo*, this is not possible in our system as the chyme was toxic to the cells in undiluted form. The chyme from the digestion-on-a-chip was therefore mixed with transport buffer HBSS (175 $\mu\text{L}/\text{min}$) using a fourth micromixer, resulting in an eight-fold dilution of the chyme on the apical side of the cells. Note that at this stage the original sample solution had been diluted 200 times in total, so sufficiently high solubility of the compound of interest in the sample solution and the detection limit of the final analysis method must be considered. The effluent from the fourth micromixer was connected to the apical side of the flow-through transwell (Fig. 5.1b), with a total flow rate of 200 $\mu\text{L}/\text{min}$, causing a realistic shear stress on the cells in accordance with the *in vivo* range (0.002-0.08 dyne/cm²) [19, 28]. Finally, the effluent from the flow-through transwell was either connected to a fraction collector or to the automated online analysis system (Fig. 5.1c).

A consideration for especially the online UPLC-QTOF-MS analysis of the apical effluent is that through the addition of chyme, the chemical interference will increase compared to previous studies when the sample was only dissolved in much cleaner HBSS buffer [24]. However, even though there was an increased background caused by the increased complexity of the sample matrix, it was

still possible to record mass spectra and reconstructed ion chromatograms of characteristic drug ions. Our system is unique in the fact that it combines a microfluidic digestion-on-a-chip, an *in vitro* intestinal barrier model and mass spectrometry analysis in one automated online total analysis system, whereas in the past these processes were performed offline and using static cell culture systems [2, 33]. But most importantly, as mentioned above, pure chyme is toxic to the Caco-2 and HT29-MTX-E12 cells used in our flow-through transwell model. Therefore, it was crucial to first investigate the effects of chyme on the barrier integrity of the cell layer, both before and after the experiments.

Ensuring a biologically relevant intestinal cell barrier is vital when performing *in vitro* permeability studies. As alluded to above, pure chyme is toxic to the Caco-2 and HT29-MTX-E12 cells used in our flow-through transwell model. Therefore, it was crucial to investigate the effects of chyme on the barrier integrity of the cell layer, both before and after experiments in which cell layers were exposed to chyme. Therefore, we studied the co-culture of Caco-2 and HT29-MTX-E12 cells in the presence of chyme using three different techniques. First, to determine the toxicity of the digestive juices coming from the digestion-on-a-chip, we used a WST-1 viability assay on proliferating cells, to assess the mitochondrial activity as a measure of cell viability. The combined digestive juices from the mouth, stomach and intestine (chyme) did not affect the cell viability up to a concentration of 62.5% (v/v) in cell culture medium after 24 h exposure (Fig. 5.2a). These results are comparable with a previous *in vitro* study in the literature [34], suggesting that the living cells in the modular system can be exposed to a mixture containing chyme.

For experiments with the digestion-on-a-chip connected to the flow-through transwell, we used 12.5% chyme in HBSS in the apical compartment as it is compatible with the desired flow rate (200 $\mu\text{L}/\text{min}$) for the apical compartment. This yielded a 12.5% chyme solution in HBSS, which is well below the upper acceptable concentration of 62.5% reported above to maintain proper cell viability during experiments. For our second series of experiments, then, we statically exposed a 21-day old co-culture of Caco-2 and HT29-MTX-E12 cells to 12.5% chyme for 24 hours and subsequently stained the tight junction protein ZO-1/TJP1. Co-cultured cells were exposed to 0% chyme (control, Fig. 5.2b) and to 12.5% chyme (Fig. 5.2c), and an interconnecting network of tight junction proteins is shown in red. No differences in the quality of

the tight junctions were observed for the two co-cultures, indicating good barrier integrity. Moreover, cell barrier integrity was also confirmed after each permeability experiment using the fluorescent marker, lucifer yellow, which is not transported by the cells. Any translocation of this compound to the basolateral compartment amounting to more than 5% of the total amount present in the apical compartment thus indicates leakiness of the barrier. Cell layers were exposed to 500 $\mu\text{g}/\text{mL}$ lucifer yellow in HBSS for 30 min after every permeability experiment. Cell layers translocating more than 5% of lucifer yellow to the basolateral side were judged as leaking, and data from these cultures were discarded. The cell barriers used for calculating permeability showed $0.9 \pm 0.4\%$ lucifer yellow transport, confirming that the biointegrity of living cells can be fully maintained in the presence of chyme.

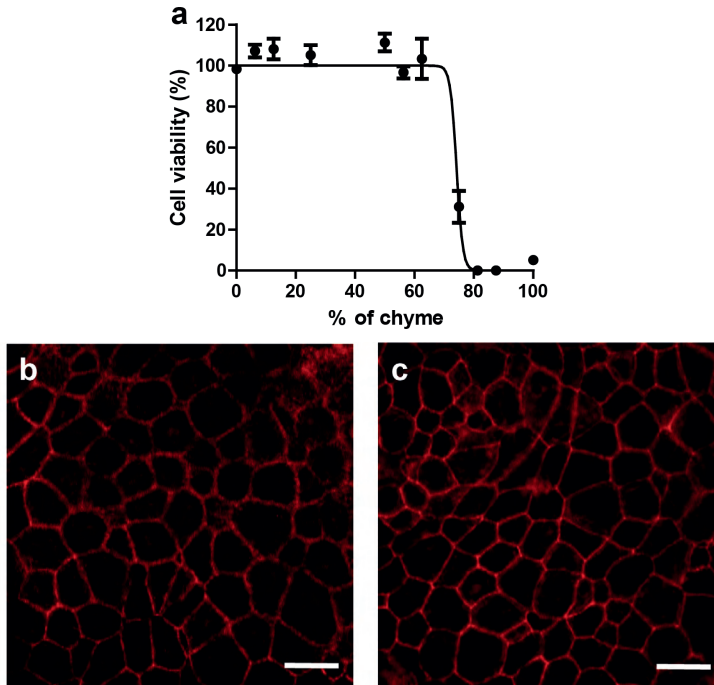


Figure 5.2: a) Cell viability of Caco-2/HT29-MTX-E12 co-culture after 24 h exposure to increasing concentrations of chyme using the WST-1 mitochondrial activity assay. Viability is given as a percentage of the control ($\% \pm$ standard error of the mean (SEM); triplicates). A nonlinear curve was fitted through the points for clarity using GraphPad Prism. b) Confocal image of Caco-2/HT29-MTX-E12 cells cultured in a transwell for 21 days (control). c) Confocal image of Caco-2/HT29-MTX-E12 cells cultured in a transwell for 21 days (exposed to 12.5% chyme for 24 hours). All exposures under static conditions. Cells were stained for tight junction protein ZO-1/TJP1 (red). Scale bar: 20 μm .

5.3.2 In vitro digestion and intestinal permeability of omeprazole

To evaluate digestion-on-a-chip in combination with our dynamic model of the intestinal barrier, we used the model drug compound, omeprazole (molecular structure, Fig. S5.1, SI). Omeprazole is a proton pump inhibitor that irreversibly blocks the last step of acid production in the stomach wall, thereby increasing the gastric pH [35]. Omeprazole is preferably administered orally via a suspension, tablet or capsule. As omeprazole itself is acid-labile, these drug formulations contain an enteric coating to protect omeprazole from acid degradation in the stomach [36]. Omeprazole is then released in the small intestine and absorbed. Prior to evaluation of the combined set-up comprising digestion and cellular uptake of omeprazole, we determined a 5 $\mu\text{g}/\text{mL}$ concentration of this drug to be non-toxic to the cell coculture, using the WST-1 assay (Fig. S5.2, SI). Static co-cultures of Caco-2 and HT29-MTX-E12 cells were then exposed to omeprazole at 5 $\mu\text{g}/\text{mL}$ for 3 hours. In Figure 5.3, the cumulative percentage of omeprazole that has crossed the cell barrier to the basolateral side is given at different time points, reaching 36.1% of the apical concentration after 3 h. The apparent permeability coefficient (P_{app}) was calculated to be $54.9 \pm 12.9 \times 10^{-6} \text{ cm/s}$, which is in the same range as P_{app} data found for omeprazole in literature ($13.4\text{-}53.2 \times 10^{-6} \text{ cm/s}$) [37, 38].

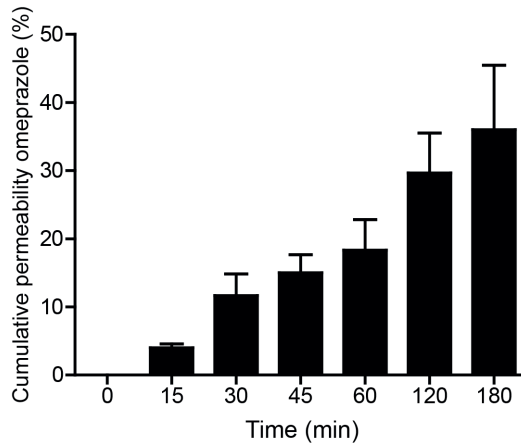


Figure 5.3: Permeability of omeprazole across a monolayer of Caco-2/HT29-MTX-E12 cells in a static transwell, without digestive juices in the apical matrix. Permeability is given as a percentage of the initial apical concentration ($\% \pm \text{SEM}$; $n=3$).

Next, we coupled digestion-on-a-chip to the dynamic model of the intestine, using two different set-ups. In the first set-up, all three chaotic micromixers simulating the mouth, stomach and intestine were implemented, and connected via a fourth micromixer to the flow-through transwell, using the modular set-up depicted in Fig. 5.1a+b. Every minute, apical and basolateral samples were collected in two separate 96-well plates using two fraction collectors. In the second set-up, we emulated the working mechanism of an enteric-coated tablet of omeprazole, which only releases omeprazole in the intestinal compartment to prevent exposure to gastric acid. This was done by excluding the mixers for the mouth and stomach compartments to realize a simplified version of chip-based digestion. Only one micromixer was used to mix the sample (omeprazole) and the pre-mixed digestive juices (saliva, gastric juice, and intestinal juice). After dilution in the fourth mixer and perfusion of the dynamic cell coculture, samples were collected from the apical and basolateral side in two separate 96-well plates. In Fig. 5.4, the reconstructed ion currents of the $[M+H]^+$ ion of omeprazole at m/z 346 are given for both complete digestion and exposure to only intestinal digestion after 90 minutes. The figure clearly shows that the unprotected omeprazole is fully degraded in the total digestion system, in accordance with expectations; no signal remains for the m/z 346 ion (in grey). We did not observe any clear degradation products of omeprazole in the MS data [39].

In the second experiment mimicking the ingestion of enteric-coated omeprazole, we clearly observed the omeprazole ion in the apical effluent (Fig. 5.4, in black), as expected. However, we did not observe any translocation of omeprazole to the basolateral site. This is in contrast to the static permeability data for omeprazole (Fig. 5.3), and *in vivo* data which predict that uptake of omeprazole could be expected in the dynamic flow-through system [37, 38]. From the literature, it is known that omeprazole heavily binds to plasma proteins [40]. A control experiment was conducted to examine the effect of digestive juices (chyme) on the translocation of omeprazole in a static transwell (Fig. S5.3, SI). It was found that the uptake of omeprazole in the presence of digestive juices was about three times lower compared to omeprazole dissolved in only HBSS buffer. This may explain why no omeprazole was detected in the basolateral compartment of the flow-through transwell after fraction collection and offline analysis. Translocation appears to have been lowered due to binding with proteins in the chyme matrix. Moreover, omeprazole will generally be more difficult to detect in the flow-through case than in the static

case, as in a dynamic system no accumulation of the translocated compound occurs due to the collection of samples every minute.

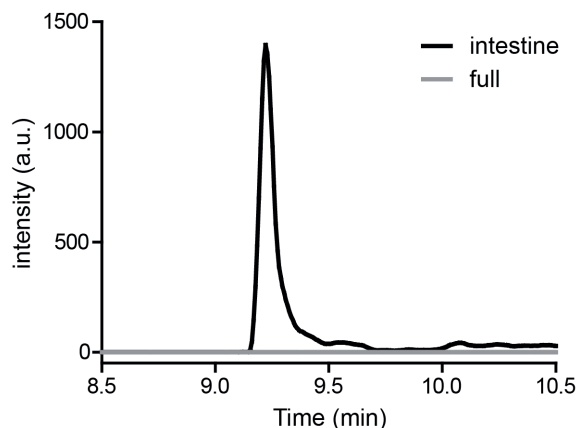


Figure 5.4: Reconstructed-ion chromatogram of m/z 346 ($[M+H]^+$) at time point 90 minutes on the apical side after only intestinal digestion (black) or full digestion (grey). The latter used the set-up of Fig. 5.1b and Fig. 5.1a+b, respectively. Samples were collected by a fraction collector followed by offline analysis using chip-based UPLC-QTOF-MS.

5.3.3 Integrated modular microfluidic *in vitro* gastrointestinal tract with online analysis: proof of principle with and without co-exposure to a food matrix

All the elements of our system: digestion-on-a-chip, flow-through transwell with co-cultured intestinal cells, and MS analysis were combined in one hyphenated, online system (Fig. 5.1a+b+c), creating a multi-module gastrointestinal tract with automated online analysis to monitor *in vitro* oral bioavailability over time. In a previous study, [24] the flow-through transwell was combined with online MS analysis. In this study, we further challenged the system by including microfluidic digestion-on-a-chip (Fig. 5.1a), allowing pre-treatment of samples with digestive juices before studying translocation through a model of the gut wall. We used the model compound, verapamil, a drug for treatment of high blood pressure and other conditions, for evaluation of the modular *in vitro* gastrointestinal tract. Verapamil has the advantage that there are plenty of data available in the literature for both static and dynamic transwell systems, making it possible to benchmark our system [24, 41, 42]. First, we examined if verapamil is affected by digestion in the different phases by performing a test tube digestion. As can be seen in Fig. S5.4 in the supplementary information, verapamil is not affected by digestion. Therefore,

it was hypothesized that verapamil would exhibit similar behaviour in our modular *in vitro* gastrointestinal tract compared to its behaviour in the earlier flow-through set-up reported previously [24]. Figure 5.5 shows the cumulative permeability of verapamil over 195 minutes measured in the entire system shown in Fig. 5.1a+b+c (in white). The results are very similar to the data from Santbergen et al. indicating that including the additional digestion-on-a-chip functionality affects neither the biointegrity of the co-culture of Caco-2 and HT29-MTX-E12 cell model, nor the overall analytical performance [24]. In contrast to the reduced absorption of omeprazole in the presence of digestive juices, the translocation of verapamil is not affected at all.

To emulate the functions of the gastrointestinal tract even further, a final experiment was performed in which verapamil was not administered in ultrapure water, but in apple juice as a simplified food matrix. In Fig. 5.5, the uptake of verapamil dissolved in apple juice (black) is depicted versus the control (white). As mentioned above, the data in the absence of apple juice are very similar to Santbergen et al. [24]. Moreover, it can be clearly observed that the absorption of verapamil is much slower in the presence of an apple juice matrix compared to the control. It is well known that food (or certain food ingredients) alter the bioavailability of drugs, for example by binding to proteins, fats, or calcium ions contained in food [43, 44]. Fruit juices have been shown to inhibit the transport of organic anion-transporting polypeptides [45]. The latter however is believed to be irrelevant since verapamil is mainly transported via passive diffusion [46]. Nevertheless, the uptake of verapamil seems to be affected by apple juice in this proof-of-principle experiment, but of course more experiments with different sample matrices are required in a follow-up study to confirm this hypothesis.

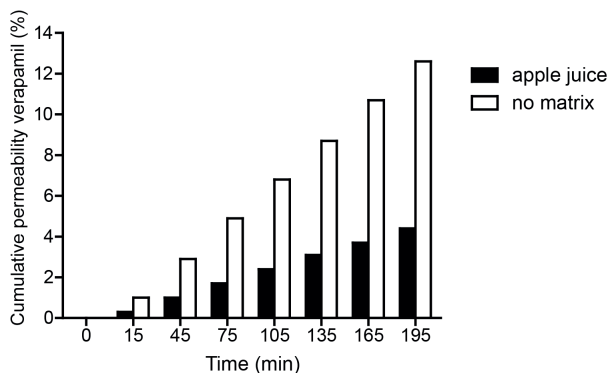


Figure 5.5: Permeability of verapamil in apple juice matrix (black) or no food matrix (ultra-pure water, white) across a monolayer of Caco-2/HT29-MTX-E12 cells, measured in the integrated gastrointestinal tract with online analysis set-up of Figure 5.1a-c. Permeability is given as a calculated cumulative percentage of the starting apical concentration ($\% \pm \text{SEM}$; $n=1$)

Conclusions

The integrated modular model of the gastrointestinal tract described in this paper comprises pre-treatment of samples with digestive juices, followed by translocation of sample molecules and their possible metabolites through an *in vitro* intestinal barrier. Online coupling to UPLC-QTOF-MS resulted in an automated online read-out of oral bioavailability. This system encompasses the two-key processes of the human intestinal tract, namely digestion and absorption. The hyphenation of these miniaturized model systems into one multi-modular system makes it perfectly suited to replace separate *in vitro* digestions and uptake studies in the fields of pharmacology, toxicology, and the nutritional sciences in the future. Systems like ours have a bright future for the automation of oral bioavailability testing in novel drug development and next generation risk assessment.

Acknowledgements

We thank Arjen Gerssen (Wageningen Food Safety Research), Klaus Mathwig and Jean-Paul S.H. Mulder (Pharmaceutical Analysis, University of Groningen) for technical support and stimulating discussions. This research received funding from the Dutch Research Council (NWO) in the framework of the Technology Area PTA-COAST3 (GUTTEST, project nr. 053.21.116) of the Fund New Chemical Innovations. The partners in this project were Wageningen University, University of Groningen, Wageningen Food Safety Research, FrieslandCampina, Micronit Microtechnologies, Galapagos and R-Biopharm as partners.

References

- [1] Fernandez-Garcia E, Carvajal-Lerida I, Perez-Galvez A. In vitro bioaccessibility assessment as a prediction tool of nutritional efficiency. *Nutr Res.* 2009;29(11):751-760.
- [2] Walczak AP, Fokkink R, Peters R, Tromp P, Herrera Rivera ZE, Rietjens IM, et al. Behaviour of silver nanoparticles and silver ions in an in vitro human gastrointestinal digestion model. *Nanotoxicol.* 2013;7(7):1198-1210.
- [3] Alegria A, Garcia-Llatas G, Cilla A. Static digestion models: General introduction. In: Verhoecx K, Cotter P, Lopez-Exposito I, Kleiveland C, Lea T, Mackie A, et al., editors. *The impact of food bioactives on health: in vitro and ex vivo models.* Cham (CH)2015. p. 3-12.
- [4] DeSesso JM, Jacobson CF. Anatomical and physiological parameters affecting gastrointestinal absorption in humans and rats. *Food Chem Toxicol.* 2001;39(3):209-228.
- [5] Trout GE, Fruton JS. The side-chain specificity of pepsin. *Biochemistry.* 1969;8(10):4183-4190.
- [6] Whitcomb DC, Lowe ME. Human pancreatic digestive enzymes. *Dig Dis Sci.* 2007;52(1):1-17.
- [7] Carey MC, Small DM, Bliss CM. Lipid digestion and absorption. *Annu Rev Physiol.* 1983;45:651-677.
- [8] Artursson P, Palm K, Luthman K. Caco-2 monolayers in experimental and theoretical predictions of drug transport. *Adv Drug Deliver Rev.* 1996;22(1-2):67-84.
- [9] Liu X, Testa B, Fahr A. Lipophilicity and its relationship with passive drug permeation. *Pharm Res.* 2011;28(5):962-977.
- [10] Musther H, Olivares-Morales A, Hatley OJD, Liu B, Hodjegan AR. Animal versus human oral drug bioavailability: do they correlate? *Eur J Pharm Sci.* 2014;57:280-291.
- [11] Lea T. Epithelial cell models; General introduction. In: Verhoecx K, Cotter P, Lopez-Exposito I, Kleiveland C, Lea T, Mackie A, et al., editors. *The impact of food bioactives on health: in vitro and ex vivo models.* Cham (CH)2015. p. 95-102.
- [12] Costa J, Ahluwalia A. Advances and current challenges in intestinal in vitro model engineering: a digest. *Front Bioeng Biotechnol.* 2019;7:144.
- [13] de Haan P, Janovska MA, Mathwig K, van Lieshout GAA, Triantis V, Bouwmeester H, et al. Digestion-on-a-chip: a continuous-flow modular microsystem recreating enzymatic digestion in the gastrointestinal tract. *Lab Chip.* 2019;19(9):1599-1609.
- [14] Kulthong K, Duivenvoorde L, Mizera BZ, Rijkers D, ten Dam G, Oegema G, et al. Implementation of a dynamic intestinal gut-on-a-chip barrier model for transport studies of lipophilic dioxin congeners. *Rsc Adv.* 2018;8(57):32440-32453.
- [15] Bein A, Shin W, Jalili-Firoozinezhad S, Park MH, Sontheimer-Phelps A, Tovaglieri A, et al. Microfluidic organ-on-a-chip models of human intestine. *Cell Mol Gastroenter.* 2018;5(4):659-668.
- [16] Villenave R, Wales SQ, Hamkins-Indik T, Papafragkou E, Weaver JC, Ferrante TC, et al. Human gut-on-a-chip supports polarized infection of coxsackie B1 virus in vitro. *Plos One.* 2017;12(2):e0169412.
- [17] Imura Y, Asano Y, Sato K, Yoshimura E. A microfluidic system to evaluate intestinal absorption. *Anal Sci.* 2009;25(12):1403-1407.
- [18] Gao D, Liu HX, Lin JM, Wang YN, Jiang YY. Characterization of drug permeability in Caco-2 monolayers by mass spectrometry on a membrane-based microfluidic device. *Lab Chip.* 2013;13(5):978-985.
- [19] Kim HJ, Huh D, Hamilton G, Ingber DE. Human gut-on-a-chip inhabited by microbial flora that experiences intestinal peristalsis-like motions and flow. *Lab Chip.* 2012;12(12):2165-2174.
- [20] Kulthong K, Duivenvoorde L, Sun H, Confederat S, Wu J, Spenkelink B, et al. Microfluidic chip for culturing intestinal epithelial cell layers: characterization and comparison of drug transport between dynamic and static models. *Toxicol in Vitro.* 2020:104815.
- [21] Kim HJ, Ingber DE. Gut-on-a-chip microenvironment induces human intestinal cells to undergo villus differentiation. *Integr Biol (Camb).* 2013;5(9):1130-1140.
- [22] Santbergen MJC, van Der Zande M, Bouwmeester H, Nielen MWF. Online and in situ analysis of organs-on-a-chip. *Trac-Trend Anal Chem.* 2019;115:138-146.
- [23] Zhang YS, Aleman J, Shin SR, Kilic T, Kim D, Mousavi Shaegh SA, et al. Multisensor-integrated organs-on-chips platform for automated and continual in situ monitoring of organoid behaviors. *Proc Natl Acad Sci U S A.* 2017;114(12):E2293-E2302.
- [24] Santbergen MJC, van der Zande M, Gerssen A, Bouwmeester H, Nielen MWF. Dynamic in vitro intestinal barrier model coupled to chip-based liquid chromatography mass spectrometry for oral bioavailability studies. *Anal Bioanal Chem.* 2020;412(5):1111-1122.

- [25] Mallet CR, Lu Z, Mazzeo JR. A study of ion suppression effects in electrospray ionization from mobile phase additives and solid-phase extracts. *Rapid Commun Mass Spectrom.* 2004;18(1):49-58.
- [26] Rowland M, Tozer TN. *Clinical pharmacokinetics and pharmacodynamics.* 4th Ed ed: Lippincott Williams & Wilkins; 2011.
- [27] Bouwman-Boer Y, le Brun P, Woerdenbag H, Tel R, Oussoren C. *Recepteerkunde.* 5th ed: Bohn Stafleu van Loghum; 2009.
- [28] Giusti S, Sbrana T, La Marca M, Di Patria V, Martinucci V, Tirella A, et al. A novel dual-flow bioreactor simulates increased fluorescein permeability in epithelial tissue barriers. *Biotechnol J.* 2014;9(9):1175-1184.
- [29] de Haan P, Mulder JP, Lötters JC, Verpoorte E. A highly stable, pressure-driven, flow control system based on Coriolis mass flow sensors for organs-on-chips. Manuscript in Preparation. n.d.
- [30] Yeon JH, Park JK. Drug permeability assay using microhole-trapped cells in a microfluidic device. *Anal Chem.* 2009;81(5):1944-1951.
- [31] Oomen AG, Rompelberg CJ, Bruil MA, Dobbe CJ, Pereboom DP, Sips AJ. Development of an in vitro digestion model for estimating the bioaccessibility of soil contaminants. *Arch Environ Contam Toxicol.* 2003;44(3):281-287.
- [32] Minekus M, Alminger M, Alvito P, Ballance S, Bohn T, Bourlieu C, et al. A standardised static in vitro digestion method suitable for food - an international consensus. *Food Funct.* 2014;5(6):1113-1124.
- [33] Versantvoort CH, Oomen AG, Van de Kamp E, Rompelberg CJ, Sips AJ. Applicability of an in vitro digestion model in assessing the bioaccessibility of mycotoxins from food. *Food Chem Toxicol.* 2005;43(1):31-40.
- [34] Deat E, Blanquet-Diot S, Jarrige JF, Denis S, Beyssac E, Alric M. Combining the dynamic TNO-gastrointestinal tract system with a Caco-2 cell culture model: application to the assessment of lycopene and alpha-tocopherol bioavailability from a whole food. *J Agr Food Chem.* 2009;57(23):11314-11320.
- [35] Castell D. Review of immediate-release omeprazole for the treatment of gastric acid-related disorders. *Expert Opin Pharmacol.* 2005;6(14):2501-2510.
- [36] Riedel A, Leopold CS. Degradation of omeprazole induced by enteric polymer solutions and aqueous dispersions: HPLC investigations. *Drug Dev Ind Pharm.* 2005;31(2):151-160.
- [37] Pauli-Magnus C, Rekersbrink S, Klotz U, Fromm MF. Interaction of omeprazole, lansoprazole and pantoprazole with P-glycoprotein. *N-S Arch Pharmacol.* 2001;364(6):551-557.
- [38] Hellinger E, Veszelka S, Toth AE, Walter F, Kittel A, Bakk ML, et al. Comparison of brain capillary endothelial cell-based and epithelial (MDCK-MDR1, Caco-2, and VB-Caco-2) cell-based surrogate blood-brain barrier penetration models. *Eur J Pharm Biopharm.* 2012;82(2):340-351.
- [39] Shankar G, Borkar RM, Udutha S, Kanakaraju M, Charan GS, Misra S, et al. Identification and structural characterization of the stress degradation products of omeprazole using Q-TOF-LC-ESI-MS/MS and NMR experiments: evaluation of the toxicity of the degradation products. *New Journal of Chemistry.* 2019;43(19):7294-7306.
- [40] Andersson T, Hassan-Alin M, Hasselgren G, Rohss K, Weidolf L. Pharmacokinetic studies with esomeprazole, the (S)-isomer of omeprazole. *Clin Pharmacokinet.* 2001;40(6):411-426.
- [41] Pauli-Magnus C, von Richter O, Burk O, Ziegler A, Mettang T, Eichelbaum M, et al. Characterization of the major metabolites of verapamil as substrates and inhibitors of P-glycoprotein. *Journal of Pharmacology and Experimental Therapeutics.* 2000;293(2):376-382.
- [42] Lozoya-Agullo I, Araujo F, Gonzalez-Alvarez I, Merino-Sanjuan M, Gonzalez-Alvarez M, Bermejo M, et al. Usefulness of Caco-2/HT29-MTX and Caco-2/HT29-MTX/Raji B coculture models to predict intestinal and colonic permeability compared to Caco-2 monoculture. *Mol Pharm.* 2017;14(4):1264-1270.
- [43] Tesoriere L, Gentile C, Angileri F, Attanzio A, Tutone M, Allegra M, et al. Trans-epithelial transport of the betalain pigments indicaxanthin and betanin across Caco-2 cell monolayers and influence of food matrix. *Eur J Nutr.* 2013;52(3):1077-1087.
- [44] Parada J, Aguilera J. Food microstructure affects the bioavailability of several nutrients. *Journal of food science.* 2007;72(2):R21-R32.
- [45] Dresser GK, Bailey DG. The effects of fruit juices on drug disposition: a new model for drug interactions. *Eur J Clin Invest.* 2003;33 Suppl 2:10-16.
- [46] Engman H, Tannergren C, Artursson P, Lennernas H. Enantioselective transport and CYP3A4-mediated metabolism of R/S-verapamil in Caco-2 cell monolayers. *Eur J Pharm Sci.* 2003;19(1):57-65.

Supplementary information

Table S5.1 Optimized composition of the artificial digestive juices, dissolved in ultrapure water (De Haan et al. [13])

Compound	Saliva (mg/L)	Gastric Juice (mg/L)	Duodenal juice (mg/L)	Bile (mg/L)
CaCl ₂		302	151	167.5
Glucosamine HCl		330		
Glucose		650		
Glucuronic acid		20		
KCl	896	824	564	376
KH ₂ PO ₄			80	
KSCN	200			
MgCl ₂ ·6H ₂ O			50	
Na ₂ SO ₄	570			
NaCl	298	2752	7012	5259
NaH ₂ PO ₄ ·H ₂ O	1021	306		
NaHCO ₃			3388	5785
NH ₄ Cl		306		
Urea	200	85	100	250
Uric acid	15			
HCl		4.16 mM	5.57 mM	6.17 mM
NaOH	2.9 mM			
α-Amylase (<i>Bacillus sp.</i>)	145			
Bile (bovine)				6000
Lipase (porcine pancreas)			500	
Pancreatin (porcine pancreas)			3000	
Pepsin (porcine gastric mucosa)		1000		

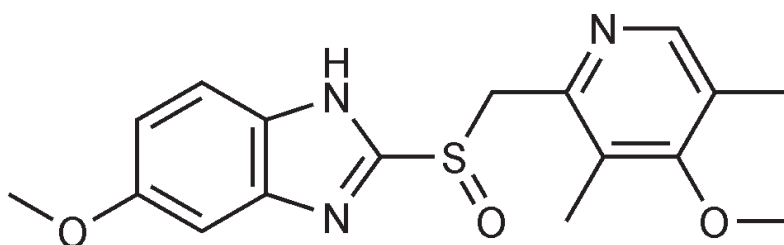


Figure S5.1: Molecular structure omeprazole

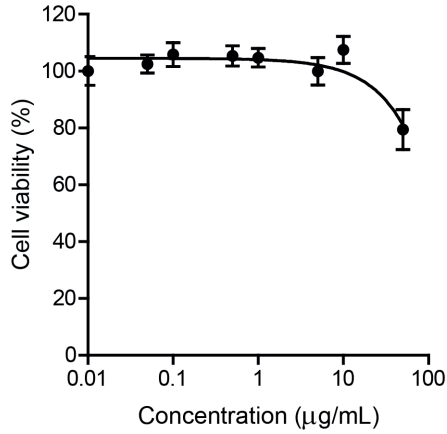


Figure S5.2: Cell viability of a Caco-2/HT29-MTX-E12 co-culture after 24 h exposure to increasing concentrations of omeprazole using the WST-1 mitochondrial activity assay. Viability is given as a percentage of the control (% ± SEM; n=3).

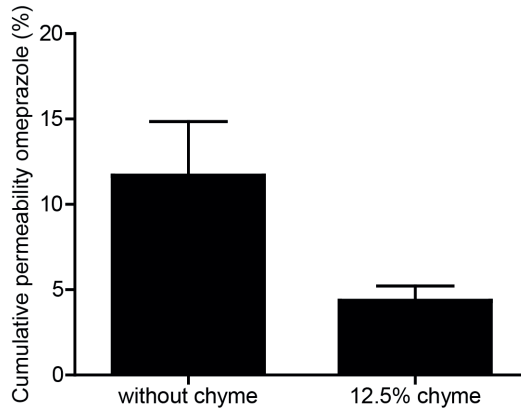


Figure S5.3: Permeability of omeprazole in the absence and presence of 12.5% chyme (composition as mentioned in table S1) across a monolayer of Caco-2/HT29-MTX-E12 cells in a static transwell after 30 minutes. Permeability is given as a percentage of the apical concentration (% ± SEM; triplicates).

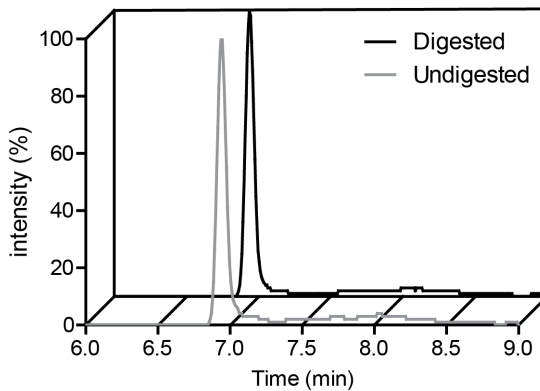
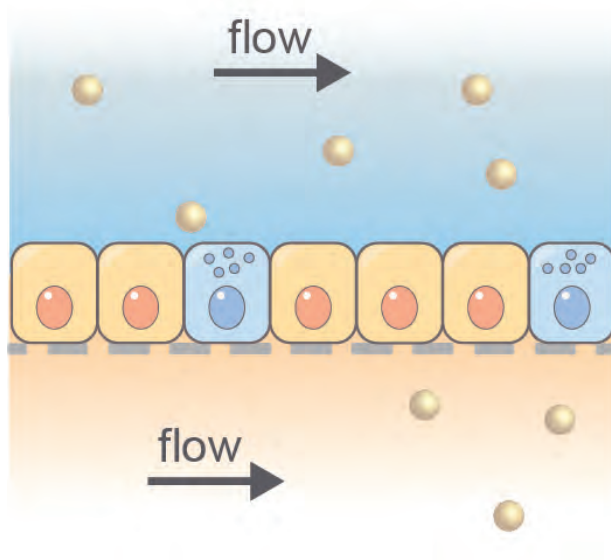


Figure S5.4: Reconstructed-ion chromatogram of m/z 455 $[M+H]^+$ ion of verapamil after digestion (conditions as mentioned in table S5.1) in a test tube (black) or no digestion (grey).

5



Chapter 6

The effect of flow on the translocation of gold nanoparticles in a dynamic *in vitro* intestinal barrier model

Milou J.C. Santbergen, Meike van der Zande, Ruud J.B. Peters, Greet van Bommel, Hans Bouwmeester and Michel W.F. Nielen

Unpublished results

Abstract

Nanoparticles (NPs) can be found in a variety of food products, which has led to concerns about their potential adverse effects for consumers upon ingestion. Currently, static *in vitro* cell culture models of the intestine are used to predict the uptake and translocation of NPs in the human gastrointestinal tract. However, in a static environment NP sedimentation or flotation can cause altered exposure levels on the cells. By including flow into the cell model these problems might be solved. Nevertheless, the effect of flow on the translocation of NP across the *in vitro* intestinal barrier is largely unknown. In this study, we compared the cell associated fraction and translocation of gold nanoparticles (AuNPs) between a static *in vitro* cell culture system and a dynamic flow-through transwell system using single particle inductively coupled plasma mass spectrometry (sp-ICP-MS). The translocation of three sizes of AuNPs was examined in the static system (15, 30 and 70 nm). Only the smallest particles translocated through the static *in vitro* cell layer. For the dynamic experiments only, the smallest particles were used. The translocation and cell associated fraction of the 15 nm AuNPs in the flow-through transwell was increased compared to the static system. This is most likely due to the higher total amount of particles that the cell layer was exposed to in the flow-through transwell and the flow directing the particles towards the cell layer. Even though, the inclusion of flow might solve NP sedimentation/flotation problems present in static barrier models. The results show that accurate measurements of the number of particles that reaches the cells is of great importance to determine the (apparent) bioavailability of NPs for both the static and dynamic model. It is therefore recommended that in future studies the effect of flow on nanoparticle deposition on the cell layer and subsequent translocation should be carefully considered when using a dynamic cell culture model to study NP translocation.

keywords: gold nanoparticles, translocation, transwell, gut-on-a-chip, sp-ICP-MS

6.1 Introduction

Nanoparticles (NPs) can be found in a variety of food products serving multiple applications, like increasing shelf life, improving microbiological safety or altering sensory attributes (e.g. appearance, flavour, odour) [1, 2]. Silica and titanium dioxide NPs have been found in several organs throughout the human body, such as the liver and the intestinal tract [3]. Because of their large surface-to-volume ratio, NPs are strongly reactive and may cause adverse effects in the body [4]. Examining the absorption, distribution, and excretion profiles of NPs and their effects on human health is thus imperative [5]. Animal models are still the golden standard to predict the uptake and biodistribution of NPs in humans [4]. However, due to physiological and anatomical differences between the animal model and the human body, results derived from animal data have shown to not always give an accurate prediction [6]. Furthermore, studying molecular mechanisms underlying cellular uptake of NPs in a spatiotemporal controlled manner in animals is difficult.

Currently, as an alternative for animal models, static *in vitro* human intestinal cell barrier models are used to assess the cellular uptake and translocation of NPs [7-9]. Generally, a monolayer of one or more intestinal cell types is grown on a transwell insert and exposed to the NPs for several hours [9, 10]. One of the most commonly used cell models, mimicking the intestinal epithelial barrier, is a combination of Caco-2 cells (representing the enterocytes) and HT29-MTX cells (representing the goblet cells). Incorporation of the mucus secreting goblet cells in the *in vitro* model is especially important when examining NP translocation as mucus may have an impact on their permeability due to the gel-like properties and negative charge of the mucus [4].

Depending on the physical chemical properties of the particle, translocation across the intestinal epithelial barrier can be measured using different techniques. When particles are labelled with a fluorescent dye a simple fluorescence plate reader can be used [8]. Disadvantage of this system is that nothing can be said about the particle size distribution and it is less sensitive, also there may be leaching of the label into the matrix. Other techniques like atomic absorption spectroscopy and inductively coupled plasma mass spectrometry (ICP-MS) are more sensitive, but are only applicable for inorganic

materials and cannot distinguish between particles and ions as the entire solution is treated before measurement to convert all material into ions [11]. So, nothing can be said about the particle concentration or size distribution only the total concentration of ions. With the development of single particle (sp) ICP-MS it became possible to analyse the concentration, size and size distribution of metal NPs with high sensitivity [9, 12, 13].

Static intestinal cell barrier systems fail to represent the dynamic conditions that intestinal cells experience due to the presence of flow in the gut. The development of dynamic *in vitro* models based on microfluidic technology allows for the inclusion of *in vivo* relevant shear stresses on the cells, mimicking intestinal fluid flow [14]. Furthermore, a drawback of using static cell culture models for nanoparticle research is the effect of NP sedimentation/flotation on cellular exposure levels. The inclusion of flow might solve these problems. Currently, several microfluidic devices for *in vitro* intestinal barrier models exist [15-17]. In a microfluidic system mimicking a blood vessel by culturing endothelial cells it has been shown that upon exposure to gold NPs the cell viability in the dynamic system was less affected compared to the effects on cells grown in its static counterpart [18]. Esch and colleagues studied the uptake of carboxylated polystyrene NPs in a body-on-a-chip system, which included an intestinal and liver compartment. They found that most particles did not cross the intestinal epithelial barrier, however at very high exposure concentrations the liver cells showed increased expression of an intracellular enzyme indicating liver cell injury [19]. Yet, further research investigating the effect of flow on cellular uptake and translocation of NPs in the gastrointestinal tract is limited.

Therefore, in this chapter we aimed to investigate the effect of flow by comparing the cellular association and translocation of gold (Au) NPs across a co-culture of Caco-2 and HT29-MTX-E12 cells grown in a static transwell and a dynamic flow-through transwell system. For this purpose, cells in both systems were exposed to gold particles. These were chosen as a model particle as they do not dissolve or aggregate in biological fluids. Furthermore, AuNPs can be detected with high sensitivity and with low size detection limits (i.e. ~10 nm) using single particle (sp) ICP-MS analysis. To the best of our knowledge, this work

represents the first attempt of using a dynamic *in vitro* system in combination with sp-ICP-MS detection to study the translocation of nanoparticles.

6.2 Material and Methods

6.2.1 Nanoparticles and chemicals

Gold nanoparticles were purchased from Nanocomposix Inc. (San Diego, CA, USA) in different sizes, 15, 30, 60 and 70 nm (Citrate, BioPure). The particles were suspended in Milli-Q water at a gold mass concentration of 1 mg/mL. Ionic standard solution for gold was purchased from Merck (Darmstadt, Germany). Penicillin-streptomycin, sodium bicarbonate (NaHCO_3), 4-(2-hydroxyethyl)-1-piperazineethanesulfonic acid (HEPES), lucifer yellow, triton-X100 and Hank's balanced salt solution (HBSS), were purchased from Sigma-Aldrich/Merck (Zwijndrecht, the Netherlands). Dulbecco's Modified Eagle Medium (DMEM) with 4.5 g/L glucose and l-glutamine with and without phenol red and heat-inactivated fetal bovine serum (FBS) were purchased from Gibco (Bleiswijk, the Netherlands). Trace analysis grade nitric acid and non-essential amino acids (NEAA) were obtained from Thermo Fisher Scientific (Landsmeer, the Netherlands). WST-1 reagent from Roche Diagnostics GmbH (Mannheim, Germany) and water was prepared daily using a Milli-Q Reference Water Purification System from Millipore (Burlington, MA, USA).

6.2.2 Cell viability assay

The cytotoxic effects of the AuNPs were assessed using the WST-1 cell viability assay. Caco-2 (American Type Culture Collection, USA) and HT29-MTX-E12 (European Collection of Authenticated Cell Culture, Salisbury, UK) cells were seeded in a 3:1 ratio in 96-well plate, each well containing 100 μL of a 1×10^5 cells/mL suspension. Plates were incubated for 24 hours, at 37°C under 5% CO_2 . After 24 hours cells were exposed to 0-100 $\mu\text{g}/\text{mL}$ of the different sizes of gold particles in cell culture medium, for 24 hours at 37°C. Subsequently, the exposure medium was discarded, and cells were washed with pre-heated HBSS followed by an incubation of the cells with 100 μL WST-1 reagent in cell culture medium (without phenol red) at a 1:10 ratio. After 90 minutes of incubation at 37°C, plates were centrifuged for 5 min at 200xg, to settle particles at the bottom of the well and avoid particle interference as suggested by Kong et

al. [20]. Supernatant (50 μL) was transferred to a new plate and absorbance was measured at 440nm using a Bio-Tek (Winooski, VT, USA) Synergy HT Multi-Mode microplate reader. Cell viability was expressed as a percentage of the negative control consisting of cell culture medium. Triton-X100 (0.25%, v/v) was used as a positive control and decreased the cell viability to $0.1\% \pm 0.2\%$.

6.2.3 NP transport exposure

A co-culture of Caco-2 and HT29-MTX-E12 was used for all experiments in a 3:1 ratio. Caco-2 cells were used at passage numbers 29-40 and HT29-MTX-E12 cells were used at passage numbers 52-70 for all experiments. Cells were cultured in DMEM containing 10% FBS, 1% NEAA and 1% penicillin-streptomycin and maintained at 37°C in a 5% CO_2 -humidified air atmosphere and subcultured every 2 to 3 days. For permeability experiments cells were seeded at a density of 40,000 cells/ cm^2 on the apical side of a polycarbonate transwell insert (area: 0.6 cm^2 , 0.4 μm pore size, Millipore). Cell culture medium was refreshed every 2-3 days. Transwells were used for permeability experiments after 21 days of culturing. For the static transwell experiments, the cells were exposed to 400 μL /insert of 25 $\mu\text{g}/\text{mL}$ of 15 nm AuNPs in cell culture medium for 24 hours at 37°C, 5% CO_2 . After 24 hours the medium from the apical and basolateral chamber was collected. The cell layer was washed 3 times with HBSS to remove the NPs that were loosely attached to the cell layer. These wash solutions were added to the apical samples of the respected inserts. Subsequently, the cells were removed from the insert by trypsinization and sonication (40 kHz for 15 min). For the dynamic flow-through transwell experiments the transwell inserts were placed in the Kirkstall QV600 system (York, UK) at day 20 of culture and exposed to an apical flow of cell culture medium containing 25 mM of HEPES of 200 $\mu\text{L}/\text{min}$ and a basolateral flow of 100 $\mu\text{L}/\text{min}$ as suggested by Giusti et al. [21] at 37°C for 24 hours. For the permeability experiments the apical syringe was replaced with a syringe containing 25 $\mu\text{g}/\text{mL}$ 15 nm AuNPs. Apical and basolateral samples were collected continuously for 60 minutes. The apical sample was collected in a 50 mL tube for the full 60 minutes, the basolateral samples were collected in 15 mL tubes which were changed every 10 minutes. The cell fraction was collected in the same fashion as for the static experiments.

6.2.4 Single particle ICP-MS analysis

Prior to analysis the samples were sonicated for 10 minutes and diluted to a concentration suitable for single particle ICP-MS analysis (i.e. concentration of 15 nm AuNPs between 0.2 – 20 ng/L). Samples were analysed using a Thermo Scientific iCAP Q equipped with a MicroFlow 54 PFA_ST nebulizer and a quartz cyclonic spray chamber with baffle. The ICP-MS was operated at a forward power of 1550 W with the following settings: plasma (cool flow), 14 L/min; nebulizer, 1.1 L/min; and auxiliary, 0.8 L/min (all argon gas). The peristaltic pump was set at 40 rpm resulting in a flow speed of 0.2 mL/min. Data acquisition was done in time resolved mode with a dwell time of 3 ms and a total acquisition time of 60 s per analysis. With rinse steps in between each sample (3% nitric acid in water). To determine nebulizer transport efficiency a concentration of 25 ng/L 60 nm AuNPs was used [12]. For gold the following isotope was monitored ^{197}Au . The particle sizes and amount together with the mass concentrations in the samples were calculated using a single particle calculation tool [22]. This calculation tool has been validated and described in detail by Peters and colleagues [12, 13].

6.2.5 In vitro sedimentation, diffusion and dosimetry model for 15 nm AuNPs

The deposited fraction of the 25 $\mu\text{g/mL}$ 15 nm AuNPs in the two systems was calculated using the *in vitro* sedimentation, diffusion and dosimetry (ISDD) model [23]. The parameters listed in table 6.1 were used.

Table 6.1: Parameters used in the *in vitro* sedimentation, diffusion and dosimetry model

Particle characteristics		
Particle diameter	15 nm	
Particle density	19.3 g/mL	
Particle concentration	25 $\mu\text{g/mL}$	
Liquid conditions		
Temperature	310 °K	
Cell culture medium density	1 g/mL	
Cell culture medium viscosity	0.0009 N s/m ² [24]	
	Transwell	FTTW
Hight liquid column	0.0105 m	0.0165 m
Volume	0.4 mL	2 mL

6.3 Results and Discussion

6.3.1 Cytotoxicity of AuNPs

To determine a non-toxic concentration of the AuNPs for the translocation experiments the cell viability assay WST-1 was used. The AuNPs, all three sizes (15, 30 and 70 nm), were exposed to proliferating cells and did not affect the cell viability up to a concentration of 75 $\mu\text{g}/\text{mL}$ (Fig. 6.1) after 24 h of exposure. By using proliferating cells likely an overestimation of the cytotoxic effects is made as proliferating cells are more sensitive than differentiated cells, which were used for translocation experiments [25]. For all sizes, the highest concentration of 100 $\mu\text{g}/\text{mL}$ resulted in a decrease in cell viability compared to the control namely; $79 \pm 4\%$ (15 nm), $80 \pm 8\%$ (30 nm) and $68 \pm 6\%$ (70 nm). A non-toxic, a concentration of 25 $\mu\text{g}/\text{mL}$ was chosen for translocation experiments.

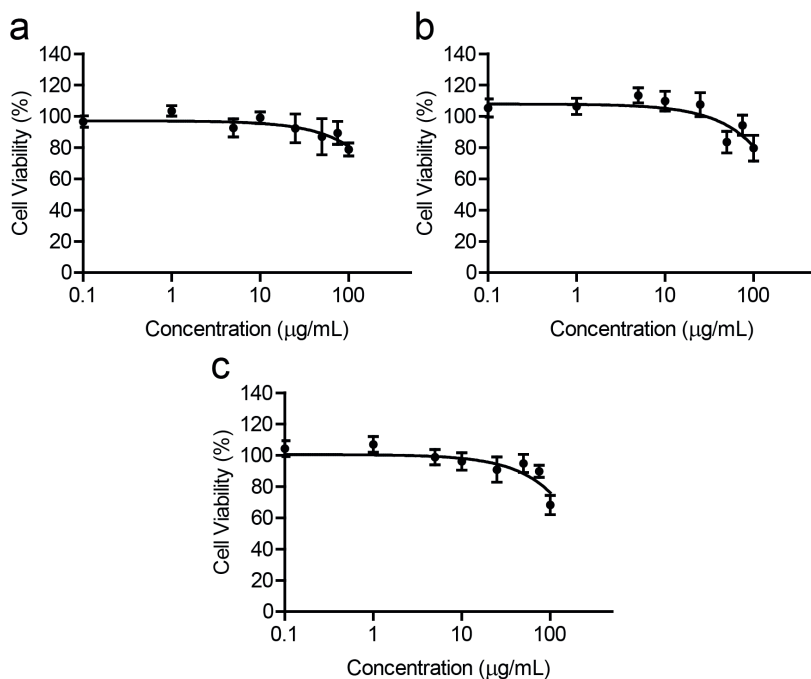


Figure 6.1: Cell viability after 24 h exposure to increasing concentrations of **a)** 15 nm, **b)** 30 nm and **c)** 70 nm AuNPs. Viability is given as a percentage of the control ($\% \pm$ standard error of the mean (SEM); $n=3$).

6.3.2 Comparison of AuNP translocation characteristics in the static versus dynamic intestinal barrier model

Fully differentiated co-cultures of Caco-2 and HT29-MTX-E12 cells were exposed to three different sizes (15, 30 and 70 nm) of AuNPs at 25 $\mu\text{g}/\text{mL}$ for 24 h, in a static environment. For the 15 nm AuNPs, translocation of 2.03×10^7 particles/mL was measured using sp-ICP-MS, which corresponds to 0.003% of the apical concentration. For the larger sizes, 30 and 70 nm, no translocation of particles was observed after 24 hours of exposure. These results correlate to previous findings, where 15 nm AuNPs were more rapidly absorbed by a monolayer of Caco-2 cells, compared to 50 and 100 nm AuNPs [26]. Furthermore, Walczak et al. investigated the difference between 50 and 100 nm polystyrene NP translocation in different static *in vitro* models and also found a significant decrease in translocation of the larger size particles [8]. Additionally, a study examining the translocation of 5, 10 and 20 nm polymer coated AuNPs again showed the highest translocation for the smallest (5 nm) particles [27]. Therefore, for the translocation experiments in the dynamic system we focussed on the 15 nm AuNPs only. For the dynamic experiments investigating the effect of flow on AuNP translocation, transwell inserts with a fully differentiated cell layer of Caco-2 and HT29-MTX-E12 cells were placed in the flow-through transwell device and exposed for 24 hours to flow before starting exposure to the AuNPs. On the day of the translocation experiments the apical side of the flow-through transwell device was exposed to 25 $\mu\text{g}/\text{mL}$ of 15 nm AuNPs at a flow speed of 200 $\mu\text{L}/\text{min}$ for 60 minutes. In figure 6.2a the cumulative translocation of the 15 nm AuNPs is shown. After 60 min $0.006 \pm 0.004\%$ (triplicates) of the apical AuNP exposure concentration crossed the cell barrier, corresponding to a particle concentration of $4.2 \pm 3.2 \times 10^7$ particles/mL. Variation among the individual experiments is large, this has been observed more frequently for intestinal barrier models including flow [28-30]. However, in figure 6.2b, the translocation measurements of the individual flow-through transwells (FTTW) show that the variation within each replicate was stable over time. Comparison of the results of the static model with the dynamic model shows that, the dynamic model already had a higher number of particles translocate after 1 hour than the static model after 24 hours. This most likely is related to the flow and its influence on particle exposure to the cells, which will be discussed in more detailed in section 6.3.3.

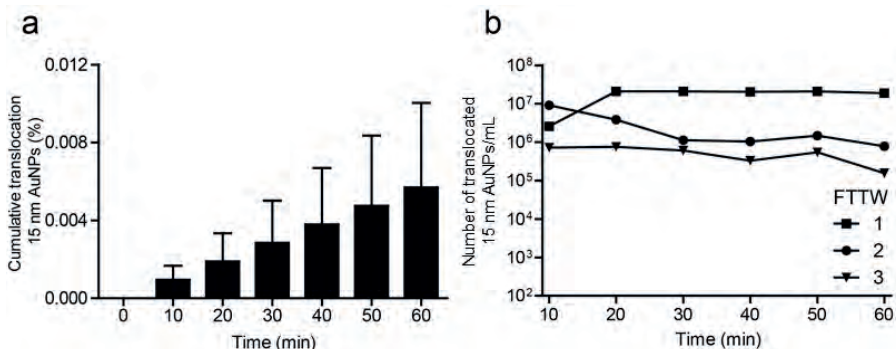


Figure 6.2: **a)** Translocation of 15 nm AuNPs across a monolayer of Caco-2/HT29-MTX-E12 cells in the dynamic flow-through transwell (FTTW). Translocation is given as a calculated cumulative percentage of the apical concentration (% \pm SEM; triplicates). **b)** Translocation of 15 nm AuNPs for the individual dynamic FTTWs. Uptake is given as the number of particles per mL.

Overall, translocation of 15 nm AuNPs is low, nevertheless due to the high sensitivity of the sp-ICP-MS method it is possible to detect such low concentrations of particles in a sample. Figure 6.3 shows the time scan of the sp-ICP-MS analysis of a blank sample (Fig. 6.3a) and of the 15 nm AuNPs in the basolateral sample of the third flow-through transwell sample at timepoint $t=60$ min (Fig. 6.3b). Each peak above the background represents a particle, meaning the number of peaks is directly correlated to the particle concentration. The height of the peak is proportional to the mass of the particle that can be translated into the diameter of the particle (assuming spherical particles). Ideally, we would also want to investigate even smaller particles as they might have a higher translocation rate [27]. However, the size limit of detection of sp-ICP-MS is approximately 10 nm, so single particle peaks for AuNPs smaller than 15 nm wouldn't be distinguishable from the background.

6.3.3 Comparison of the cell associated fraction of 15 nm AuNP in the static versus dynamic intestinal barrier model

Besides analysing particle translocation across the cell barrier, the number of particles in or on the cell layer itself was also analysed using sp-ICP-MS by collection of the cells from the membrane. Before cell trypsinization the cell layer was washed three times with HBSS to remove any loosely bound nanoparticles from the cell layer. Figure 6.4a shows the total number of 15 nm gold nanoparticles associated with the cell layer for the static transwell experiments (black) and the dynamic flow-through transwell experiment (grey). The term

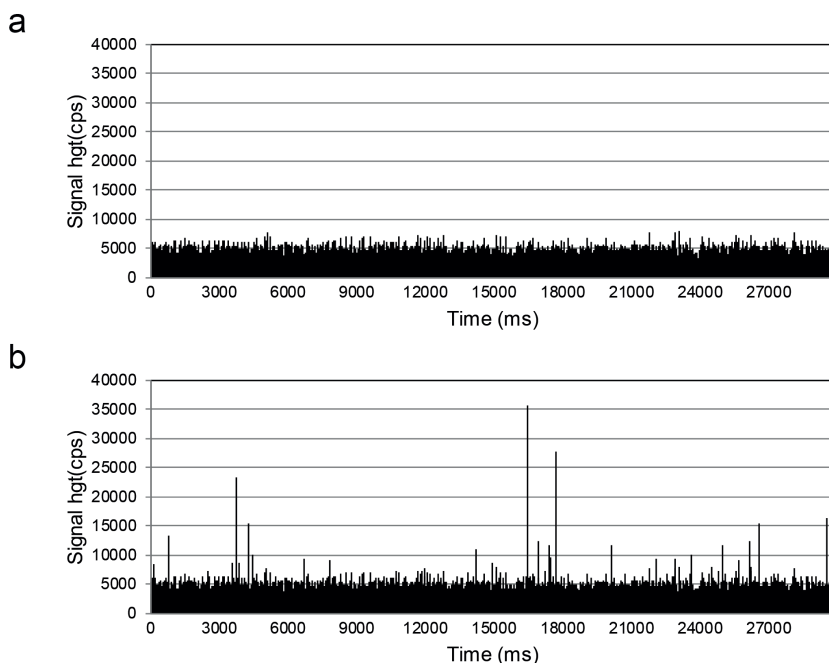


Figure 6.3: Time scan of the sp-ICP-MS analyses of **a)** a blank sample and **b)** a 15 nm AuNP basolateral flow-through transwell sample at $t=60$ min.

associated is used as it cannot be confirmed if the nanoparticles are present in the cells or surface bound using this technique. For the static experiment 5.6×10^{10} AuNPs were detected in the cell associated fraction, however for the dynamic experiments this was 10-fold higher, being 6.0×10^{11} AuNPs. This is a striking difference as the static transwell was exposed for 24 hours and the dynamic FTTW only for 1 hour. If we would correlate these results to the total amount of AuNPs the cell layer was exposed to in the static experiment this would mean a fraction of 19% of the total amount of AuNPs was associated with the cell layer (after 24 h). For the dynamic experiments using the flow-through transwell the fraction of AuNPs associated with the cell layer of the total amount of AuNPs it was exposed to was 7% (after 1 h). Clearly there is a large difference in translocation of the AuNPs between both systems. In order to gain insight in what is causing this difference we calculated the deposited dose for both systems assuming static conditions as the in vitro sedimentation, diffusion and dosimetry (ISDD) model cannot account for flow. The deposited dose indicates the amount of AuNPs that actually is in contact with the cells. Differences in deposited dose are due to varying volumes in the two systems

(Fig. 6.4b), as the same particles and cell surface was used. The deposited dose, without flow, was lower in the FTTW, especially considering a 1 h exposure (Fig. 6.4c and d). So, based on the deposited dose under static conditions translocation would likely be highest in the static system. This means that another factor besides the geometry of the FTTW (Fig. 6.4b) affects cellular association of particles. Due to the design of the model unequal flow speeds in the apical (200 $\mu\text{L}/\text{min}$) and basolateral (100 $\mu\text{L}/\text{min}$) compartment are used. This is necessary in order for the flow to reach the cells, as modelled previously [21], and results in a flow that is directed towards the cell culture membrane. This downward flow most likely forces the particles into contact with the cells to a much higher extent than deposition takes place in a static environment. Furthermore, in absolute numbers the cell layer in the FTTW is exposed to much higher numbers of particles (8.8×10^{12}) than the static transwell (2.9×10^{11}), even though the concentration of the exposure suspension was the same (25 $\mu\text{g}/\text{mL}$ or 7.3×10^{11} NPs/mL). Taken together, this is probably the reason for the increased cell associated fraction. Furthermore, the flow dynamics and its influence on particle exposure to the cells likely also account for the differences in translocation of AuNPs through the cell layer as discussed above.

This raises the question whether the dynamic flow-through transwell, as used in this chapter, is suited for nanoparticle research. A dynamic *in vitro* cell culture device containing a straight channel or tube would probably be better suited for investigation of nanoparticle translocation, as an equilibrium in flow, and thus pressure, will likely affect the particle exposure to the cells less. Clearly, particle sedimentation under flow [31], which will change depending on the geometry and flow speeds used in the device, needs to be considered in future research. An adapted ISDD model that can account for the effect of flow on particle sedimentation would be a helpful tool for predicting nanoparticle behaviour in a dynamic system. Literature addressing nanoparticle translocation using an *in vitro* dynamic intestinal cell culture system is extremely limited. Nevertheless, a dynamic environment has the potential to solve NP sedimentation and flotation issues currently present in static *in vitro* cell culture systems. Translocation of nanoparticles in the intestine is a complex question with parameters like shape/size, material, surface charge, sedimentation and protein corona all affecting particle uptake resulting in diverse outcomes between studies [32, 33]. However, for future studies the effect of flow on nanoparticle translocation should not be overlooked.

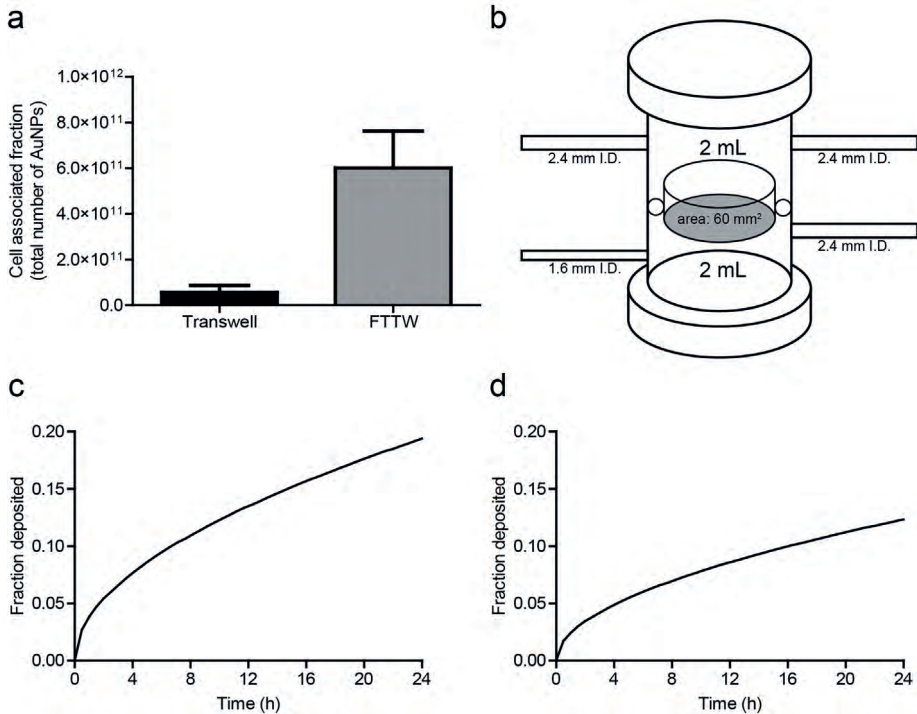


Figure 6.4: **a**) 15 nm AuNPs associated with the monolayer of Caco-2/HT29-MTX-E12 cells in the static transwell and the dynamic flow-through transwell (FTTW) (total number of AuNPs \pm SEM; triplicates). **b**) Schematic representation flow-through transwell. **c**) ISDD calculated fraction of 15 nm AuNPs deposited on the cell layer in the static transwell and **d**) the flow-through transwell (assuming static conditions)

6.4 Conclusions

In this chapter, we aimed to investigate the effect of flow on the uptake and translocation of nanoparticles across an *in vitro* intestinal barrier model by comparing a static transwell system with a dynamic flow-through transwell system. The translocation of gold nanoparticles in the static transwell depends on the size of the particles, as only the smallest (15 nm) particle translocated through the cell layer after 24-hour exposure in our experiments. The introduction of flow into the *in vitro* cell culture system increased the translocation and cell associated fraction of 15 nm AuNPs. The higher absolute number of particles on the apical side of the cell layer in the dynamic culture system in combination with the downward flow, influencing nanoparticle exposure to the cells, are presumably the reason for this increase. The flow

dynamics of the flow-through transwell, as used in this chapter, therefore render this system less suitable as a model to study nanoparticle translocation *in vitro*. Other flow systems consisting of a straight channel or tube appear to be better suited for that purpose, but more research on this topic is needed. Nevertheless, the incorporation of flow to better mimic *in vivo* physiology of the intestine is essential for studies examining NP translocation in the future as it can help solve NP sedimentation/flotation issues.

Acknowledgements

This research received funding from the Dutch Research Council (NWO) in the framework of the Technology Area PTA-COAST3 (GUTTEST, project nr. 053.21.116) of the Fund New Chemical Innovations. The partners in this project were Wageningen University, University of Groningen, Wageningen Food Safety Research, FrieslandCampina, Micronit Microtechnologies, Galapagos and R-Biopharm as partners.

References

- [1] Peters RJ, van Bommel G, Herrera-Rivera Z, Helsper HP, Marvin HJ, Weigel S, et al. Characterization of titanium dioxide nanoparticles in food products: analytical methods to define nanoparticles. *J Agric Food Chem*. 2014;62(27):6285-6293.
- [2] Souza VGL, Fernando AL. Nanoparticles in food packaging: Biodegradability and potential migration to food—A review. *Food Packag Shelf Life*. 2016;8:63-70.
- [3] Peters RJ, Oomen AG, van Bommel G, van Vliet L, Undas AK, Munniks S, et al. Silicon dioxide and titanium dioxide particles found in human tissues. *Nanotoxicol*. 2020:1-13.
- [4] Frohlich E, Roblegg E. Oral uptake of nanoparticles: human relevance and the role of in vitro systems. *Arch Toxicol*. 2016;90(10):2297-2314.
- [5] Bergin IL, Witzmann FA. Nanoparticle toxicity by the gastrointestinal route: evidence and knowledge gaps. *Int J Biomed Nanosci Nanotechnol*. 2013;3(1-2).
- [6] Li M, Zou P, Tyner K, Lee S. Physiologically based pharmacokinetic (PBPK) modeling of pharmaceutical nanoparticles. *Aaps J*. 2017;19(1):26-42.
- [7] Lefebvre DE, Venema K, Gombau L, Valerio LG, Raju J, Bondy GS, et al. Utility of models of the gastrointestinal tract for assessment of the digestion and absorption of engineered nanomaterials released from food matrices. *Nanotoxicol*. 2015;9(4):523-542.
- [8] Walczak AP, Kramer E, Hendriksen PJ, Tromp P, Helsper JP, van der Zande M, et al. Translocation of differently sized and charged polystyrene nanoparticles in in vitro intestinal cell models of increasing complexity. *Nanotoxicol*. 2015;9(4):453-461.
- [9] Abdelkhalig A, van der Zande M, Undas AK, Peters RJB, Bouwmeester H. Impact of in vitro digestion on gastrointestinal fate and uptake of silver nanoparticles with different surface modifications. *Nanotoxicol*. 2020;14(1):111-126.
- [10] Mortensen NP, Caffaro MM, Patel PR, Uddin MJ, Aravamudhan S, Sumner SJ, et al. Investigation of twenty metal, metal oxide, and metal sulfide nanoparticles' impact on differentiated Caco-2 monolayer integrity. *NanoImpact*. 2020;17:100212.
- [11] De la Calle I, Menta M, Séby F. Current trends and challenges in sample preparation for metallic nanoparticles analysis in daily products and environmental samples: a review. *Spectrochim acta B*. 2016;125:66-96.
- [12] Peters R, Herrera-Rivera Z, Undas A, van der Lee M, Marvin H, Bouwmeester H, et al. Single particle ICP-MS combined with a data evaluation tool as a routine technique for the analysis of nanoparticles in complex matrices. *J Anal At Spectrom*. 2015;30(6):1274-1285.
- [13] Peters RJ, Rivera ZH, van Bommel G, Marvin HJ, Weigel S, Bouwmeester H. Development and validation of single particle ICP-MS for sizing and quantitative determination of nano-silver in chicken meat. *Anal Bioanal Chem*. 2014;406(16):3875-3885.
- [14] Sambale F, Stahl F, Bahnemann D, Scheper T. In vitro toxicological nanoparticle studies under flow exposure. *J Nanopart Res*. 2015;17(7):298.
- [15] Kim HJ, Huh D, Hamilton G, Ingber DE. Human gut-on-a-chip inhabited by microbial flora that experiences intestinal peristalsis-like motions and flow. *Lab Chip*. 2012;12(12):2165-2174.
- [16] Trietsch SJ, Naumovska E, Kurek D, Setyawati MC, Vormann MK, Wilschut KJ, et al. Membrane-free culture and real-time barrier integrity assessment of perfused intestinal epithelium tubes. *Nat Commun*. 2017;8(1):262.
- [17] Guo Y, Li Z, Su W, Wang L, Zhu Y, Qin J. A biomimetic human gut-on-a-chip for modeling drug metabolism in intestine. *Artif Organs*. 2018;42(12):1196-1205.
- [18] Fede C, Albertin G, Petrelli L, De Caro R, Fortunati I, Weber V, et al. Influence of shear stress and size on viability of endothelial cells exposed to gold nanoparticles. *J Nanopart Res*. 2017;19(9):316.
- [19] Esch MB, Mahler GJ, Stokol T, Shuler ML. Body-on-a-chip simulation with gastrointestinal tract and liver tissues suggests that ingested nanoparticles have the potential to cause liver injury. *Lab Chip*. 2014;14(16):3081-3092.
- [20] Kong B, Seog JH, Graham LM, Lee SB. Experimental considerations on the cytotoxicity of nanoparticles. *Nanomedicine*. 2011;6(5):929-941.

- [21] Giusti S, Sbrana T, La Marca M, Di Patria V, Martinucci V, Tirella A, et al. A novel dual-flow bioreactor simulates increased fluorescein permeability in epithelial tissue barriers. *Biotechnol J.* 2014;9(9):1175-1184.
- [22] WFSR. single particle calculation tool 2015 [Available from: <https://www.wur.nl/nl/show/Single-Particle-Calculation-tool.htm>.]
- [23] Hinderliter PM, Minard KR, Orr G, Chrisler WB, Thrall BD, Pounds JG, et al. ISDD: A computational model of particle sedimentation, diffusion and target cell dosimetry for in vitro toxicity studies. *Part Fibre Toxicol.* 2010;7.
- [24] Frohlich E, Bonstingl G, Hofler A, Meindl C, Leitinger G, Pieber TR, et al. Comparison of two in vitro systems to assess cellular effects of nanoparticles-containing aerosols. *Toxicol in Vitro.* 2013;27(1):409-417.
- [25] Bohmert L, Niemann B, Lichtenstein D, Juling S, Lampen A. Molecular mechanism of silver nanoparticles in human intestinal cells. *Nanotoxicology.* 2015;9(7):852-860.
- [26] Yao MF, He LL, McClements DJ, Xiao H. Uptake of gold nanoparticles by intestinal epithelial cells: Impact of particle size on their absorption, accumulation, and toxicity. *J Agr Food Chem.* 2015;63(36):8044-8049.
- [27] Lin IC, Liang MT, Liu TY, Ziora ZM, Monteiro MJ, Toth I. Interaction of densely polymer-coated gold nanoparticles with epithelial Caco-2 monolayers. *Biomacromolecules.* 2011;12(4):1339-1348.
- [28] Gao D, Liu HX, Lin JM, Wang YN, Jiang YY. Characterization of drug permeability in Caco-2 monolayers by mass spectrometry on a membrane-based microfluidic device. *Lab Chip.* 2013;13(5):978-985.
- [29] Santbergen MJC, van der Zande M, Gerssen A, Bouwmeester H, Nielen MWF. Dynamic in vitro intestinal barrier model coupled to chip-based liquid chromatography mass spectrometry for oral bioavailability studies. *Anal Bioanal Chem.* 2020;412(5):1111-1122.
- [30] Kulthong K, Duivenvoorde L, Sun HY, Confederat S, Wu J, Spenkelink B, et al. Microfluidic chip for culturing intestinal epithelial cell layers: Characterization and comparison of drug transport between dynamic and static models. *Toxicol in Vitro.* 2020;65.
- [31] Fede C, Fortunati I, Weber V, Rossetto N, Bertasi F, Petrelli L, et al. Evaluation of gold nanoparticles toxicity towards human endothelial cells under static and flow conditions. *Microvasc Res.* 2015;97:147-155.
- [32] Frohlich E. The role of surface charge in cellular uptake and cytotoxicity of medical nanoparticles. *Int J Nanomed.* 2012;7:5577-5591.
- [33] Cao Y, Li J, Liu F, Li XY, Jiang Q, Cheng SS, et al. Consideration of interaction between nanoparticles and food components for the safety assessment of nanoparticles following oral exposure: A review. *Environ Toxicol Phar.* 2016;46:206-210.

Chapter 7

General discussion and future perspectives

7.1 General discussion

The use of animals for the development of novel drugs or the risk assessment of hazardous chemicals has been under pressure by society. Besides the ethical issues performing animal tests, the high costs and lack of predictive power for the human situation has prompted researcher to develop a better alternative for animal testing than current *in vitro* cell culture models. By combing microfluidic lab-on-a-chip technology with advanced cell biology techniques researcher created the organ-on-a-chip, an *in vitro* cell culture system that is subjected to a dynamic physiological microenvironment. Aiming towards better mimicking the *in vivo* microenvironment. Organ-on-a-chip technology has quickly expanded over the last decade, where both the biological and technological aspects increased in complexity [1]. Dynamic *in vitro* intestinal barrier models were introduced and provided a more realistic dynamic microenvironment, compared to current static *in vitro* cell culture systems [2]. The technological advancement of integrating these models with high-end analytical equipment is the next step. The main aim of this thesis was to integrate a dynamic intestinal cell culture device with advanced mass spectrometry equipment for automated and online analysis of oral bioavailability for an array of compounds. In this chapter, the potential and limitations of the developed system are discussed, and recommendations are given for future research.

7.1.1 Biological quality of the *in vitro* intestinal barrier model

Many aspects need to be considered when integrating a dynamic *in vitro* cell culture system with analytical equipment. Therefore, in **Chapter 2**, the literature was reviewed for online and *in situ* analysis of organ-on-a-chip models focussing on biological relevance of the model, analytical compatibility, system integration and final applicability. One of the conclusions of this chapter was that the bio-integrity of models integrated with sensors and analytical equipment is largely overlooked or underreported. Hence, in our studies we assured good integrity of our *in vitro* barrier model.

In **Chapter 3**, the key parameters involved in permeability experiments were assessed, including barrier integrity and cell viability. Furthermore, when integrating the dynamic model with analytical equipment the cell model was placed outside a temperature and CO₂ controlled incubator, adjustments to

assure stable temperature and CO₂ levels were examined as well. The barrier integrity of the co-culture of Caco-2 and HT29-MTX-E12 cells was evaluated both by visualizing the tight junction protein ZO-1 using an antibody staining and by assessing the permeability of lucifer yellow. Tight junctions were unaffected by the introduction of flow as no clear differences were observed between a static culture and one exposed to flow according to confocal imaging (**Chapter 3**). Furthermore, after every permeability experiment in this thesis (except for chapter 6) the cell layer was exposed to lucifer yellow to check if the cell layer showed any sign of paracellular transport, which would indicate barrier leakage. Including a barrier integrity check after a permeability experiment is essential to ensure a relevant biological barrier transport experiment. Trans epithelial electrical resistance (TEER) measurements are also considered a good barrier check after permeability experiments as they are easy and non-toxic for the cells (long-term lucifer yellow exposure can cause toxicity to the cells). However, TEER values might vary between laboratories using the same cell line as parameters like, type of cell culture medium, membrane material and passage number of the cells can already influence the measurement [3]. Furthermore, incorporating a TEER sensor in a dynamic cell culture system brings along its own challenges [4]. Therefore, lucifer yellow permeability evaluation is easier to perform and yields more stable results throughout literature.

A second approach to ensure the quality of the *in vitro* intestinal barrier model is to exclude any cytotoxic effects of the compound of interest or digestive juices, for this a WST-1 cell viability test was used. Experiments were performed on two-day old proliferating cells and exposed to the compound for 24 hours. Two-day old cells are more sensitive for potential cytotoxic effects than fully differentiated 21-day old cells as used in the permeability experiments. In **Chapter 3**, no comparison was made between the static and dynamic culture system in terms of toxicity. The literature on this topic is non-conclusive where some have found no difference between a static and dynamic culture [5], while others report lower sensitivity in the dynamic system [6]. Nevertheless, using the concentrations as determined by the static toxicity test for the permeability experiments in the dynamic system, we did not observe loss of barrier function as found by the lucifer yellow experiments, indicating absence of cytotoxicity.

The main aim of this thesis is the integration of a dynamic *in vitro* model system of the intestine with mass spectrometry analysis, this requires the cell model to be located outside of a CO₂ and temperature-controlled incubator. With current technology it is easier to bring the cell model to the mass spectrometer than the other way around. However, this does require some adaptations to provide a physiological environment suitable for cell growth. As discussed in **Chapter 3** the cell culture medium in conventional static systems uses a sodium bicarbonate buffering system to keep a stable pH of 7. However, this also requires access to the surrounding air containing stable level of 5% CO₂. The dynamic system is a closed system, so the sodium bicarbonate was replaced with a HEPES buffer. HEPES is already commonly used within the field of intestinal cell culture and does not require CO₂ [7]. Placement outside of a temperature-controlled incubator means that the temperature needs to be controlled by other means. Therefore, the cell culture medium was heated using a syringe heater system prior to entering the cell model. The syringe heater system consisted of a thermo-kinetic heater control unit, a primary heating pad with a thermocouple temperature sensor and a secondary heating pad. A benefit is that the syringe heaters are easy to use and nearly take up any extra space. However, ideally the cell model and the incoming cell culture medium would be directly heated by being in some sort of small incubator as the cell culture medium cools down on its way to the flow-through transwell when using a syringe heating system. This is less stable, also increasing or decreasing the tubing length towards the flow-through transwell will require re-optimization of the temperature settings. Having a stable temperature of 37°C is essential, as too high temperatures results in cell death and too low temperatures downregulate the energy metabolism in the cell [7]. Furthermore, stability of the compound of interest at higher temperatures is also something to keep in mind when using a syringe heater.

With the adaptations and evaluations discussed above a biologically relevant *in vitro* barrier model of the intestine was established. Ideally, this is further verified and characterized by measuring the presence and functionality of different transporters and metabolic enzymes under flow conditions, as others have shown differences in the expression of these proteins between a static and dynamic culture [8-10].

7.1.2 Evaluation of fluid dynamics and geometry for the dynamic *in vitro* model

Besides assuring that the biology within the dynamic *in vitro* model is relevant the geometry of the device together with the applied flow speed are of great influence on the integration with mass spectrometry. Initially, the organ-on-a-chip system from Micronit Microtechnologies was used for the integration. This technologically advanced system consisted of three glass slides stacked on top of each other with the middle slide containing the porous membrane creating an apical and basolateral chamber [9]. However, when integrating this system with mass spectrometry more frequently than not the system started leaking at the tubing in/outlet or the cell culture membrane ruptured during the experiment, resulting in unreliable permeability data. Due to the lack of robustness for routine analysis using the Micronit system we decided to use a more reliable but less advanced set-up throughout this thesis. The dynamic *in vitro* intestinal barrier model used was the QV600 system from Kirkstall, further referred to in this chapter as flow-through transwell. The initial design and use of Caco-2 cells in this system were modelled and evaluated by Guisti *et al.* [11]. They calculated the shear force on the cell layer and modelled the flow, in figure 7.1 the flow lines are depicted for different flow speeds. Figure 7.1b shows the flow lines for the flow speeds used throughout this thesis, showing a downward trajectory for the apical flow reaching the cell layer. For the other flow speeds modelled by Guisti and colleagues, the flow lines either did not reach the cells (Fig. 7.1a) or resulted into vortices (Fig. 7.1c). Using a higher flow velocity for the top than the bottom compartment in dynamic *in vitro* intestinal barrier models is rarely seen in microfluidic barrier models as it can cause a pressure difference between the top and bottom compartment. However, due to the design of the flow-through transwell the cell layer would only be slightly exposed to the compound of interest when using equal flows. This raises another question, to which extent do more physiologically relevant parameters enhance the *in vitro* model system. Literature has shown that fluid shear stress on the cells influences the cell layer, increasing the presence of transporter proteins and affecting the shape and differentiation of the cells and cell layer [8]. However, minor changes in fluid shear stress already altered the cytoskeleton (F-actin levels), expression of tight junction, microvilli formation and the expression of cytochrome P450 of the Caco-2 monolayer, as studied by Delon *et al.* [12]. Therefore, optimization of the cellular model system should

aim for a functionally relevant microenvironment within the dynamic model instead of recapitulating an *in vivo* accurate fluid shear stress as this might not result in a functional cellular model system. Furthermore, due to the complex structure of the intestine and the non-constant exposure to flow extrapolating an *in vivo* accurate fluid shear stress is difficult.

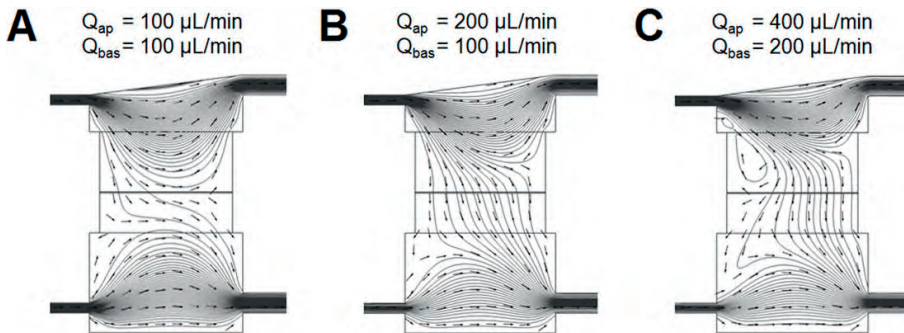


Figure 7.1: Flow line evaluation with different inlet velocities of a) 100 $\mu\text{L}/\text{min}$ (apical) and 100 $\mu\text{L}/\text{min}$ (basolateral), b) 200 $\mu\text{L}/\text{min}$ (apical) and 100 $\mu\text{L}/\text{min}$ (basolateral) and c) 400 $\mu\text{L}/\text{min}$ (apical) and 200 $\mu\text{L}/\text{min}$ (basolateral) reproduced from [11] with permission of John Wiley & Sons

In the flow-through transwell both the apical and basolateral compartment have an internal volume of 2 mL. Due to this rather large geometry, relative high flow speeds, and thus amount of media, are necessary. The advantage of the setup was that in **Chapter 5** diluting the digestive juices coming from the digestion-on-a-chip was easily managed. However, the disadvantage of the setup was that high amounts of the compound of interest were needed to result in a significant concentration at the cell culture system. Smaller devices use less media and the compound of interest, however resulting in smaller sample sizes as well which in term affects the analysis.

When comparing the flow-through transwell system used in this thesis with other organ-on-a-chip systems developed for barrier models, a few things stand out. Firstly, commercially available transwell inserts can be used in the flow-through transwell system, which is beneficial in many aspects. Cell layers can be grown in series in standard well plates before they are transferred to the flow-through transwell system, allowing for higher throughput of experiments compared to systems that require the growth of the cell layer already in the chip

system [9, 13, 14]. Another benefit is that the porous membrane material and surface area of the insert are identical for the static and dynamic experiments, in other words there is no need for normalization of these parameters. Especially membrane material has been proposed as a possible cause for differences in uptake between a static and dynamic culture system [9]. Additionally, the flow-through transwell is cheap for initial purchase and doesn't require any special equipment to operate besides a syringe- or peristaltic pump. Lastly, the system is easy to use. The porous membrane insert is placed inside the QV600 system using an O-ring which seals of the top and bottom chamber. Another platform with a high throughput is the Organoplate system from Mimetas, which has a total of 40 units on one plate, however this is not a full perfusion system and can therefore not be online connected to analytical detection equipment as used in our studies [15].

7.1.3 Integration of the *in vitro* model with mass spectrometry

Sample collection

The integration of *in vitro* models of the digestive tract with mass spectrometry, as used in this thesis, came with several challenges related to sample collection, sample preparation and analysis. Three methods of sample collection for the dynamic cell culture system have been used for various reasons throughout this thesis. The first method used two fraction collectors (one for the apical and one for the basolateral flow) and collected samples in two 96-well plates (**Chapter 3 and 5**). This method allowed for samples to be collected every minute, which for fast permeating compounds is highly desirable. Furthermore, sample preparation steps like dilutions or sample clean-up using Zip tips can be easily performed using a multichannel pipet. Zip tips are pipette tips containing a chromatography bed, which can bind the analyte of interest, subsequently any contaminants (like salts) can be washed away using a wash solution. Disadvantage of this method is that sample sizes per well can slightly vary and the samples are exposed to the ambient environment for the duration of the experiment, which might affect the stability of certain compounds.

The second method eliminated manual handling all together (**Chapter 4 and 5**), samples from the apical and basolateral flow were collected for 20 minutes in a 5 μL sample loop and alternatingly measured. This method gives high control over the sample size and removes the risk of human error.

However, something to consider with this type of sample collection is that due to the narrowing of the outlet in the sample loop a backpressure builds up in the system. If not balanced on the apical and basolateral sides, this pressure can negatively impact the biological cell barrier or result in leakage of the model. This phenomenon was observed when trying to integrate the Micronit system with the automated sample collection system (data not shown). Another key concern is the risk of carry-over between apical and basolateral samples when interface valves and/or capillaries are alternatingly in contact with high and low levels of analytes of interest. Therefore, the integrated design developed in **Chapter 4** has separate valves and capillaries for the apical and basolateral effluent to prevent carry-over between the two streams. This however compromises the continuous online analysis of the two sides of the flow-through transwell. Others have collected sample from their microfluidic chip onto a solid phase extraction (SPE) column directly [16, 17], mostly using (non-commercial) on chip SPE columns which adds to the variability between chips. The last method used for sample collection was used in **Chapter 6** for the nanoparticle sample collection. Apical samples were continuously collected in a 50 mL tube and basolateral samples were collected every 10 minutes in a 15 mL tube by manually changing the collection tube. As the samples were analysed with single particle inductively coupled plasma mass spectrometry (sp-ICP-MS) extensive dilution of mainly the apical sample was required before analysis, which adds complexity to automated collection and online analysis of the sample. The use of a fraction collector in this case was also undesirable as this would increase the volume to surface area per sample and for example titanium dioxide nanoparticles tend to stick heavily to the plastic of a 96-well plate. In literature, an integrated online analysis system for the detection of nanoparticles using ICP-MS has yet to be described. In figure 7.2 a proposed online coupling scheme for the flow-through transwell to ICP-MS is visualised. A single micromixer is connected to the basolateral outlet of the flow-through transwell to dilute the sample with an aqueous eluent which can contain a percentage of nitric acid to prevent sticking of particles to the wall of the micromixer. Followed by a switching valve containing a sample loop to collect the diluted sample. When the sample loop is filled it can be flushed towards the ICP-MS with an aqueous eluent for analysis. Apical samples would be collected separately to determine the exposure concentration.

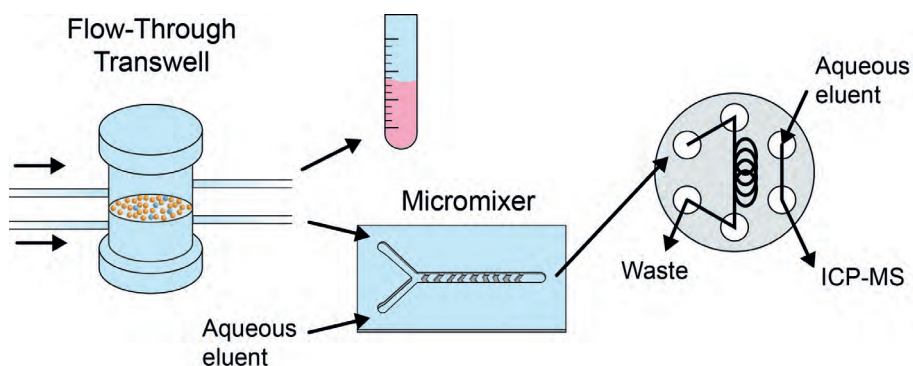


Figure 7.2: Schematic overview of proposed online coupling of the flow-through transwell to ICP-MS.

Sample clean-up

A reliable *in vitro* cell model starts with providing the cells with the right nutrients to grow and keep a stable energy balance. In **Chapter 2**, a list of common ingredients in cell culture medium was provided to emphasize the complexity of the sample matrix. This complex matrix will induce problems during analytical measurements, indicating the need for sample preparation. For **Chapters 3-5**, when performing permeability experiments the compound of interest was dissolved in Hank's balanced salt solution (HBSS). As the name already suggests high levels of salts are present in this mixture. In **Chapter 5** the matrix was even more complex due to the addition of digestive juices. Salts can heavily interfere with the electrospray ionization (ESI) process and cause ion suppression in the MS analysis [18]. Therefore, it is of great importance to get rid of these salts before introducing the sample to the electrospray. In this thesis, a C8 (nano) trap column was used to retain the compounds of interest and wash away the salts present in the mixture (**Chapter 4**). A disadvantage of this method is that the compound of interest needs to be sufficiently retained, furthermore if a more hydrophilic metabolite is formed it will most likely not be fully retained on the C8 (nano) trap column and thus not detected during the final measurement. However, the trap column (and the analytical column) can be easily adapted to suite the physicochemical characteristics of the analytes of interest. For example, a C4 trap column with a larger pore size can be used for the analysis of proteins. However, it should always be considered that other components of the sample matrix might be retained as well. In **Chapter 6**, nanoparticles were suspended in cell culture medium, this

was important as the proteins in the medium form a protein corona around the particles hereby affecting the interacting the cells and uptake, which also occurs *in vivo* [19]. For the analysis of gold particles, the high content of salts and sugars did not interfere with the ICP-MS analysis. However, when looking at a more food relevant particle like titanium dioxide particles for example the presence of high levels of calcium can pose a problem for ICP-MS analysis. The most abundant isotope for titanium is ^{48}Ti , which experiences interference of isobaric ^{48}Ca . With a quadrupole ICP-MS instrument no distinction can be made between calcium and titanium, however this problem can be resolved when moving towards the high resolution ICP-MS measuring the less abundant ^{47}Ti isotope. Other solutions to remove the interference of calcium from the matrix are incorporating an ion exchange column or membrane in order to remove the Ca^{2+} ions from the Ti particles, or reacting the titanium with an ammonia reaction gas [20].

7.1.4 Advances in online and *in situ* analysis platforms for organ-on-a-chip devices

Chapter 2 was published mid-2019 and since then a few interesting papers have been published on the integration of organ-on-a-chip models with high-end analytical equipment. In this paragraph, selected newly emerged literature is highlighted. In **Chapter 2**, one of the drawbacks of integrated electrochemical sensors in organ-on-a-chip systems was discussed being that only one or two analytes could be measured at the same time. Recently, Giménez-Gómez and colleagues developed a multiplexed electrochemical lab-on-a-chip device, they were able to measure four different parameters in parallel namely, glucose, hydrogen peroxide, cell conductivity and the oxidation reduction potential. They showed the applicability of the system by exposing human lung fibroblast cells to hydrogen peroxide inducing oxidative stress. Another great feature of this system is that the cell culture chamber is upstream from the sensor chambers, so the reactions taking place at the sensor surface are separate from the cell model [21]. This also allows for regeneration of the sensors without compromising the cell model, reducing the effect of biofouling on the integrated sensor. New studies on the integration of an organ-on-a-chip system with mass spectrometry are limited. However, one nice example was developed by Cahill et al. They designed a chip that allowed for liquid microjunction surface sampling probe mass spectrometry (LMJ-SSP

MS). The microfluidic device consisted of a porous membrane top section through which sampling of the chip below could occur. With this technique a spatial distribution of chemicals along the microfluidic channel was visualized [22]. Even though the authors did not show a biological application for this technique, it is easy to imagine that this type of mass spectrometry imaging would be well suited for the analysis of the digestion-on-a-chip used in **Chapter 5**. This would allow for direct analysis of digestion products in the different compartments (e.g. mouth, stomach and intestine), without the need for manual sampling.

7.2 Future perspectives

The possibilities of integrating microfluidic cell culture and analysis techniques seem almost endless, ranging from single organ-on-a-chip devices with manual sample collection to multi-organ systems with integrated sensor platforms and analytical detection techniques [23]. For intestinal models mechanical and biological parameters, like peristaltic motion, fluid shear stress, presences of all cell types, 3D crypt/villi structure and the incorporation of the microbiome have all been realised, separately. It is nearly impossible to recapitulate all these factors in one *in vitro* intestinal barrier system. Furthermore, depending on the scientific question addressed not all factors have to be included in future integrated designs to establish a functional *in vitro* model. A critical look at which factors will contribute to an *in vitro* intestinal barrier model suited for predicting oral bioavailability of chemicals in humans is highly desirable. In the section 'future biology' these factors are discussed. Almost the same goes for the integration of analytical read-out system, **Chapter 2** already explored the current *in situ* and online integration systems for organ-on-a-chip models, in the paragraph 'future integration' suggestions are given for future integration platforms and which aspects to consider.

7.2.1 Future biology

In this thesis and throughout literature most dynamic *in vitro* intestinal models have incorporated the cancer cell line Caco-2 as a mimic for the enterocytes present in the small intestine. Sometimes a combination with the mucus producing cell line HT29-MTX representing the goblet cells is also described.

The simple culturing methods, widespread availability and the large data sets available for these cell lines as reference make them an attractive cell model system for the intestinal barrier. Nevertheless, these cancerous cell lines do not fully recapitulate the intestinal tissue (cellular and molecular machinery) and environment *in vivo*, as they fail to express important transporter and metabolic proteins and do not represent cellular diversity [24]. Since the discovery of mouse small intestinal organoids in 2009 [25], the ability to culture human small intestinal organoids containing all the cell types present in the human gut soon followed [26]. The benefit of an organoid culture lies in the cells ability to mimic *in vivo* cellular programming and a higher order of tissue organization. Furthermore, organoid cultures can be set-up from induced pluripotent stem cells or biopsies getting a step closer to personalized medicine. The one downside of small intestinal organoid cultures is that they grow in an extracellular matrix and form a closed sphere with the lumen on the inside making it difficult to expose the intestinal cells to a compound of interest. Researchers have been successful in growing the organoids as a flat 2D culture making it more accessible for permeability experiments [27] and the first studies incorporating these 2D cultures in a microfluidic chip have been established as well [10, 28, 29].

With the rise of microfluidic technology, dynamic intestinal barrier models were one of the first flow based cell culture models developed and flow has since been included in many devise [2, 8, 9, 13]. Inducing fluid shear stress on an intestinal cell layer is achieved relatively easy with current microfluidic engineering techniques and has a high impact on the biological microenvironment [12]. The inclusion of flow was followed by the incorporation of peristaltic motion by stretching and releasing the cell culture membrane, resulting in cyclic strain on the cells. Results on how this affects the properties of the cell barrier are mixed. Kim *et al.* has shown that peristaltic motion together with applying flow results in increased permeability and aminopeptidase activity of the Caco-2 monolayer [13]. However, other studies have presented that only applying flow is enough to modulate these properties [30, 31]. According to this, including peristaltic motion as a parameter in a dynamic intestinal barrier model might unnecessarily complicate the model, without much added benefit. This is also backed up by the limited number of studies incorporating peristaltic motion in the model.

Another aspect that highly influences the behaviour of chemicals and cells in the gastrointestinal tract is the intestinal microbiome. The potential impact of microbes on immune regulation, compound metabolism, nutrition and infection in the gut is starting to be revealed and would be a valuable addition to a dynamic *in vitro* cell culture model of the intestine. However, incorporating aspects of the microbiome on a microfluidic chip is tricky. Several studies have incorporated commensal or pathogenic bacteria, however growing under aerobic circumstances [32-34], this only partly represents the wide variety of microorganisms present in the gut as several species require anaerobic conditions to grow. The HuMix (human-microbial crosstalk) model does provide microbial exposure under anaerobic conditions, by incorporating the bacteria via a separate channel allowing oxygen free conditions [35, 36], yet making the model as a whole more complex. In the case of incorporating the microbiome on chip the balance between added biological effects and the increased complexity of the system itself largely depends on the biological questions asked. For research into the uptake of nutrients, especially complex carbohydrates that are metabolised by gut microbes the addition of the microbiome in the *in vitro* model is essential.

Lastly, one of the striking features of the intestinal epithelium is its 3D structures of crypts and villi. The 3D structure increases the absorptive surface area and affects the differentiation of the epithelial cells. This notion has resulted in the development of 3D scaffolds that can be placed inside dynamic intestinal barrier models mimicking the crypt/villi structure [14, 37, 38]. Selecting the right material for the scaffold is essential for permeability experiments, for example the use of a collagen hydrogel negatively impacted the transport of lipophilic drug antipyrine in a study by Yu *et al.* [37]. Limited research has been performed examining the effect of 3D scaffolds in combination with microfluidic intestinal chips and to which extent it improves the biological model. Therefore, future developments of the biological model within a dynamic cell culture device should aim for a basic system including all relevant cell types and flow with the option to include the microbiome if the application calls for it.

7.2.2 Future integrations

Current integrated platforms with online or *in situ* analysis of the organ-on-a-chip system consist of individual cellular units mimicking one or two organs

and only a few parameters are monitored at the same time. Furthermore, the integrated chip systems are often fabricated using PDMS, as it is biocompatible and easy for rapid prototyping. However, adsorption of analytes and nanoparticles [39] and limited possibilities in upscaling the fabrication process make it a material unsuited for future integrations. The organ-on-a-chip field is highly diverse with bioengineers, cell biologists and analytical chemists all contributing to novel integrated systems. However, for future integrations the biological questions that we want answered need to lead the engineering process and not the other way around. As presented in this thesis and other literature, organ-on-a-chip systems can be integrated with multiple sensors and high-end analytical equipment providing a lot of information for one individual biological experiment [40-42]. Figure 2.6 (Chapter 2), depicts a total analysis system for a single chip device envisioning a self-regulating organ-on-a-chip system with sensors for active feedback control of the microenvironment (oxygen, glucose). The theoretical system also includes a sensor for continuous read-out of the barrier integrity via TEER measurements. Furthermore, the system is coupled to miniaturized analytical equipment for the analysis of target analytes and metabolites thereof. This will eventually lead to an online analysis system that provides continuous data to uphold a stable microenvironment needed for relevant biological experiments. This, however, makes the integrated system highly complex and will affect user friendliness and throughput. Therefore, besides developing vastly integrated systems, increasing the throughput and user friendliness of the systems is desired as well. Meaning the number of biological replicates per system needs to be increased, but also the automated online analysis system needs to match the upscaling process. Throughout this thesis the focus was on the analysis of intestinal permeability in the flow-through transwell by measuring the compound of interest in the effluent. Besides examining permeability, the accumulation within the cell layer itself is highly important for toxicity and overall bioavailability. Analytical techniques incorporating laser ablation (LA), like LA-ICP-MS and LAESI-MS would be well equipped to analyse the uptake of molecules or metal nanoparticles by the cell layer in a spatial manner [43-46].

7.2.3 Benchmarking in vitro dynamic models

The multidisciplinary field of organ-on-a-chip technology has for a long time focussed on technological development, pushing the boundaries of

microfluidic *in vitro* cell culture systems. This has resulted in an array of different designs and integrations each with its own advantages and disadvantages. However, the use of organ-on-a-chip technology in drug development trials or for regulatory purposes is non-existent. Going forward more attention needs to be given towards validation and improvement of current model systems and user friendliness, to realize the end goal of organ-on-a-chip technology as alternative to animal testing. To reach that goal first large-scale studies need to be performed comparing the different dynamic *in vitro* model systems amongst each other and to the current experimental models used. Aspects to consider are predictability of *in vivo*, throughput, user friendliness, compatibility with analysis and costs.

References

- [1] Azizipour N, Avazpour R, Rosenzweig DH, Sawan M, Ajji A. Evolution of biochip technology: A review from lab-on-a-chip to organ-on-a-chip. *Micromachines (Basel)*. 2020;11(6).
- [2] Bein A, Shin W, Jalili-Firoozinezhad S, Park MH, Sontheimer-Phelps A, Tovaglieri A, et al. Microfluidic organ-on-a-chip models of human intestine. *Cell Mol Gastroenter*. 2018;5(4):659-668.
- [3] Volpe DA. Variability in Caco-2 and MDCK cell-based intestinal permeability assays. *J Pharm Sci-U.S.* 2008;97(2):712-725.
- [4] Srinivasan B, Kolli AR, Esch MB, Abaci HE, Shuler ML, Hickman JJ. TEER measurement techniques for in vitro barrier model systems. *Jala-J Lab Autom*. 2015;20(2):107-126.
- [5] Jie MS, Li HF, Lin LY, Zhang J, Lin JM. Integrated microfluidic system for cell co-culture and simulation of drug metabolism. *Rsc Adv*. 2016;6(59):54564-54572.
- [6] Esch MB, Mahler GJ, Stokor T, Shuler ML. Body-on-a-chip simulation with gastrointestinal tract and liver tissues suggests that ingested nanoparticles have the potential to cause liver injury. *Lab Chip*. 2014;14(16):3081-3092.
- [7] Hubatsch I, Ragnarsson EGE, Artursson P. Determination of drug permeability and prediction of drug absorption in Caco-2 monolayers. *Nat Protoc*. 2007;2(9):2111-2119.
- [8] Kim HJ, Ingber DE. Gut-on-a-Chip microenvironment induces human intestinal cells to undergo villus differentiation. *Integr Biol-Uk*. 2013;5(9):1130-1140.
- [9] Kulthong K, Duivenvoorde L, Sun HY, Confederat S, Wu J, Spenkelink B, et al. Microfluidic chip for culturing intestinal epithelial cell layers: Characterization and comparison of drug transport between dynamic and static models. *Toxicol in Vitro*. 2020;65.
- [10] Kasendra M, Tovaglieri A, Sontheimer-Phelps A, Jalili-Firoozinezhad S, Bein A, Chalkiadaki A, et al. Development of a primary human small intestine-on-a-chip using biopsy-derived organoids. *Sci Rep-Uk*. 2018;8.
- [11] Giusti S, Sbrana T, La Marca M, Di Patria V, Martinucci V, Tirella A, et al. A novel dual-flow bioreactor simulates increased fluorescein permeability in epithelial tissue barriers. *Biotechnol J*. 2014;9(9):1175-1184.
- [12] Delon LC, Guo ZB, Oszmiana A, Chien CC, Gibson R, Prestidge C, et al. A systematic investigation of the effect of the fluid shear stress on Caco-2 cells towards the optimization of epithelial organ-on-chip models. *Biomaterials*. 2019;225.
- [13] Kim HJ, Huh D, Hamilton G, Ingber DE. Human gut-on-a-chip inhabited by microbial flora that experiences intestinal peristalsis-like motions and flow. *Lab Chip*. 2012;12(12):2165-2174.
- [14] Shim KY, Lee D, Han J, Nguyen NT, Park S, Sung JH. Microfluidic gut-on-a-chip with three-dimensional villi structure. *Biomed Microdevices*. 2017;19(2).
- [15] Trietsch SJ, Naumovska E, Kurek D, Setyawati MC, Vormann MK, Wilschut KJ, et al. Membrane-free culture and real-time barrier integrity assessment of perfused intestinal epithelium tubes. *Nat Commun*. 2017;8.
- [16] Gao D, Liu HX, Lin JM, Wang YN, Jiang YY. Characterization of drug permeability in Caco-2 monolayers by mass spectrometry on a membrane-based microfluidic device. *Lab Chip*. 2013;13(5):978-985.
- [17] Marasco CC, Enders JR, Seale KT, McLean JA, Wikswo JP. Real-time cellular exometabolome analysis with a microfluidic-mass spectrometry platform. *Plos One*. 2015;10(2).
- [18] Annesley TM. Ion suppression in mass spectrometry. *Clin Chem*. 2003;49(7):1041-1044.
- [19] Walczak AP, Kramer E, Hendriksen PJM, Helsdingen R, van der Zande M, Rietjens IMCM, et al. In vitro gastrointestinal digestion increases the translocation of polystyrene nanoparticles in an in vitro intestinal co-culture model. *Nanotoxicology*. 2015;9(7):886-894.
- [20] Tharaud M, Gondikas AP, Benedetti MF, von der Kammer F, Hofmann T, Cornelis G. TiO₂ nanomaterial detection in calcium rich matrices by spICPMS. A matter of resolution and treatment. *J Anal Atom Spectrom*. 2017;32(7):1400-1411.
- [21] Gimenez-Gomez P, Rodríguez-Rodríguez R, Rios JM, Perez-Montero M, Gonzalez E, Gutierrez-Capitan M, et al. A self-calibrating and multiplexed electrochemical lab-on-a-chip for cell culture analysis and high-resolution imaging. *Lab Chip*. 2020;20(4):823-833.

- [22] Cahill JF, Khalid M, Retterer ST, Walton CL, Kertesz V. In situ chemical monitoring and imaging of contents within microfluidic devices having a porous membrane wall using liquid microjunction surface sampling probe mass spectrometry. *J Am Soc Mass Spectr.* 2020;31(4):832-839.
- [23] Zhang YS, Aleman J, Shin SR, Kilic T, Kim D, Shaegh SAM, et al. Multisensor-integrated organs-on-chips platform for automated and continual in situ monitoring of organoid behaviors. *P Natl Acad Sci USA.* 2017;114(12):E2293-E2302.
- [24] Mochel JP, Jergens AE, Kingsbury D, Kim HJ, Martin MG, Allenspach K. Intestinal stem cells to advance drug development, precision, and regenerative medicine: A paradigm shift in translational research. *Aaps J.* 2018;20(1).
- [25] Sato T, Vries RG, Snippert HJ, van de Wetering M, Barker N, Stange DE, et al. Single Lgr5 stem cells build crypt-villus structures in vitro without a mesenchymal niche. *Nature.* 2009;459(7244):262-U147.
- [26] Sato T, Stange DE, Ferrante M, Vries RGJ, van Es JH, van den Brink S, et al. Long-term expansion of epithelial organoids from human colon, adenoma, adenocarcinoma, and barrett's epithelium. *Gastroenterol.* 2011;141(5):1762-1772.
- [27] van der Hee B, Loonen LMP, Taverne N, Taverne-Thiele JJ, Smidt H, Wells JM. Optimized procedures for generating an enhanced, near physiological 2D culture system from porcine intestinal organoids. *Stem Cell Res.* 2018;28:165-171.
- [28] Workman MJ, Gleeson JP, Troisi EJ, Estrada HQ, Kerns SJ, Hinojosa CD, et al. Enhanced utilization of induced pluripotent stem cell-derived human intestinal organoids using microengineered chips. *Cell Mol Gastroenter.* 2018;5(4):669-677.
- [29] Park SE, Georgescu A, Huh D. Organoids-on-a-chip. *Science.* 2019;364(6444):960-965.
- [30] Tan HY, Trier S, Rahbek UL, Dufva M, Kutter JP, Andresen TL. A multi-chamber microfluidic intestinal barrier model using Caco-2 cells for drug transport studies. *Plos One.* 2018;13(5).
- [31] Pocock K, Delon L, Bala V, Rao S, Priest C, Prestidge C, et al. Intestine-on-a-chip microfluidic model for efficient in vitro screening of oral chemotherapeutic uptake. *ACS Biomater Sci Eng.* 2017;3(6):951-959.
- [32] Kim HJ, Li H, Collins JJ, Ingber DE. Contributions of microbiome and mechanical deformation to intestinal bacterial overgrowth and inflammation in a human gut-on-a-chip. *P Natl Acad Sci USA.* 2016;113(1):E7-E15.
- [33] Mortensen NP, Mercier KA, McRitchie S, Cavallo TB, Pathmasiri W, Stewart D, et al. Microfluidics meets metabolomics to reveal the impact of *Campylobacter jejuni* infection on biochemical pathways. *Biomed Microdevices.* 2016;18(3).
- [34] Kim J, Hegde M, Jayaraman A. Co-culture of epithelial cells and bacteria for investigating host-pathogen interactions. *Lab Chip.* 2010;10(1):43-50.
- [35] Shah P, Fritz JV, Glaab E, Desai MS, Greenhalgh K, Frachet A, et al. A microfluidics-based in vitro model of the gastrointestinal human-microbe interface. *Nat Commun.* 2016;7.
- [36] Eain MMG, Baginska J, Greenhalgh K, Fritz JV, Zenhausern F, Wilmes P. Engineering solutions for representative models of the gastrointestinal human-microbe interface. *Engineering-Proc.* 2017;3(1):60-65.
- [37] Yu JJ, Peng SM, Luo D, March JC. In vitro 3D human small intestinal villous model for drug permeability determination. *Biotechnol Bioeng.* 2012;109(9):2173-2178.
- [38] Wu J, Chen QS, Liu W, He ZY, Lin JM. Recent advances in microfluidic 3D cellular scaffolds for drug assays. *Trac-Trend Anal Chem.* 2017;87:19-31.
- [39] Berthier E, Young EWK, Beebe D. Engineers are from PDMS-land, biologists are from polystyrenia. *Lab Chip.* 2012;12(7):1224-1237.
- [40] Santbergen MJC, van Der Zande M, Bouwmeester H, Nielen MWF. Online and in situ analysis of organs-on-a-chip. *Trac-Trend Anal Chem.* 2019;115:138-146.
- [41] Mao SF, Li WW, Zhang Q, Zhang WL, Huang QS, Lin JM. Cell analysis on chip-mass spectrometry. *Trac-Trend Anal Chem.* 2018;107:43-59.
- [42] Kieninger J, Weltin A, Flamm H, Urban GA. Microsensor systems for cell metabolism - from 2D culture to organ-on-chip. *Lab Chip.* 2018;18(9):1274-1291.

- [43] Drescher D, Giesen C, Traub H, Panne U, Kneipp J, Jakubowski N. Quantitative imaging of gold and silver nanoparticles in single eukaryotic cells by laser ablation ICP-MS. *Anal Chem.* 2012;84(22):9684-9688.
- [44] Wang M, Zheng LN, Wang B, Chen HQ, Zhao YL, Chai ZF, et al. Quantitative analysis of gold nanoparticles in single cells by laser ablation inductively coupled plasma-mass spectrometry. *Anal Chem.* 2014;86(20):10252-10256.
- [45] Shrestha B, Sripadi P, Walsh CM, Razunguzwa TT, Powell MJ, Kehn-Hall K, et al. Rapid, non-targeted discovery of biochemical transformation and biomarker candidates in oncovirus-infected cell lines using LAESI mass spectrometry. *Chem Commun.* 2012;48(31):3700-3702.
- [46] Sripadi P, Shrestha B, Easley RL, Carpio L, Kehn-Hall K, Chevalier S, et al. Direct detection of diverse metabolic changes in virally transformed and tax-expressing cells by mass spectrometry. *Plos One.* 2010;5(9).

Summary

Currently, animals are used for the risk assessment of hazardous chemicals and the development of novel drugs. Apart from the ethical issues when using animals, the lack of predicative power for the human body has stimulated researchers to develop an intricate *in vitro* cell culture models that better mimic the human situation. The combination of microfluidic lab-on-a-chip technology with cell biology techniques resulted in the organ-on-a-chip, an *in vitro* cell culture system that is subjected to a dynamic physiological microenvironment. For almost every organ in the human body a chip equivalent was created, as was for the intestine. The main aim of this thesis was to integrate a dynamic *in vitro* intestinal barrier model with advanced mass spectrometry equipment for automated and online analysis of oral bioavailability for an array of compounds.

In chapter 2, the literature was reviewed for online and *in situ* analytical techniques integrated with organ-on-a-chip devices with special emphasis on maintaining the biological relevance, achieving analytical compatibility, system integration and final applicability. It was found that *in situ* optical and electrochemical sensors, when integrated, were easy to use and could be placed inside a gas and temperature-controlled incubator aiding biological compatibility. However, lower sensitivity compared to its benchtop counterparts and susceptibility to biofouling were the major issues for these integrations. Online coupling of an organ-on-a-chip to a mass spectrometer was also discussed in chapter 2. Continuous online mass spectrometric detection of organ-on-a-chip systems is currently not feasible, due to the high levels of sugars, salts and antibiotics in the cell culture medium. A sample preparation step was required usually by incorporation of SPE columns and a wash step to prevent ionization suppression. In recent interfacing designs, the organ-on-a-chip device was generally placed outside the gas and temperature-controlled incubator to allow interfacing with a mass spectrometer. Obviously, this is still a serious drawback as it compromises a biological accurate environment.

In this thesis oral bioavailability of chemicals was studied as this is essential information for novel drug development and in the field of toxicology. Intestinal uptake of the chemical is a crucial factor in oral bioavailability, highlighting the importance of *in vitro* intestinal models that correctly predict this phenomenon. In chapter 3a, a dynamic *in vitro* model of the intestine for permeability studies of chemicals was developed and evaluated. A co-culture

of Caco-2 and HT29-MTX-E12 cells was grown in a flow-through transwell system. Proper gut barrier function was assessed by showing absence of Lucifer yellow permeability, and examination of the morphology of the cell barrier using confocal microscopy. The permeability of the model compound verapamil was determined and showed similar permeability compared to the traditional static transwells. Furthermore, the system was benchmarked against *in vitro* and *in vivo* permeability data found in literature. In chapter 3b the permeability of the mycotoxin ergotamine(in)e was evaluated in the static and dynamic *in vitro* intestinal model systems. A higher permeability of the epimer ergotaminine was observed compared to ergotamine in the static *in vitro* model. This difference was lost in the dynamic model experiments. Highlighting the importance of flow and flow induced shear stress on the cell monolayer and subsequently on permeability of a compound.

Despite a few recent integration attempts, ensuring a biological relevant microenvironment while coupling with a fully online detection system still represents a major challenge. Herein, in chapter 4 an online technique to measure drug permeability and analyse (un)known product formation across an intestinal epithelial layer was designed, while ensuring the quality and relevance of the biological model. Chip-based ultra-performance liquid chromatography quadrupole time-of-flight mass spectrometry (UPLC-QTOF-MS) was coupled to the dynamic flow-through transwell via a series of switching valves, thus allowing alternating measurements of the apical and basolateral side of the *in vitro* model. Two trap columns were integrated for online sample pre-treatment and compatibility enhancement. Temporal analysis of the intestinal permeability was successfully demonstrated using verapamil as a model drug and ergotamine epimers as a model for natural mycotoxins present in foods. Evidence was obtained that the newly developed dynamic online analysis system provides reliable results versus offline analysis. Finally, initial experiments with the drug granisetron suggest that metabolic activity can be studied as well, thus highlighting the versatility of the bio-integrated online analysis system developed.

In chapter 5, a novel, integrated, *in vitro* gastrointestinal system was presented including three hyphenated modules for digestion, intestinal absorption and analysis. In the first module, a compound was exposed dynamically to enzymatic

digestion in three consecutive microreactors, mimicking the processes of the mouth, stomach, and intestine. The resulting solution (chyme), continued to the second module, a flow-through barrier model of the intestine allowing translocation of the compound and metabolites thereof. The final module analysed the composition of both effluents from the barrier model by chip-based electrospray ionization mass spectrometry. Apart from technical challenges interfacing the modules, a key challenge is ensuring proper barrier integrity of the intestinal layer under these hyphenated conditions. Two model drugs were used to test the integrated model, omeprazole and verapamil. Omeprazole was shown to be broken down upon treatment with gastric acid but reached the cell barrier unharmed when emulating an enteric-coated formulation. In contrast, verapamil was unaffected by digestion. Finally, a simple food matrix, apple juice, was introduced into the system resulting in a reduced uptake of verapamil.

For chapter 6, the effect of flow on gold nanoparticle (AuNP) uptake and translocation was studied in a flow-through transwell. NPs can be found in a variety of food products, which has led to concerns about their potential adverse effects for consumers upon ingestion. Currently, static *in vitro* cell culture models of the intestine are used to predict the uptake and translocation of NPs in the human gastrointestinal tract. However, in a static environment NP sedimentation or flotation can cause altered exposure levels on the cells. By including flow into the cell model these problems might be solved. Nevertheless, the effect of flow on the translocation of NP across the *in vitro* intestinal barrier is largely unknown. In chapter 6, the cell associated fraction and translocation of gold nanoparticles (AuNPs) between a static *in vitro* cell culture system and a dynamic flow-through transwell system were compared using single particle inductively coupled plasma mass spectrometry (sp-ICP-MS). The translocation of 15, 30 and 70 nm AuNPs was examined in the static system. Only the smallest particles translocated through the static *in vitro* cell layer. For the dynamic experiments only, the smallest particles were used. The translocation and cell associated fraction of the 15 nm AuNPs in the flow-through transwell was increased compared to the static system. This is most likely due to the higher total amount of particles that the cell layer was exposed to in the flow-through transwell and the flow directing the particles towards the cell layer. Even though, the inclusion of flow might solve NP sedimentation/flotation problems present in static barrier models. The results show that

accurate measurements of the number of particles that reaches the cells is of great importance to determine the (apparent) bioavailability of NPs for both the static and dynamic model.

In this thesis, *in vitro* models of the digestive tract were integrated with advanced mass spectrometry equipment to study the oral bioavailability of small drug compounds, toxins and nanoparticles. In chapter 7, the potential and limitations of the developed system were discussed, and recommendations were given for future research.

Samenvatting

Hedendaags, worden voor de ontwikkeling van nieuwe medicijnen en de risico beoordeling van gevaarlijke stoffen proefdieren gebruikt. Buiten de ethische aspecten omtrent proefdieren geven ze ook niet genoeg voorspellende informatie over wat er daadwerkelijk gebeurt in het menselijk lichaam. Dit heeft onderzoekers gestimuleerd om een beter alternatief te gaan ontwikkelen in de vorm van een complex *in vitro* cel model. De combinatie van lab-on-a-chip technologie en cel biologie technieken heeft geleid tot de ontwikkeling van het organ-on-a-chip systeem. Dit is een *in vitro* cel model dat wordt blootgesteld aan een dynamisch fysiologisch micro-omgeving. Voor bijna ieder orgaan in het menselijk lichaam is er een chip variant ontwikkeld zo ook voor de darmen. Het doel van dit proefschrift is het integreren van een dynamisch *in vitro* darm model met geavanceerde massa spectrometers voor geautomatiseerde en online analyse van biologische beschikbaarheid voor een verscheidenheid aan stoffen.

In hoofdstuk 2, is er in de literatuur gekeken naar huidige online en *in situ* analytische technieken die zijn geïntegreerd met organ-on-a-chip systemen met de nadruk op biologische relevantie, analytische compatibiliteit, systeem integratie en toepasbaarheid. Geïntegreerde *in situ* optische en electrochemische sensoren konden makkelijk in een gas en temperatuur gecontroleerde incubator worden geplaatst, wat de biologische compatibiliteit aanzienlijk verhoogde. Echter, deze geïntegreerde sensoren konden minder gevoelig meten in vergelijking met de standaard meet system en waren vatbaar voor biofouling. Verder werd in hoofdstuk 2 ook de online koppeling van een massa spectrometer aan de organ-on-a-chip besproken. Op het moment is het niet mogelijk om voortdurend een organ-on-a-chip systeem te analyseren met gebruik van een massa spectrometer. Dit komt door het hoge gehalte aan suikers, zouten en antibiotica in het te analyseren celweek medium. Het gebruik van een SPE kolom en was stappen is nodig als een voorbereidingsstap, dit om ion onderdrukking in de massa spectrometer te voorkomen. Voor recente integraties wordt het organ-on-a-chip systeem buiten een incubator geplaatst om het te kunnen koppelen aan de massa spectrometer. Logischer wijs is dit een nadeel aangezien dit niet een biologische relevante omgeving is voor cellen.

In dit proefschrift is er gekeken naar de orale biologische beschikbaarheid van stoffen, dit is essentiële informatie voor de ontwikkeling van nieuwe medicijnen en toxicologisch onderzoek. Doorgifte van een chemische stof door de darm is een cruciaal onderdeel van orale bio-beschikbaarheid. Het gebruik van *in vitro* darm modellen is daarom ook van belang om de opname van stoffen te kunnen voorspellen. In hoofdstuk 3a, is er een dynamisch *in vitro* darm model ontwikkeld om de doorgifte van stoffen te evalueren. In een doorstroom transwell systeem werd een co-culture van Caco-2 en HT29-MTX-E12 cellen gegroeid. Vervolgens werd er vastgesteld dat de *in vitro* darm cellaag niet lekte, door de afwezigheid van lucifer yellow opname en de visuele beoordeling van de morfologie van de cellaag door het gebruik van een confocale microscoop. De doorgifte van de model stof verapamil werd vastgesteld in de doorstroom transwell en was vergelijkbaar aan de opname in de traditionele statische transwell. Verder, is het systeem ook nog vergeleken met *in vitro* en *in vivo* data vanuit de literatuur. In hoofdstuk 3b, werd er gekeken naar de opname van de mycotoxine ergotamin(in)e in het statische en doorstroom darm model. Een hogere doorgifte werd gevonden voor de ergotaminine epimeer in vergelijking met ergotamine in het statische model. Het verschil tussen de doorgifte van de twee epimeren was verdwenen in de experimenten met het dynamische model. Dit laat zien dat de vloeistof stroom in het dynamische model en de kracht die dat uitoefent op de cellaag invloed heeft op de doorgifte van stoffen door de cellaag.

Ondanks meerdere pogingen om een organ-on-a-chip systeem te koppelen aan een online detectie systeem blijft het garanderen van een biologische relevant omgeving de grootste uitdaging. In hoofdstuk 4 werd een online analyse techniek ontwikkeld voor de detectie van medicijn doorgifte in het dynamische celsysteem, terwijl tegelijkertijd de biologische omgeving werd behouden. Een ultra-performance liquid chromatography quadrupole time-of-flight massa spectrometer (UPLC-QTOF-MS) werd gekoppeld aan de doorstroom transwell via een serie van schakelkranen. Dit zorgde ervoor dat de apicale en basolaterale kant van het *in vitro* model afwisselend konden worden gemeten. Twee trap kolommen werden geïntegreerd als monster voorbereidingsstap. De doorgifte van verapamil en ergotamine kon worden vastgesteld in de tijd. Als laatste experiment voor dit hoofdstuk werd er gekeken

naar het medicijn granisetron, wat suggereerde dat metaboliëet formatie ook kan worden gemeten met het huidige geïntegreerde systeem.

Hoofdstuk 5 beschrijft de integratie van een *in vitro* mond, maag, darm systeem dat bestaat uit drie digestie modules, een darm cellaag en online analyse. In het eerste deel werd een stof blootgesteld aan drie enzymatische digestie modules die de processen in de mond, maag en darm nabootste. Na de digestie werd de stof geïntroduceerd aan de doorstroom transwell en vervolgens werd de doorgifte door de cellaag gemeten met de massa spectrometer. Buiten de technische uitdagingen om alle systemen aan elkaar te koppelen, was de integriteit van de cellaag van cruciaal belang. Twee model stoffen werden gekozen om het integratie model te testen, omeprazol en verapamil. Puur omeprazol degradeerde wanneer het in aanraking kwam met de maagsappen. Maar wanneer gecoat omeprazol werd nagebootst bereikte omeprazol de cellaag intact. In tegenstelling tot omeprazol was verapamil onaangetast na digestie. Tenslotte, werd een simpele voedsel matrix (appelsap) geïntroduceerd in het systeem tegelijkertijd met verapamil, dit zorgde voor verminderde doorgifte van verapamil door de cellaag.

Voor hoofdstuk 6, werd de opname en doorgifte van goud nanodeeltjes bestudeerd in het doorstroom transwell systeem. Nanodeeltjes kunnen in allerlei soorten voedsel worden gevonden, wat soms kan leiden tot schadelijke effecten wanneer ze worden ingeslikt. In huidige statische *in vitro* cel systemen sedimenteren of drijven de nanodeeltjes in het systeem, wat de uiteindelijke concentratie op de cellen beïnvloed. Een dynamisch doorstroom cel system zou dit probleem kunnen verhelpen. Maar het effect van een vloeistof stroom op de opname en doorgifte van nanodeeltjes in *in vitro* modellen is tot op heden nooit onderzocht. In hoofdstuk 6, werd de opname en doorgifte van goud nanodeeltjes vergeleken tussen een statisch en dynamisch transwell systeem. De goud deeltjes werden gemeten met behulp van single particle inductively coupled plasma massa spectrometrie. De doorgifte van 15, 30 en 70 nanometer goud deeltjes werd gemeten in het statische systeem. Alleen het allerkleinste deeltje werd terug gevonden aan de basolaterale kant van de cellaag. Hogere opname en doorgifte werd gevonden voor het 15 nm goud deeltje in de doorstroom transwell. Dit kwam waarschijnlijk doordat de cellen aan een hogere concentratie deeltjes werden blootgesteld in verhouding tot

het statische systeem. De hypothese is dat de vloeistof stroom de deeltjes naar de cellaag toe drukt. Hoewel, een vloeistof stroom misschien het probleem van sedimentatie/drijven kan oplossen zijn er ook beperkingen aan het dynamische systeem. Voor de toekomst zijn accurate metingen van het aantal deeltjes in het statische en dynamische model en het effect daarvan van groot belang om de biologische beschikbaarheid van deeltjes te kunnen bestuderen.

In dit proefschrift zijn *in vitro* modellen van het spijsverteringssysteem geïntegreerd met geavanceerde massa spectrometers om de orale bio beschikbaarheid van medicijnen, toxine en deeltjes te kunnen bepalen. In hoofdstuk 7 zijn de mogelijkheden en beperkingen van het ontwikkelde systeem besproken en aanbevelingen voor toekomstig onderzoek werden gegeven.

Curriculum Vitae

Milou Johanna Cornelia Santbergen was born on the 19th of November 1991 in Zevenbergen, the Netherlands. After graduating from high school (Markland college, Oudenbosch) in 2010, she started the bachelor Biology at Wageningen University. Followed by the Master Biology with an emphasis on human and animal health. For her MSc thesis project she joined the host-microbe interactomics group at Wageningen University, after which she spent six months at the Babraham institute in the United Kingdom as an intern. Both projects had a strong focus on the small intestine and how external triggers might affect the immune system. In January 2016 she started her PhD at the Laboratory of Organic Chemistry under the supervision of Prof. Dr. Michel Nielen, Dr. Hans Bouwmeester and Dr. Meike van der Zande, the results of this work are described in this thesis. Milou currently works as a study director in vitro drug metabolism and pharmacokinetics at Charles River, den Bosch.



Publications

Santbergen, M. J., van Der Zande, M., Bouwmeester, H., & Nielen, M. W. (2019). Online and in situ analysis of organs-on-a-chip. *TrAC Trends in Analytical Chemistry*.

Santbergen, M. J., van der Zande, M., Gerssen, A., Bouwmeester, H., & Nielen, M. W. (2020). Dynamic in vitro intestinal barrier model coupled to chip-based liquid chromatography mass spectrometry for oral bioavailability studies. *Analytical and Bioanalytical Chemistry*, 412(5), 1111-1122.

de Haan, P.*, Santbergen, M. J.*, van der Zande, M., Bouwmeester, H., Nielen, M. W. & Verpoorte, E. An integrated modular in vitro gastrointestinal tract total analysis system for oral bioavailability studies. *Submitted*

Stubbs, T. M., Bonder, M. J., Stark, A. K., Krueger, F., BI Ageing Clock Team, von Meyenn, F., Stegle, O., & Reik, W. (2017). Multi-tissue DNA methylation age predictor in mouse. *Genome biology*, 18(1), 68.

Acknowledgements

Eind 2015 via Skype had ik mijn eerste gesprek met Michel en Hans, ze waren opzoek naar iemand die verstand had van in vitro darm modellen en massa spectrometrie voor het PhD project GUTTEST. Nou, die persoon konden ze niet vinden, dus toen was het zaak om iemand te vinden die een van de twee disciplines wilde aanleren. Ik was ervan overtuigd dat de keuze zou vallen op een analytisch chemicus die wel even ging leren over celletjes. Ik was daarom ook verbaasd toen Hans belde en het project aanbood. Misschien, dachten ze onbewust: "haar initialen spellen MS, moet goed komen toch?". De afgelopen jaren waren een rollercoaster aan emoties, ik heb van mijn project gehouden, heb het vervloekt en zoveel geleerd in de tussentijd. Via dit dankwoord wil ik alle mensen bedanken die direct en indirect hebben bijgedragen aan mijn proefschrift.

Traditie getrouw begin ik met het bedanken van mij (co)-promotoren Michel, Hans en Meike. Michel, bedankt voor al je input over de jaren en je kritische blik. Jou no-nonsense style van begeleiding is mij altijd goed bevallen en ik kon altijd binnenlopen om even kort iets te bespreken. Verder bedankt voor je vertrouwen in mij als bioloog in dit analytische project het is niet altijd makkelijk geweest. Hans, de eerste twee jaar was jij officieel betrokken bij mijn project waarna je overgestapt bent naar de universiteit, maar gelukkig bleef je interesse voor mijn project. Ik kon mijn data nog wel eens somber inzien, maar jou enthousiasme en optimisme lieten me vaak zien dat het allemaal zo slecht nog niet was, bedankt daarvoor. Dan Meike, jou creativiteit en oog voor detail zijn ongekend en zijn dit proefschrift zeker ten goede gekomen. Buiten dat kon ik met jou ook altijd goed praten over niet wetenschappelijke dingen, films, series, een fijne afwisselingen van al die data. Dank je wel.

Nu dan iemand die nooit officieel mijn begeleider was, maar ik weet zeker zonder jou Arjen was ik dit dankwoord nu niet aan het schrijven. Hoe vaak ik wel niet aan jou bureau heb gestaan met een sip gezicht en de mededeling: dat ding doet het niet, is ongelofelijk. Bedankt voor je geduld met mij en de MS. Je moet vast meerdere keren hebben gedacht: "ohw nee komt ze weer", maar ik heb daar nooit iets van gemerkt, bedankt daarvoor.

Then my two paranymphs, ladies first. Gina, throughout our PhD journeys we were the two biologists among the chemistry bunch and had our fair share

of coffee breaks where we talked about our PhD struggles, feministic views, tattoos and all things related to snakes. You even trusted me enough to babysit your pet snake Irwin when you were on holiday (I still miss him). And of course the very exciting presenting with impact course, Shakespeare will never be the same. Thank you for being my paranympth.

Dan Menno, hoewel wij allebei in 2010 aan de studie biologie begonnen hier in Wageningen leerde we elkaar pas echt kennen toen jij begon als aio bij het WFSR. Het is maar goed dat je samen met Hans naar de toxicologie afdeling van de universiteit bent verhuist, anders was mijn PhD nooit af gekomen denk ik, want onze gesprekken duurde nooit een paar minuten maar altijd een aantal uur. Bedankt voor het luisterend oor, alle diners, thee, biertjes, ciders en gin-tonics.

Even though as a PhD student you're part of the university my real home was at WFSR, office 3057. Phim, Ashraf we started this PhD journey together and are also all defending in the same year, we made it! We actually made it, I still can't believe it really. Thank you both for the talks, cookies, chocolates and help in the lab. Dan voor de andere ongelukkige in ons kantoor, sorry dat jullie al onze PhD stress indirect mee hebben gekregen. Loes jij was altijd de rust zelve in het kantoor, bedankt daarvoor het was soms echt nodig. En Nicole, ik was heel blij toen jij naar het WFSR kwam, nu kon ik iets van mijn MS wijsheden aan jou overdragen. Hopelijk kun jij dat nu doen bij de volgende.

Het liefst zou ik over iedereen individueel iets zeggen, maar dan wordt dit dankwoord net zo lang als mijn proefschrift. Jullie zijn allemaal mijn helden, bedankt voor alle koffie/lunch pauzes, borrels, spelletjes avonden, laser gamen, tafeltennissen, eetentjes, hulp in het lab, input voor mijn project en jullie betrokkenheid: Deborah, Liza, Astrid, Marcia, Toine, Gerlof, Henri, Yoran, Ans, Jochem, Aafke, Geert, Ad, Ron, Lonneke, Greet, Sandra en Ruud.

Then everyone at Organic Chemistry, Monday morning was always my university morning and I think I sat in almost every PhD office as a stray. Even though most of you probably found my project a bit odd as it did not involve any organic chemistry whatsoever. You still came to my presentations and provided me with valuable input I would have never gotten elsewhere, thank

you for that. During my PhD I also assisted at several practical courses at the University which I dreaded beforehand but with the help of some amazing people it was easy: Hendra, Carel, Erik, Judith, Jean, Frank, Barend, Andrada and Kris, thank you. I also want to thank my two students Nienke and Bram, for working with me and all the trouble shooting that you both did for my project. Being part of the university and WFSR was double the amount of responsibilities, but also double the fun. To all the PhDs thank you for the amazing and memorable game nights, We-day, Christmas drinks, lab- and PhD trips. A PhD is not always easy and I'm happy I got to share this experience with you. I want to address some people individually, Alice thank you for your food, energy and chaos, never change. Jorick, ik zal nooit meer navigeren voor je belooft. Esther, bedankt voor al onze cafeïne gevulde dates. Ian, even lekker zeuren op het bankje, ik mis het zo. Jordi, waarom jij nooit biologie bent gaan studeren is mij een raadsel. Bedankt voor al onze gesprekken lang of heel lang. Een badmintonveld zal nooit meer hetzelfde zijn.

My PhD project was part of a larger consortium and the benefit of that is, that you get a lot of input on your research from different backgrounds. I want to thank each and every one of the project partners involved for your interest and enthusiasm for my project, I learned a great deal from you. A special thanks to Pim de Haan and Sabeth Verpoorte, we worked together with ease throughout the whole project, but all the puzzle pieces fell into place in Chapter 5 of this thesis and I think we put forward something great. Thank you.

Zoals hierboven te lezen is had ik best wel toffe collega's en als je naar een nieuwe baan gaat is het altijd maar weer afwachten waar je terecht komt. Nu ik dit schrijf werk ik drie maanden bij Charles River in Den Bosch en ook al zitten we midden in de corona quarantaine en is alles een beetje anders dan normaal weet ik dat ik op een goede plek terecht gekomen ben. Bedankt dat jullie me zo welkom laten voelen.

Gelukkig is er buiten werk nog een heel ander leven, ver weg van onderzoek. Marije wij zijn al vrienden sinds we 10 jaar oud zijn en hebben lief en leed gedeeld. Ik kan me mijn leven zonder jou niet voorstellen. Bedankt voor je vriendschap door al die jaren heen.

Rebecca en Marjon, bedankt voor alle keren waar we ouderwets herinneringen konden ophalen we moesten meestal wel het halve land doorreizen ervoor, maar dat hadden we er allemaal wel voor over.

Aan mijn andere vrienden en (schoon) familie, bedankt voor jullie interesse in mijn PhD project en jullie geduld een PhD vraagt veel tijd en dat gaat meestal ten kosten van de sociale aspecten. Maar vooral bedankt voor de afleiding, mijn wereld buiten mijn PhD project om.

Dan mijn ouders, woorden schieten te kort hoeveel jullie voor mij betekenen. Bedankt voor jullie steun en vertrouwen in mij. Studeren in Wageningen, half jaar in Engeland wonen en dan nog die PhD jullie waren er voor mij iedere dag, wanneer maar nodig. Lydia, het beste zusje dat ik maar kan wensen, jou deur (en die van Jeroen) staat altijd open en niks is te gek. Bedankt voor alles wat je bent en doet. Ik hou zoveel van jullie.

Lieve Rob, toen ik het wilde idee kreeg om te gaan promoveren ben jij met me mee verhuisd naar Wageningen. De afgelopen jaren heb jij mij gesteund, voor me gezorgd en me afgeleid wanneer dat nodig was. Ik mag je ondertussen al een tijdje mijn man noemen en we hebben eindelijk ons eerste huis samen gekocht. Ik kijk uit naar de rest van onze toekomst samen. Ik hou van je.

Milou

p.s. Mariska, Roelof en Machteld jullie ook bedankt

Overview of Completed Training Activities

Discipline specific activities	Organizing institute	year
COAST meeting ^a	COAST	2016
Advanced Food Analysis ^a	VLAG	2017
Dutch Society of Mass Spectrometry Spring meeting ^a	NVMS	2017
Forum for Analytical Science and Technology conference ^{ab}	COAST	2017
Chemistry as Innovating Science conference ^a	NWO	2017
MicroNano conference ^a	MinacNED	2017
Forum for Analytical Science and Technology conference ^a	COAST	2018
Forum for Analytical Science and Technology conference ^{ab}	COAST	2019

General courses

VLAG PhD week	VLAG	2016
Effective Behaviour in your Professional surrounding	WGS	2016
Efficient Writing Strategies	WGS	2017
Presenting with Impact	WGS	2018
Interpersonal communication for PhD students	WGS	2018
Brain training	WGS	2018

Other activities

Preparation of PhD research proposal		2016
Analytical Methods in Organic Chemistry	WUR	2016
Project meetings		2016-19
Weekly group meetings		2016-19
PhD study tour to Denmark and Sweden		2017
VLAG PhD council member		2017-19
PhD study tour to Israel		2019
Organizing committee PhD study tour to Israel		2019

^a Poster; ^b Oral presentation

The research presented in this thesis was financially supported by The Dutch Research Council (NWO) in the framework of the Technology Area PTA-COAST3 of the Fund New Chemical Innovations (GUTTEST, project nr. 053.21.116). Financial support from Wageningen University for printing this thesis is gratefully acknowledged.

Lay-out: Ferdinand van Nispen, *my-thesis.nl*

Printed by: GVO Drukkers & Vormgevers B.V., Ede, The Netherlands

